TUNED VIBRATION ABSORBER DESIGN METHODOLOGY FOR SYSTEMS WITH CUBIC STIFFNESS NONLINEARITY

A THESIS SUBMITTED TO
THE GRADUATE SCHOOL OF NATURAL AND APPLIED SCIENCES
OF
MIDDLE EAST TECHNICAL UNIVERSITY

BY

EGE ÖZGÜVEN

IN PARTIAL FULFILLMENT OF THE REQUIREMENTS
FOR
THE DEGREE OF MASTER OF SCIENCE
IN
MECHANICAL ENGINEERING

APRIL 2024

Approval of the thesis:

TUNED VIBRATION ABSORBER DESIGN METHODOLOGY FOR SYSTEMS WITH CUBIC STIFFNESS NONLINEARITY

submitted by **EGE ÖZGÜVEN** in partial fulfillment of the requirements for the degree of **Master of Science** i**n Mechanical Engineering, Middle East Technical University** by,

Prof. Dr. Naci Emre Altun
Dean, **Graduate School of Natural and Applied Sciences** _____

Prof. Dr. M. A. Sahir Arıkan
Head of the Department, **Mechanical Engineering** _____

Assoc. Prof. Dr. Mehmet Bülent Özer
Supervisor, **Mechanical Engineering, METU** _____

Examining Committee Members:

Prof. Dr. Yiğit Yazıcıoğlu
Mechanical Engineering, METU _____

Assoc. Prof. Dr. Mehmet Bülent Özer
Mechanical Engineering, METU _____

Assoc. Prof. Dr. Ali Emre Turgut
Mechanical Engineering, METU _____

Assist. Prof. Dr. Orkun Özşahin
Mechanical Engineering, METU _____

Prof. Dr. S. Çağlar Başlamışlı
Mechanical Engineering, Hacettepe University _____

Date: 22.04.2024

I hereby declare that all information in this document has been obtained and presented in accordance with academic rules and ethical conduct. I also declare that, as required by these rules and conduct, I have fully cited and referenced all material and results that are not original to this work.

Name Last name : Ege Özgüven

Signature :

ABSTRACT

TUNED VIBRATION ABSORBER DESIGN METHODOLOGY FOR SYSTEMS WITH CUBIC STIFFNESS NONLINEARITY

Özgüven, Ege
Master of Science, Mechanical Engineering
Supervisor: Assoc. Prof. Dr. Mehmet Bülent Özer

April 2024, 122 pages

This thesis investigates a novel Tuned Vibration Absorber (TVA) design methodology tailored for weakly nonlinear structural systems, specifically those that contain cubic stiffness nonlinearity. Vibration control is essential in various engineering applications to obtain system stability, reduce structural vibrations, and mitigate potential damage. While traditional linear approaches have been widely employed, weakly nonlinear systems pose unique challenges that demand a more mathematically advanced design methodology. This research develops a systematic approach to optimize TVA parameters, considering weak nonlinearity effects. The proposed method leverages analytical and numerical tools to model and analyze the system's dynamic response, enabling the identification of optimal tuning parameters for the TVA. The effectiveness of the proposed design methodology is demonstrated through theoretical analyses and numerical simulations, showcasing improved vibration suppression performance in weakly nonlinear systems. The findings contribute to the advancement of vibration control techniques and offer valuable insights for engineers and researchers working on designing and optimizing vibration absorbers for a wide range of applications in mechanical, civil, and aerospace engineering when nonlinearities exist in the structure.

Keywords: Tuned Vibration Absorber, Cubic Stiffness, Weakly Nonlinear Systems, Describing Functions, Harmonic Balance Method, Sherman-Morrison Matrix Inversion

ÖZ

DOĞRUSAL OLMAYAN KÜBİK DİRENGENLİĞE SAHİP SİSTEMLER İÇİN AYARLI TİTREŞİM SÖNÜMLEYİCİ TASARIM METODOLOJİSİ

Özgüven, Ege
Yüksek Lisans, Makina Mühendisliği
Tez Yöneticisi: Doç. Dr. Mehmet Bülent Özer

Nisan 2024, 122 sayfa

Bu tez, zayıf doğrusal olmayan sistemler (özellikle de kübik direngenlik içeren sistemler) için uyarlanmış yeni bir Ayarlı Titreşim Sönümleyici (TVA) tasarım metodunu incelemektedir. Titreşim kontrolü, çeşitli mühendislik uygulamalarında sistem kararlılığını sağlamak, yapısal titreşimleri azaltmak ve potansiyel hasarı azaltmak için gereklidir. Geleneksel doğrusal yaklaşımlar yaygın olarak kullanılırken, zayıf derecede doğrusal olmayan sistemler, matematiksel olarak daha gelişmiş bir tasarım metodolojisi gerektiren benzersiz zorluklar ortaya çıkarmaktadır. Bu araştırma, zayıf doğrusal olmayan etkileri dikkate alarak TVA parametrelerini optimize etmek için sistematik bir yaklaşım geliştirmektedir. Önerilen yöntem, sistemin dinamik tepkisini modellemek ve analiz etmek için analitik ve sayısal araçlardan yararlanır ve TVA için en uygun ayar parametrelerinin tanımlanmasına olanak tanır. Önerilen tasarım metodolojisinin etkinliği, zayıf doğrusal olmayan sistemlerde gelişmiş titreşim sönümleme performansını sergileyen teorik analizler ve sayısal simülasyonlar yoluyla gösterilmiştir. Bulgular, titreşim kontrol tekniklerinin ilerlemesine katkıda bulunmakta ve yapıda doğrusal olmayan durumlar mevcut olduğunda makine, inşaat ve havacılık mühendisliğinde çok çeşitli uygulamalar için titreşim sönümleyici tasarlanması ve optimize edilmesi üzerinde çalışan mühendisler ve araştırmacılar için değerli bilgiler sunmaktadır.

Anahtar Kelimeler: Ayarlı Titreşim Sönümleyici, Kübik Direngenlik, Zayıf Doğrusal Olmayan Sistemler, Tanımlama Fonksiyonları, Harmonik Denge Yöntemi, Sherman-Morrison Matris Ters Çevirme

To my lovely wife

ACKNOWLEDGMENTS

I want to start by expressing my sincere thanks to my advisor, Dr. M. Bülent Özer, for their constant support and helpful guidance throughout my research. His expertise and encouragement have really helped me shape this thesis, and I feel fortunate to have such a dedicated mentor.

I would like to express my deepest appreciation to my family and friends, who have been my pillars of strength throughout this journey. Their encouragement, understanding, and belief in my abilities have been a constant source of motivation.

A special note of appreciation goes to my wife, Melis. Her encouragement and belief in my goals have been the driving force behind my success. I am truly fortunate to have a life partner who stands by me in every effort, offering both love and inspiration.

To everyone who has been a part of this academic journey, whether with ideas, emotional support, or just understanding, I extend my heartfelt thanks. Your presence in my life has made this journey richer, and I'm grateful for the combined support that made this thesis possible.

TABLE OF CONTENTS

ABSTRACT v

ÖZ vii

ACKNOWLEDGMENTS x

TABLE OF CONTENTS xi

LIST OF TABLES xiv

LIST OF FIGURES xv

LIST OF ABBREVIATIONS xx

LIST OF SYMBOLS xxi

CHAPTERS

1 INTRODUCTION 1

1.1 Tuned Vibration Absorbers 1

1.2 Nonlinear Systems 4

1.2.1 Cubic Stiffness 6

1.2.2 Other Common Nonlinearities 8

1.3 Literature Survey 9

1.3.1 Vibration Absorbers on Linear Systems 10

1.3.2 Vibration Absorbers on Nonlinear Systems 11

1.4 Objective of the Thesis 14

1.5 Outline of the Thesis 14

2 IDENTIFICATION AND LINEARIZATION OF NONLINEARITIES IN STRUCTURES 17

2.1 Describing Function Method 17

2.2 Forced Harmonic Response Analysis of Nonlinear Structures Using Describing Functions 19
2.3 Closed Form Solutions of Weakly Nonlinear Multi-Degree of Freedom Systems with Single Nonlinear Element 22
2.4 Tuned Vibration Absorber for Weakly Nonlinear Systems 25
3 HARMONIC RESPONSE ANALYSIS OF NONLINEAR SYSTEMS WITH LINEAR VIBRATION ABSORBER 27
3.1 Tuned Vibration Absorber Attached on A Single Degree of Freedom Nonlinear System 27
3.1.1 Undamped System with Cubic Stiffness 38
3.1.2 Damped Main System with an Undamped TVA 44
3.1.3 Undamped Main System with a Damped TVA 47
3.1.4 Damped System with Cubic Stiffness 48
3.2 Tuned Vibration Absorber Attached on A Multi Degree of Freedom Nonlinear System 67
4 CASE STUDIES AND VALIDATION 71
4.1 2-Degree-of-Freedom Case Studies 71
4.1.1 Case Study #1 (Undamped & lightly damped 2-DOF system) 72
4.1.2 Case Study #2 (Damped Main System & Undamped Absorber) 77
4.1.3 Case Study #3 (Damped Main System & Vibration Absorber with low nonlinearity and high main system damping) 80
4.1.4 Case Study #4 (Damped Main System & Damped Vibration Absorber with high nonlinearity and high main system damping) 84
4.1.5 Case Study #5 (Damped Main System & Damped Vibration Absorber with low nonlinearity and low main system damping) 87

4.1.6 Case Study #6 (Damped Main System & Damped Vibration Absorber with high non-linearity and low main system damping)..... 90
4.2 Multi-Degree-of-Freedom Case Studies..... 92
4.2.1 Case Study #7..... 92
4.2.2 Case Study #8..... 95
4.3 Discussion of the Findings..... 100
5 CONCLUSION.....105
5.1 Advantages of the Method..... 105
5.2 Disadvantages and Flaws of the Method..... 106
5.3 Future Work Improvements..... 108
REFERENCES 111
APPENDICES
A. Pseudo-Code for Parameter Sweep to Obtain Optimum Damping and Frequency Ratio..... 115
B. Main Code for 2-DOF Analytical DF Method..... 117
C. Main Code for 2-DOF Iterative Method..... 118
D. Main Code for MDOF Analytical DF Method..... 119
E. Main Code for MDOF Iterative Method..... 121

LIST OF TABLES

TABLES

Table 2.1 Describing Function Representations of Common Nonlinearities 19
Table 3.1 The Comparison of Computational Time for Iterative and DF Methods 68
Table 4.1 Summary of the Case Studies #3-6 101

LIST OF FIGURES

FIGURES

Figure 1.1 System Model in Den Hartog's Work [27] 1
Figure 1.2 Before and After a (Untuned) Vibration Absorber is Attached to the System [27] 2
Figure 1.3 Before and After a Tuned Vibration Absorber is Attached to the System [27] 3
Figure 1.4 Typical Response Curves for Various Levels of Excitation [28] 6
Figure 1.5 Force vs Displacement Graphs for Softening and Hardening Stiffnesses [29] 7
Figure 1.6 Theoretical Frequency Response Curve for a Hardening Spring Type Resonant System [28] 8
Figure 1.7 Force vs Displacement Graphs for Other Common Types of Nonlinearities [29] 9
Figure 2.1 System Modeling for Linear and Nonlinear Systems 18
Figure 2.2 An Example of Weakly Nonlinear n-Degree-of-Freedom System with the Nonlinear Component Between $(k-1)^{th}$ and k^{th} Elements 22
Figure 3.1 The System Model of a Single-Degree-of-Freedom System with Cubic Stiffness 29
Figure 3.2 An Example of Frequency vs Amplitude Graph of a SDOF System Found with Describing Function Method 30
Figure 3.3 Frequency vs Discriminant Graph for the Example SDOF System 31
Figure 3.4 The 2-DOF System Model of a Tuned Vibration Absorber Attached to the Main System 32
Figure 3.5 The Frequency vs Amplitude Graphs for the First TVA Parameter Set 33
Figure 3.6 The Frequency vs Amplitude Graphs for the Second TVA Parameter Set 34
Figure 3.7 The Frequency vs Amplitude Graphs for the Third TVA Parameter Set 35

Figure 3.8 Non-Dimensional Version of the Graph in Figure 3.2 37
Figure 3.9 Non-Dimensional Version of the Graph in Figure 3.4 and Figure 3.5 .. 38
Figure 3.10 The 2-DOF Undamped System Model with Cubic Stiffness Between First Mass and the Ground 39
Figure 3.11 The Frequency vs Amplitude Graphs for the SDOF System with Parameters $\gamma = 0.5, \zeta 1 = 0$ 42
Figure 3.12 The Frequency vs Amplitude Graphs with Jump Frequencies for the 2-DOF System with Parameters $\gamma = 0.5, \mu = 0.1, \omega r = 2.0, \zeta 1 = \zeta 2 = 0$ 43
Figure 3.13 The 2-DOF System Model with Damped Main System with Cubic Stiffness and Undamped TVA 44
Figure 3.14 The Frequency vs Amplitude Graphs with Jump Frequencies for the 2-DOF System with Parameters $\gamma = 0.5, \mu = 0.1, \omega r = 2.0, \zeta 1 = 0.1, \zeta 2 = 0$ 45
Figure 3.15 The Time Domain Solution for the 2-DOF System with Parameters $\gamma = 0.5, \mu = 0.1, \omega r = 2.0, \zeta 1 = 0.1, \zeta 2 = 0$ at the Frequency Ratio $\Omega = \omega r = 2$ 46
Figure 3.16 The Frequency vs Amplitude Graphs with varying $\zeta 2$ 47
Figure 3.17 The Invariant Points of αNLC and $XNL, 1$ 48
Figure 3.18 The 2-DOF Damped System Model with Cubic Stiffness Between First Mass and the Ground 49
Figure 3.19 The Effect of $\zeta 2$ on the Frequency vs Amplitude Graphs 50
Figure 3.20 The Effect of ωr on the Frequency vs Amplitude Graphs 52
Figure 3.21 The Best Subsets for ωr in Minitab 53
Figure 3.22 The Summary of Regression Work for ωr in Minitab 55
Figure 3.23 The Frequency vs Amplitude Graphs for the SDOF System with Parameters $\gamma = 0.256, \zeta 1 = 0.1$ 56
Figure 3.24 The Frequency vs Amplitude Graphs for the SDOF System for $\mu = 0.02$ 57
Figure 3.25 The Frequency vs Amplitude Graphs for the SDOF System for $\mu = 0.1$ 58

Figure 3.26 The Frequency vs Amplitude Graphs for the SDOF System for $\mu = 0.5$ 58
Figure 3.27 The Frequency vs kc Graphs 59
Figure 3.28 The Frequency vs k_c Graphs with $kc = 5 * 106$ Plotted 60
Figure 3.29 The Frequency vs Amplitude Graph for $kc = 5 * 106$ Case 61
Figure 3.30 The Best Subsets for the Mass Ratio Regression in Minitab 62
Figure 3.31 The Summary of Regression Work for μ in Minitab 63
Figure 3.32 The Best Subsets for ωr Regression with Predetermined Mass Ratio in Minitab 64
Figure 3.33 The Summary of Regression Work for ωr with Predetermined Mass Ratio in Minitab 65
Figure 3.34 The Invariant Points of αNLC and $XNL, 1$ with the Method Developed 66
Figure 3.35 A MDOF System with Nonlinear Element Between the First Mass and The Ground 67
Figure 4.1 A 2-DOF System Model 71
Figure 4.2 The Response Curves for SDOF System with $\gamma = 0.256, \zeta 1 = 0$ 72
Figure 4.3 The Response Curves for the Parameter Set of $\gamma = 0.256, \mu = 0.2, \omega r = 1.42, \zeta 1 = \zeta 2 = 0$ 73
Figure 4.4 The Response Curves with Jump Frequencies for the Parameter Set of $\gamma = 0.256, \mu = 0.2, \omega r = 1.42, \zeta 1 = \zeta 2 = 0$ 74
Figure 4.5 The Response Curves with Jump Frequencies for $\zeta 1 = \zeta 2 = 0.001$ ... 75
Figure 4.6 The Response Curves with Jump Frequencies for Various Damping Ratios 76
Figure 4.7 The Response Curves with Jump Frequencies for the Parameter Set of $\gamma = 0.256, \mu = 0.2, \omega r = 1.42, \zeta 1 = 0.1, \zeta 2 = 0$ 78
Figure 4.8 The Response Curves with Jump Frequencies for Various Mass Ratios 79
Figure 4.9 The Response Curves for SDOF System with $\gamma = 0.25, \zeta 1 = 0.15$ 80

Figure 4.10 ODE Solution for the Response Curves for SDOF System with $\gamma = 0.25, \zeta 1 = 0.15$ 81
Figure 4.11 The Response Curves for 2DOF System with $\gamma = 0.25, \zeta 1 = 0.15, \mu = 0.0205, \omega r = 1.232, \zeta 2 = 0.0868$ 82
Figure 4.12 The Comparison of ODE Solution and Describing Function Method Solution for Case Study #3 82
Figure 4.13 The Comparison of Describing Function Method and Parameter Sweep for Case Study #3 83
Figure 4.14 The Response Curves for SDOF System with $\gamma = 1.50, \zeta 1 = 0.15$ ... 84
Figure 4.15 The Response Curves for 2DOF System with $\gamma = 1.50, \zeta 1 = 0.15, \mu = 0.118, \omega r = 1.295, \zeta 2 = 0.200$ 85
Figure 4.16 The Comparison of ODE Solution and Describing Function Method Solution for Case Study #4 85
Figure 4.17 The Comparison of Describing Function Method and Parameter Sweep for Case Study #4 86
Figure 4.18 The Response Curves for SDOF System with $\gamma = 0.25, \zeta 1 = 0.05$ ... 87
Figure 4.19 The Response Curves for 2DOF System with $\gamma = 0.25, \zeta 1 = 0.05, \mu = 0.143, \omega r = 1.106, \zeta 2 = 0.218$ 88
Figure 4.20 The Comparison of ODE Solution and Describing Function Method Solution for Case Study #5 88
Figure 4.21 The Comparison of Describing Function Method and Parameter Sweep for Case Study #5 89
Figure 4.22 The Response Curves for SDOF System with $\gamma = 1.50, \zeta 1 = 0.05$ ... 90
Figure 4.23 The Response Curves for 2DOF System with $\gamma = 1.50, \zeta 1 = 0.05, \mu = 0.272, \omega r = 1.174, \zeta 2 = 0.286$ 91
Figure 4.24 The Comparison of ODE Solution and Describing Function Method Solution for Case Study #6 91
Figure 4.25 The Comparison of Describing Function Method and Parameter Sweep for Case Study #6 92

Figure 4.26 The System Model of a TVA Attached to 4-DOF System with Cubic Stiffness Connected Between the First Mass and the Ground 93
Figure 4.27 The Response Curves for Case Study #8 Before the TVA is Attached 94
Figure 4.28 The Response Curves for Case Study #8 After the TVA is Attached. 94
Figure 4.29 The Response of the First Mass in a 4-DOF System..... 96
Figure 4.30 The Response of the First Mass in a 20-DOF System..... 96
Figure 4.31 The Response Curves for SDOF System with $\gamma = 0.148, \zeta 1 = 0.01$ 97
Figure 4.32 The Comparison of the First Mass of the 4-DOF System and its SDOF Equivalent 98
Figure 4.33: The Response Curves of The First Mass of the 4-DOF System with and without TVA Attached 99
Figure 4.34 The Comparison of ODE Solution and Describing Function Method Solution for Case Study #8 100
Figure 4.35 The Comparison of Case Studies #4 and #6..... 103
Figure 5.1 The Error at the Peaks for $\gamma = 2, \zeta 1 = 0.05$ 108

LIST OF ABBREVIATIONS

ABBREVIATIONS

TVA: Tuned Vibration Absorber

TMD: Tuned Mass Damper

SDOF: Single-Degree-of-Freedom

MDOF: Multi-Degree-of-Freedom

NLTVA: Nonlinear Tuned Vibration Absorber

IDVA: Inerter-based Dynamic Vibration Absorber

VIF: Variance Inflation Factor

LIST OF SYMBOLS

SYMBOLS

m_i: Mass of the i-th element

k_i: Linear stiffness of the i-th element

c_i: Viscous damping of the i-th element

k_c: Cubic stiffness

M: Mass matrix

K: Linear Stiffness matrix

C: Damping matrix

F: Force vector

N: Nonlinear force vector

G: Amplitude of vector N

n: Nonlinear force element

ν: Describing function

Δ: Nonlinearity matrix involving describing functions

θ: Quasilinear receptance matrix

X_L: Linear displacement

X_{NL}: Nonlinear displacement

Z: Impedence matrix

α: Receptance matrix

α_{NLC}: Nonlinear constant of receptance

ω: Frequency

Ω: Non-dimensional frequency

γ: Nonlinearity ratio

ζ_i: Damping ratio of i-th element

μ: Mass ratio

ω_r: Frequency ratio

CHAPTER 1

INTRODUCTION

1.1 Tuned Vibration Absorbers

Vibration absorbers and isolators are commonly used in many engineering applications in mechanical engineering systems. Attenuation of vibration is critical since it may cause devastating failure effects on the system. This problem is one of the engineering issues that has been studied for a long time. Various solutions have been developed to reduce the dynamic response caused by these vibrations on structures. Passive-tuned mechanical vibration dampers, founded by Hermann Frahm, are one of the widely used methods among these solutions [1].

After Frahm laid the foundations, tuned mass dampers (TMDs) were studied by Den Hartog [2]. The extra mass system added to the primary structure with a single degree of freedom is tuned to the natural frequency of the primary structure.

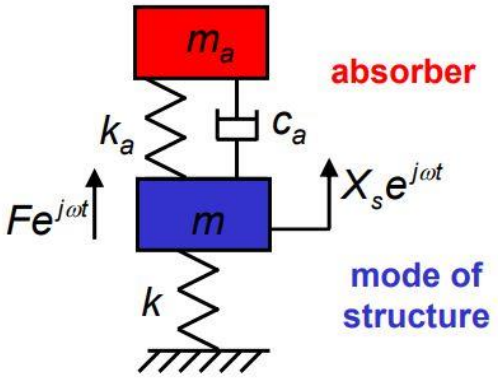

Figure 1.1 System Model in Den Hartog's Work [27]

This alteration results in the emergence of two distinct resonance peaks close to the initial natural frequency of the main structure. The amplitudes of these resonance peaks are influenced by both the mass added to the system and the characteristics of the damping and stiffness elements between the two masses.

In the figure below, the blue graph represents the displacement in the SDOF system, and the red graph represents the displacement on the first mass when TVA is attached.

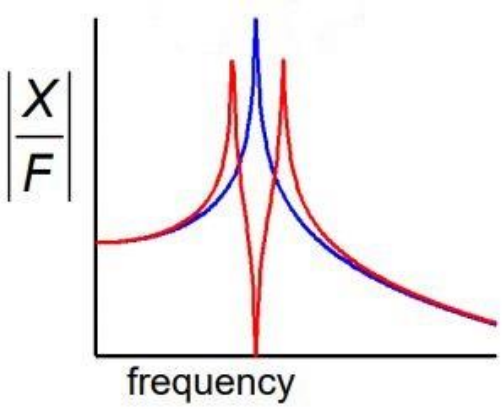

Figure 1.2 Before and After a (Untuned) Vibration Absorber is Attached to the System [27]

Den Hartog demonstrated the optimal selection and calculation of these values for single-degree-of-freedom systems. The optimal stiffness constant results in two equal resonance peaks, and the optimal damping ratio selection gives the lowest peaks possible.

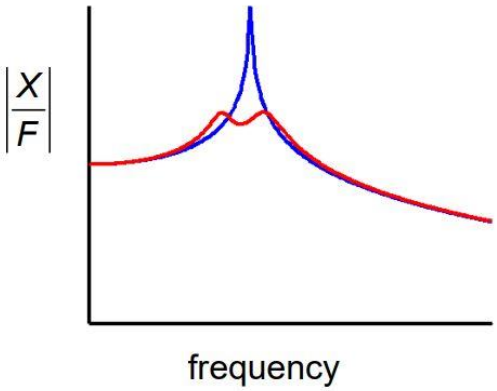

Figure 1.3 Before and After a Tuned Vibration Absorber is Attached to the System [27]

Den Hartog's simple and convenient solution to the vibration absorber problem was a breakthrough, and many research and articles were published in the upcoming years.

Den Hartog's biggest drawback was the undamped main system assumption, and many researchers tried to overcome this. One of the early papers from Randall [3] presents computational graphs for designing optimal linear vibration absorber systems for damped linear main systems. The computational graphs allow the determination of the optimal absorber system subject to design constraints on the mass ratio. The example design problem demonstrates the ease of using the design graphs and compares absorber designs resulting from the classic model and the damped linear model. It concludes that with damping included in the primary system, more accurate values for the optimal absorber system can be achieved compared to assuming a classic system.

Thompson's research paper [4] discusses the application of the frequency locus method to optimize the tuning and damping of a dynamic vibration absorber attached to a force-excited and damped main system. It presents the construction of frequency loci for the overall system and highlights the discovery of a tuning function for

determining the optimal natural frequency and relative damping rate for the absorber. The paper explores the effects of primary damping on the tuning conditions and provides an exact analysis by frequency locus methods. The findings demonstrate the reduction of the peak amplitude of the primary mass by adding an optimally tuned and damped vibration absorber.

After many approximate solutions from various researchers, a closed-form exact solution is found for this classical problem in the early 2000s. The paper from Asami and Nishihara [5] presents a new method for finding the exact solution to the optimization problem of the tuned vibration absorber attached to a linear main system. The authors introduce a new method that enables the exact algebraic solution of the H∞ optimization problem, as opposed to the previously known approximate solution. The study applies this new method to the design optimization of both a viscous damped absorber and a hysteretic damped absorber attached to main systems, considering different transfer functions for vibration suppression or isolation. The paper compares the closed-form exact solutions obtained through the new method with the approximate ones, demonstrating the accuracy and reliability of the proposed new method for finding exact solutions to the H∞ optimization problem for both types of TVAs.

Thanks to its simplicity, effectiveness, and fully passive mode of operation, tuned vibration absorbers are commonly used in real-life applications. Its main field of application includes civil structures, such as long-span bridges [6], skyscrapers [7], slender towers [8], and mechanical structures like aircraft engines [9], helicopter rotors [10], CNC machine tools [11].

1.2 Nonlinear Systems

The research papers previously discussed in Section 1.1 make certain assumptions that may not always be valid [12]. One such assumption is that damping is either viscous or linear, meaning resistance to relative motion is directly proportional to the

relative velocity. This assumption simplifies the analysis significantly. However, real-world damping in materials like wire mesh or elastomers results from a combination of localized frictional losses by individual wires and hysteresis in the cushion. Unlike the assumed linear damping, practical damping is a function of both displacement and velocity. Consequently, the terms describing damping in the equations of motion become nonlinear. At resonance, when displacement is substantial, damping is high. In off-resonance regions, where displacement is minimal, damping is relatively low. This characteristic offers a favorable scenario where damping is highly effective during resonance and can be disregarded in other conditions.

Another assumption involves the behavior of flexible members or mounts, assuming they act as linear springs. However, this assumption is not entirely accurate because many mounts exhibit a certain degree of hardening behavior, where the stiffness increases with the applied load or displacement. The extent of this hardening depends on the material of the flexible elements within the mounts.

This property has a useful effect of increasing the dynamic load-carrying capability of the mounts. Considering the natural frequency of a simple spring-mass system.

$$\omega_n = \sqrt{\frac{k}{m}}$$

As observed, an increase in the weight (mass) of an object leads to a reduction in its natural frequency. However, if the stiffness also increases, such as in the case of a hardening spring, the ratio of stiffness to mass (k/m) becomes less reliant on the object's mass. This characteristic allows the mount to accommodate a broader range of loads.

Another impact of a stiffening spring on the dynamic behavior of a system is its tendency to make the natural frequency "input sensitive." As the amplitude of the system increases, so does the displacement. Consequently, both the stiffness and natural frequency experience an increase.

The figure below illustrates typical responses to various inputs for different types of springs. It is evident that the resonant point shifts with different inputs for both hardening and softening springs.

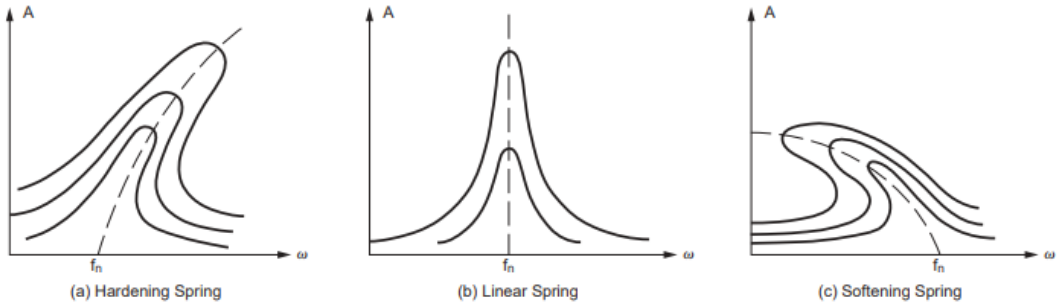

Figure 1.4 Typical Response Curves for Various Levels of Excitation [28]

1.2.1 Cubic Stiffness

Polynomial type of stiffness non-linearity is one of the most encountered types of non-linearity and cubic order is generally sufficient to represent its nonlinear behavior. Cubic stiffness means spring force is proportional to the cube of displacement.

$$F_{spring} = kx + k_c x^3$$

The cubic stiffness term k_c can be positive or negative. A system with a positive cubic stiffness exhibits bigger restoring forces at higher excitation levels, termed as having hardening characteristics. Conversely, a system demonstrating reduced stiffness as excitation levels increase is described as having softening nonlinearity.

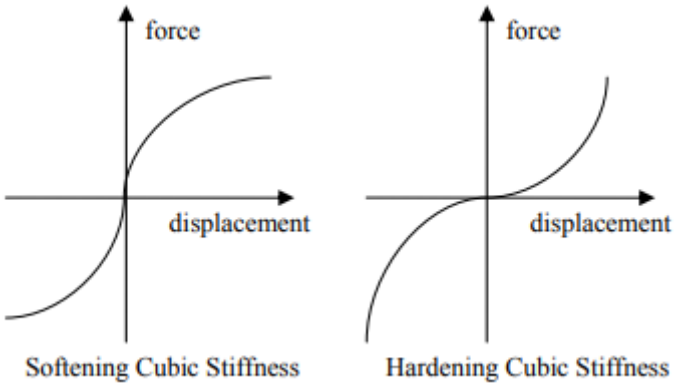

Figure 1.5 Force vs Displacement Graphs for Softening and Hardening Stiffnesses [29]

Three different displacement solutions can be found from solving the equation of motion since there is a cubic term in it. One of the solutions sets with varying frequency gives the hardening/softening curves mentioned before. The other two solutions exhibit a sharp drop or increase in amplitudes at certain frequencies. This is usually called the jump phenomenon, and the frequencies are called jump frequencies. The frequency range between two jump locations is usually referred to as the region of instability or the region of nonlinearity.

While this unstable branch does not yield a physically existing displacement, the other two solutions are both observable for the system, depending on the frequency sweep direction. While the frequency is increasing, the jump-down behavior can be observed. While the frequency is decreasing, there is a jump-up frequency at a smaller frequency than jump-down for hardening systems.

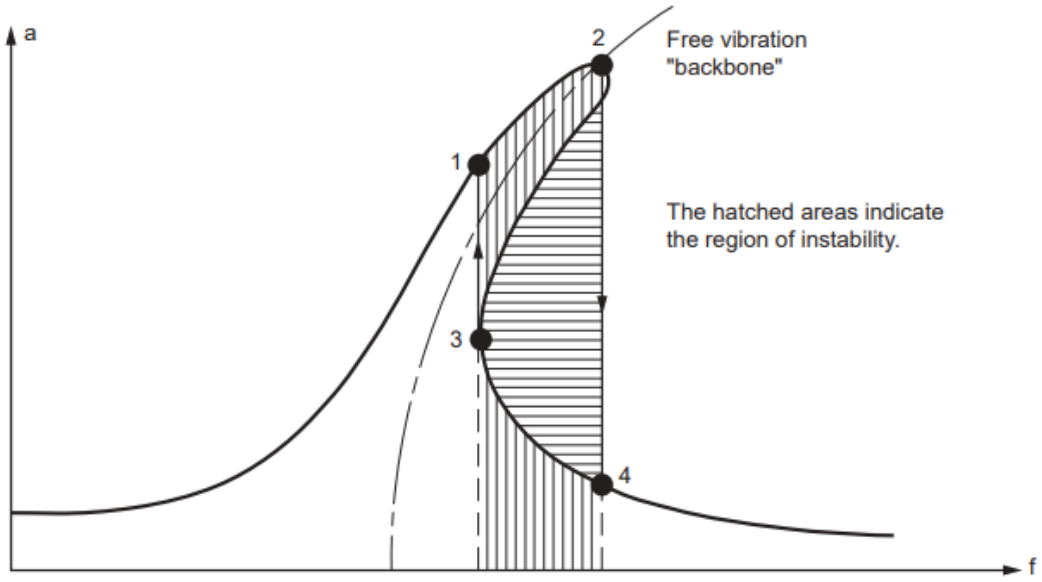

Figure 1.6 Theoretical Frequency Response Curve for a Hardening Spring Type Resonant System [28]

1.2.2 Other Common Nonlinearities

Besides cubic stiffness, there are more nonlinearities used to model the system-specific source of non-linearities, such as looseness, clearance, or friction in structural joints.

Piecewise linear stiffness may be used for modeling preloading effects or loose bolts. A typical piecewise stiffness may be modeled like below.

$$F_{spring} = \begin{cases} k_2 x + (k_1 - k_2)x' & for\ x > x' \\ k_1 x & for\ |x| < x' \\ k_2 x - (k_1 - k_2)x' & for\ x < -x' \end{cases}$$

Where k_1 and k_2 are the two different slopes on the force vs displacement graph, and x' is the point where the slope changes.

When there is a clearance on the mount, the backlash effect can be modeled as the previous equation with the addition of $k_1 = 0$.

The friction in the joints is usually known as coulomb damping. The sign of the resultant force depends on the direction of the velocity of the mass.

$F_{spring} = c\,\mathrm{sgn}(\dot{x})$

Unlike other types of nonlinearities, coulomb friction is dominant on low levels of excitation. For high levels of excitation, stick-slip motion may occur.

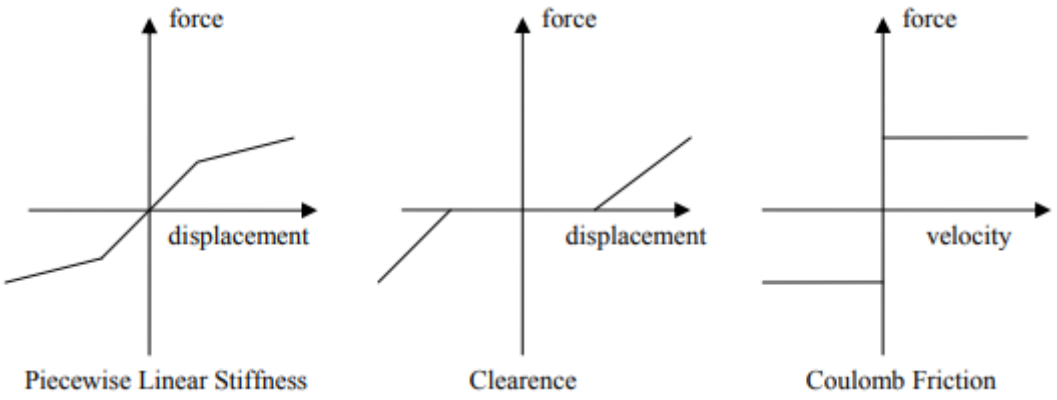

Figure 1.7 Force vs Displacement Graphs for Other Common Types of Nonlinearities [29]

1.3 Literature Survey

Throughout the history of engineering, many analytical and numerical methods have been generated to deal with the vibration absorber problem. Early concepts from the pre-computer era include developing a general analytical approach for simple systems. As the tools of engineering evolve and the problems that are trying to be solved get more and more complex, numerical methods are used. While numerical methods take more time to obtain the solution, it is advantageous for applications on large and complex systems and for optimizing and obtaining a system-specific solution.

This literature survey includes research on tuned vibration absorbers that include nonlinearities in the main system, or in the absorber, or both. Although the systems or the absorbers are different for different cases, the approach to the problem and ways to solve the problem have similarities, and they are instructive whether the nonlinearity is in the main system or in the absorber.

1.3.1 Vibration Absorbers on Linear Systems

The majority of the research in this field focuses on tuning a nonlinear vibration absorber on a linear system. Linear TVAs face a significant drawback as they typically operate within a relatively narrow frequency range. This restricts their effectiveness to mitigate vibrations in slender structures, whose natural frequency often varies concerning the oscillation amplitude [13]. To address this limitation, in addition to considering semi-active solutions [14], various researchers have suggested intentionally introducing nonlinearity into the absorber. This intentional nonlinearity aims to broaden the operational frequency range of the absorber.

Brennan and Kovacic's work [15] presents non-dimensional expressions for the jump-up and jump-down frequencies and the corresponding displacement amplitudes of a softening and hardening single-degree-of-freedom system with cubic stiffness (A Duffing oscillator) with linear viscous damping. These expressions are determined using the harmonic balance approach and are compared with those derived using perturbation methods and numerical integration. The findings highlight the complex relationship between nonlinearity, damping, and the occurrence of jump phenomena in the Duffing oscillator. The paper offers valuable insights into the analytical approach for determining jump frequencies and their amplitudes, providing a link between earlier analytical work and later numerical studies.

In Gatti and Brennan's set of papers [16-18], the dynamic behavior of a nonlinear two-degree-of-freedom system that is composed of a linear oscillator and a nonlinear

TVA attachment with cubic stiffness. The study focuses on the appearance and disappearance of the jump phenomenon in the frequency-response curve of the system. The effects of system parameters on the frequency-response curve shape, the existence of multivalued responses, and the determination of jump-up and jump-down frequencies are explored. The paper also provides approximate analytical expressions for the jump frequencies. The research contributes to the understanding of the system's behavior and provides insights into the parameters governing the jump frequencies.

Unlike other examples, Rüdinger focuses on nonlinearities in the damping term. In his paper [19], he investigates the use of a tuned mass damper with a nonlinear viscous damping element to control the vibration of lightly damped structures subjected to white-noise excitation. Statistical linearization is employed to analyze the system, and its accuracy is verified through stochastic simulation. The optimal linear tuned mass damper parameters are determined to minimize the standard deviation of the structural displacement, showing little influence of structural damping. The study demonstrates that statistical linearization leads to very accurate results, implying that the optimal nonlinear tuned mass damper is practically as effective as a linear tuned mass damper. Additionally, the paper includes an example of the design procedure for a tuned mass damper with viscous power-law damping, showcasing the process for determining optimal parameters.

1.3.2 Vibration Absorbers on Nonlinear Systems

The research on TVA attached to a nonlinear system is limited compared to the nonlinear vibration absorbers on linear systems. This is due to the advantages of using nonlinear tuned vibration absorbers that are mentioned in Section 1.3.1 and assuming the main system as a linear system always has advantages as well. However, the linear main system assumption may not be sufficient in certain cases, and the nonlinearity effect may be critical.

Even when nonlinearity is considered, these behaviors are hard to model, and usually, numerical methods are used to solve the equations of motion. In this section, the papers that can achieve an analytical solution to the tuning problem are presented.

1.3.2.1 Cubic Stiffness Nonlinearity

Habib's research paper [20] introduces the concept of using nonlinear tuned vibration absorber (NLTVA) to reduce the vibrations around a nonlinear resonance in mechanical systems. The NLTVA is designed to have a restoring force tailored to the nonlinear restoring force of the primary system. The paper proposes a method to synthesize the absorber's load-deflection characteristic to effectively reduce the considered nonlinear resonance in wide ranges of motion amplitudes. It also presents a nonlinear generalization of Den Hartog's equal-peak method to determine the NLTVA parameters. The effectiveness of the NLTVA is demonstrated through numerical simulations on a Duffing oscillator system, showing that the NLTVA can outperform the classical linear tuned vibration absorber in reducing vibrations in both weakly and strongly nonlinear regimes. The paper also discusses the occurrence of dynamical instabilities and the potential applications and areas for further research.

Chang's research [21] explores the applications and effectiveness of inerter-based dynamic vibration absorbers (IDVAs) in reducing the responses of vibration systems, specifically focusing on the application of IDVAs to nonlinear systems excited by random excitation. The study introduces translational and rotational inerters and discusses their usage in mechanical vibration, suspension systems, and civil engineering. It also evaluates IDVAs' performance when connected to other elements in parallel or series, comparing their effectiveness with traditional dynamic vibration absorbers. The paper presents numerical results to illustrate the applicability and effectiveness of IDVAs and discusses the influences of parameters on the mean-square displacement response of the nonlinear system. Additionally, it proposes approximate analytical methods to obtain the response probability density

and mean-square displacement of nonlinear systems and validates the accuracy and effectiveness of the proposed method through numerical results. The paper provides insights into the optimal design parameters for IDVAs and demonstrates the robustness of IDVAs' performance in the presence of nonlinearities and excitation intensity.

1.3.2.2 Other Nonlinearities

There are some research papers dealing with nonlinearities other than cubic stiffness. These papers present unique ways to solve the nonlinear equations of motion since different nonlinearities require different approaches.

Sgobba's research [22] investigates the optimal design of tuned vibration absorbers for seismic protection of inelastic structures using a Bouc-Wen hysteretic model. The seismic load is modeled as a filtered stochastic process. Three different objective functions are considered for the optimization problem, including the maximum peak structural displacement standard deviation, the average hysteretic dissipated energy, and a combined functional damage index. The research shows that TVAs reduce the amount of hysteretic dissipated energy, providing beneficial protection for buildings with nonlinear behavior under severe dynamic loadings. The paper also explores the effectiveness of TVAs on inelastic structures and discusses the optimal mechanical parameters for TVAs. The results suggest that the application of TVA systems reduces structural damage by lowering the dissipated energy, particularly in the inelastic range, and that the TVA's performance is sensitive to the characteristics of the ground motion. The study contributes to the preliminary design of TVAs for inelastic structures under seismic excitation.

Mohebbi's paper [23] discusses the optimization of tuned vibration absorbers for non-linear structures subjected to earthquakes. The study focuses on determining the optimal TVA parameters, including mass, stiffness, and damping, to minimize the response of non-linear frame structures to different excitations. The researcher

developed an optimization algorithm based on the minimization of a performance index defined as a function of the response of the non-linear system. They utilized a distributed genetic algorithm to solve the optimization problem. An application example for an eight-story nonlinear shear building with bilinear hysteretic material behavior subjected to earthquake illustrates the method's success in determining TVA parameters to reduce the structure response. The authors also assessed TVA efficiency in reducing the maximum drift and accumulated hysteretic energy. The results demonstrate TVA's effectiveness in minimizing the response of non-linear structures under different excitations.

1.4 Objective of the Thesis

This thesis focuses on developing a method for finding optimum tuning parameters for vibration absorbers that are connected to systems with a cubic stiffness behavior. The new method uses Describing Functions to linearize the nonlinearity and uses frequency response functions to analyze and optimize the system. The thesis includes analytical methods for 2-DOF systems with a linear tuned vibration absorber connected to the system with cubic stiffness nonlinearity and a numerical method expansion for tuned vibration absorbers for weakly nonlinear MDOF systems.

While the research focuses on cubic stiffness nonlinearity, the foundations of the method allow the user to deal with nonlinearities other than cubic stiffness as well. Although it may not be possible to obtain analytical solutions with more complex behaviors, there is always a possibility to use numerical approaches. The method promises a swift execution and saves time compared to the traditional numerical methods.

1.5 Outline of the Thesis

After the introductory chapter, Chapter 1, an identification and linearization method for nonlinearities is given in Chapter 2. This chapter focuses on some work done by

others that will be used directly in the thesis. Hence, it can be considered as a detailed literature review of specific topics that are the foundations of the methodology developed in this research.

Chapter 3 presents the method for tuning vibration absorbers for weakly nonlinear systems. Tuned vibration absorbers attached to both single and multi-degree-of-freedom systems are analyzed, and solutions are offered.

Chapter 4 is the results section of the thesis. This chapter includes case studies for the developed methods and validation of the methods by numerical methods and time-domain solutions with frequency sweep via MATLAB.

Chapter 5 is the concluding chapter of the thesis. This chapter summarizes all the work done through the thesis research, investigates the findings, and compares them with the results of others. This chapter also concludes the study with possible future work for improvements and suggestions.

CHAPTER 2

IDENTIFICATION AND LINEARIZATION OF NONLINEARITIES IN STRUCTURES

This chapter focuses on the subjects which are the foundations of this study. Section 2.1 provides a detailed explanation of the Describing Function Method, which gives an approximation of the nonlinear system with quasi-linearization of structural nonlinearities. Section 2.2 will summarize the relevant research about finding the forced harmonic response of a nonlinear system in a structural vibrations problem using the Describing Function Method by Tanrıkulu et al. [24]. Section 2.3 will explore the research by Özer [25] about applications of the describing function method for MDOF systems and linearization of weak nonlinearities by using Sherman-Morrison Matrix Inversion and separating linear and nonlinear terms. Finally, Section 2.5 will present the methodology idea for optimizing a tuned vibration absorber for systems with weak nonlinearities.

2.1 Describing Function Method

The Describing Function Method is an approximation method for analyzing certain nonlinear systems, usually used in feedback control systems. This approximation is often referred to as quasi-linearization. As an analogy, for linear systems, transfer functions are used for the relation between input and output. For nonlinear systems, a describing function does the same thing.

Figure 2.1 System Modeling for Linear and Nonlinear Systems

However, unlike transfer functions, describing functions are dependent on the inputs [26]. It is based on the following assumptions:

1. This nonlinear component should be time-invariant,
2. Its higher frequency harmonics are neglected.
3. Nonlinear characteristics are symmetric with respect to the origin.

There are also some advanced versions of describing functions, such as multi-harmonic describing functions, ignoring the low-pass filter properties, but these are the general assumptions used in this thesis.

The Describing Function Method solution is based on Fourier Expansion and the Harmonic Balancing Method. For example, for a harmonic input, describing function can be found by integrating the nonlinear forcing term, "n", which is the function of the harmonic input.

$$N = \frac{i}{\pi A}\int_0^{2\pi} n(Asin\psi)e^{i\psi}d\psi \tag{2.1}$$

Some describing function examples for common nonlinearities in structural dynamics are given below. Many others can be found with the integration above.

Table 2.1 Describing Function Representations of Common Nonlinearities [25]

Schematic representation	Nonlinearity type	Mathematical representation	Describing function representation
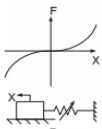	Cubic stiffness	$F_c = k_c X^3$	$N = \frac{3}{4} X^2$
	Quintic stiffness	$F_f = k_f X^5$	$N = \frac{5}{8} X^4$
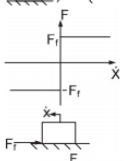	Coulomb friction	$F_c = F_f \operatorname{sign}(\dot{x})$	$N = \frac{4F_f}{\pi X}$
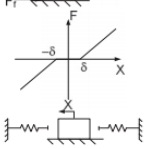	Backlash	If $x < \lvert\delta\rvert$ $F_k = 0$ If $x > \lvert\delta\rvert$ $F_k = kX$	$N = \frac{2}{\pi}\left(\arcsin\left(\frac{\delta}{X}\right) + \left(\frac{\delta}{X}\right)\sqrt{1-\left(\frac{\delta}{X}\right)^2}\right)$

2.2 Forced Harmonic Response Analysis of Nonlinear Structures Using Describing Functions

Tanrıkulu and his colleagues were the first ones to use the Describing Functions Method to find the forced harmonic response of a nonlinear system in a structural vibrations problem. They offer a semi-analytical quasi-linear solution for nonlinear equations of motion [24].

In this paper, the equation of motion of the MDOF nonlinear system is given below:

$$[M]\{\ddot{x}\} + [C]\{\dot{x}\} + [K]\{x\} + \{N\} = \{F\} \tag{2.2}$$

As can be seen, the classical equation of motion has an additional vector term. [M], [C], and [K] are mass, damping, and stiffness matrices. {F} is the external force, and vector {N} represents the internal nonlinear forces in the system. The k^{th} element of vector {N} can be expressed as a series.

$$N_k = \sum_{j=1}^{n} n_{kj} \tag{2.3}$$

n_{kj} is the nonlinear force term in the system, and it is acting between elements k and j (for the case k≠j) or between the ground and the element k (for the case k=j). Note that

$$n_{kj} = n_{jk}$$

Where n_{kj} can be any arbitrary nonlinear function of displacement and its time derivatives.

$$n_{kj} = n_{kj}(y_{kj}, \dot{y}_{kj}, \ddot{y}_{kj}, \dots)$$

Displacement is denoted by "y" instead of "x" because the nonlinear element can be between two coordinates or just attached to a simple coordinate.

$$y_{kj} = x_k - x_j \; for \; k \neq j$$

$$y_{kj} = x_k \; for \; k = j \tag{2.4a, b}$$

Assuming the force vector {F} is harmonic, the quasilinear representation of "n_{kj}", is the describing function "ν_{kj}" that can be found using the integral below. The below formula is the re-written form of Equation 2.1.

$$\nu_{kj} = \frac{i}{\pi Y_{kj}} \int_0^{2\pi} n_{kj} e^{i\omega t} d(\omega t) \tag{2.5}$$

With harmonic assumption, vector {N} can be written as combination of complex amplitude vector {G} along with its harmonic part.

$$\{N\} = \{G\} e^{i\omega t} \tag{2.6}$$

Notice that k^{th} element of vector {G} can be written as:

$$G_k = \sum_{j=1}^{n} \nu_{kj} Y_{kj} \tag{2.7}$$

Hence, {G} can be expressed as:

$$\{G\} = [\Delta]\{X\} \tag{2.8}$$

Where the nonlinearity matrix [Δ] contains describing function terms

$$\Delta_{kk} = \nu_{kk} + \sum_{j=1, j\neq k}^{n} \nu_{kj}$$

$$\Delta_{kj} = -\nu_{kj} \tag{2.9a, b}$$

When {G} term is used in {N}, and {N} term used in the equation of motion, equation of motion looks like below.

$$([K] - \omega^2[M] + i\omega[C] + [\Delta])\{X\} = \{F\} \tag{2.10}$$

Notice that the term between parentheses is similar to a receptance matrix. In the paper, it is referred as quasilinear receptance matrix, and it can be used to find nonlinear response.

$$[\theta] = ([K] - \omega^2[M] + i\omega[C] + [\Delta])^{-1} \tag{2.11}$$

However, the nonlinearity matrix [Δ] has {X} (displacement amplitude of degrees of freedom) terms in it, because describing functions are dependent on the {X} itself. Therefore, an iterative solution is needed, and it is a semi-analytic method. In addition to that, if the system is large, e.g., few thousands of degrees of freedom, the inverse of a very big matrix must be taken. For solution of large systems, the computational burden of this method becomes comparable to numerical solutions.

2.3 Closed Form Solutions of Weakly Nonlinear Multi-Degree of Freedom Systems with Single Nonlinear Element

The other paper that is significant to mention is the work of Özer [25] which provides a closed form solutions of weakly nonlinear multi degree of freedom systems with single nonlinear element. The term weak means that nonlinearity can be sufficiently expressed with a single harmonic solution. This method promises a direct analytical solution without any iteration, by using Sherman-Morrison matrix inversion.

Sherman-Morrison matrix inversion is a practical algebraic method to find the inverse of a matrix for special cases. If the matrix can be written as the summation of a matrix and product of two vectors, this formula can be used.

Sherman-Morrison formula is given below.

$$([A]^{-1} + \{u\}\{v\}^T)^{-1} = [A]^{-1} - \frac{[A]^{-1}\{u\}\{v\}^T[A]^{-1}}{1 + \{v\}^T[A]^{-1}\{u\}} \tag{2.12}$$

The figure shown below illustrates a system featuring a single nonlinear element. The system has n-degrees of freedom. It will be assumed that the nonlinear element is positioned between the $(k-1)^{th}$ and k^{th} degrees of freedom. The external force applied to the system can be exerted on one or more of its degrees of freedom.

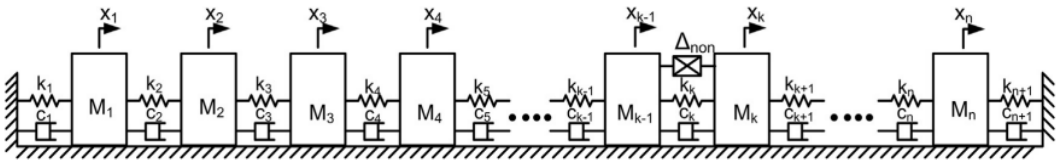

Figure 2.2 An Example of Weakly Nonlinear n-Degree-of-Freedom System with the Nonlinear Component Between $(k-1)^{th}$ and k^{th} Elements

From previous paper's work, the nonlinear response is found as multiplication of quasilinear receptance and external force. If linear equation of motion matrices of the left hand side is grouped under the impedance matrix [Z], nonlinear displacement can be written as below:

$$\{X_{NL}\} = ([Z] + [\Delta])^{-1}\{F\} \tag{2.13}$$

where,

$$[Z] = [K] - \omega^2[M] + i\omega[C] \tag{2.14}$$

For an n-DOF system case, the nonlinearity matrix becomes:

$$[\Delta] = \begin{bmatrix} 0 & 0 & \cdots & \cdots & 0 & 0 \\ \vdots & \ddots & \vdots & \vdots & \vdots & \vdots \\ 0 & \cdots & \nu & -\nu & \cdots & 0 \\ 0 & \cdots & -\nu & \nu & \cdots & 0 \\ \vdots & \vdots & \vdots & \vdots & \ddots & \vdots \\ 0 & 0 & \cdots & \cdots & 0 & 0 \end{bmatrix}$$

Notice that this matrix can also be written as below:

$$[\Delta] = \begin{bmatrix} 0 \\ \vdots \\ \nu \\ -\nu \\ \vdots \\ 0 \end{bmatrix} \begin{bmatrix} 0 \\ \vdots \\ 1 \\ -1 \\ \vdots \\ 0 \end{bmatrix}^T \tag{2.15}$$

Hence, Sherman-Morrison matrix inversion can be applied here.

$$\{X_{NL}\} = \left([Z] + \begin{bmatrix} 0 \\ \vdots \\ \nu \\ -\nu \\ \vdots \\ 0 \end{bmatrix} \begin{bmatrix} 0 \\ \vdots \\ 1 \\ -1 \\ \vdots \\ 0 \end{bmatrix}^T \right)^{-1} \{F\}$$

$$\{X_{NL}\} = \{X_L\} - \frac{[\alpha]\begin{bmatrix} 0 \\ \vdots \\ \nu \\ -\nu \\ \vdots \\ 0 \end{bmatrix}\left(X_{L(k-1)} - X_{L(k)}\right)}{1 + \begin{bmatrix} 0 \\ \vdots \\ 1 \\ -1 \\ \vdots \\ 0 \end{bmatrix}^T [\alpha]\begin{bmatrix} 0 \\ \vdots \\ \nu \\ -\nu \\ \vdots \\ 0 \end{bmatrix}} \tag{2.16}$$

Where [α] is the receptance of the linear system, which is inverse of the impedance matrix.

$$[\alpha] = [Z]^{-1} \tag{2.17}$$

When matrix multiplications are done and nonlinear response $X_{NL(k)}$ is subtracted from $X_{NL(k-1)}$ the below expression is obtained.

$$X_{NL(k-1)} - X_{NL(k)} = \frac{X_{L(k-1)} - X_{L(k)}}{1 + \upsilon\alpha_{NLC}} \tag{2.18}$$

Where α_{NLC} is the combination of terms in the linear receptance matrix

$$\alpha_{NLC} = \alpha_{(k-1)(k-1)} - \alpha_{(k-1)(k)} - \alpha_{(k)(k-1)} + \alpha_{(k)(k)} \tag{2.19}$$

Eq (2.18) in amplitude form can be expressed below

$$\left|X_{L(k-1)} - X_{L(k)}\right| = |1 + \upsilon\alpha_{NLC}|\left|X_{NL(k-1)} - X_{NL(k)}\right| \tag{2.20}$$

Notice that this nonlinear difference term is also in the describing function terms. Hence this equation is a polynomial, and the roots of this polynomial can be placed into describing function and nonlinear response of the whole system can be found. With this approach, no iterative solution is needed, and computational work is much less as the system becomes larger. Moreover, the nonlinear response equation is separated into linear terms and nonlinear terms.

2.4 Tuned Vibration Absorber for Weakly Nonlinear Systems

In summary, the idea behind this study lies in the papers discussed in this chapter. In the case of vibration absorbers, Özer's work is very useful, because linear response and receptance are theoretically known, or at least it can be measured. Computational work is significantly less than the numerical approaches for finding system response, and it can be implemented into multi degree of freedom systems easily.

CHAPTER 3

HARMONIC RESPONSE ANALYSIS OF NONLINEAR SYSTEMS WITH LINEAR VIBRATION ABSORBER

In this chapter, the implementation of a tuned vibration absorber on a nonlinear system and harmonic response analysis of the total system will be explained in detail. Section 3.1 will focus on a tuned vibration absorber attached to a single-degree-of-freedom nonlinear system. Various cases are examined under subsections of this chapter in order to find analytical relations to tune the absorbers similar to Den Hartog's method and to understand the system dynamics on a larger scale, i.e., multi-degree-of-freedom systems. Section 3.2 will explore the tuned vibration absorbers attached to multi-degree-of-freedom systems with a nonlinear component. Some numerical optimization approaches will be proposed to find the optimum response amplitude.

3.1 Tuned Vibration Absorber Attached on A Single Degree of Freedom Nonlinear System

In this section, a nonlinear system is assumed to be modeled as a single-degree-of-freedom system, and a tuned vibration absorber is attached in order to reduce the response amplitudes, just like Den Hartog did in his studies. For nonlinearity, cubic stiffness is assumed because it is a widely encountered type of polynomial nonlinearity, and it is simple enough to obtain analytical relations.

After the Sherman-Morrison application, the amplitude of the complex response is obtained as follows:

$$\left|X_{NL,(k-1)} - X_{NL,(k)}\right|\left|1 + \nu\alpha_{NLC}\right| = \left|X_{L,(k-1)} - X_{L,(k)}\right| \tag{3.1}$$

For cubic stiffness,

$$\nu = \frac{3}{4} k_c \left| X_{NL,(k-1)} - X_{NL,(k)} \right|^2 \tag{3.2}$$

Eqn. (3.1) becomes,

$$\frac{9}{16} k_c^2 |\alpha_{NLC}|^2 t^3 + \frac{3}{2} k_c Re(\alpha_{NLC}) t^2 + t - \left| X_{L,(k-1)} - X_{L,(k)} \right|^2 = 0 \tag{3.3}$$

Where

$$t = \left| X_{NL,(k-1)} - X_{NL,(k)} \right|^2 \tag{3.4}$$

$$\alpha_{NLC} = \alpha_{(k-1),(k-1)} + \alpha_{(k),(k)} - \alpha_{(k-1),(k)} - \alpha_{(k),(k-1)} \tag{3.5}$$

Discriminant of the third-degree polynomial equation

$$\Delta = 18abcd - 4b^3 d + b^2 c^2 - 4ac^3 - 27a^2 d^2 \tag{3.6}$$

Where

$$a = \frac{9}{16} k_c^2 |\alpha_{NLC}|^2, \qquad b = \frac{3}{2} k_c Re(\alpha_{NLC}), \qquad c = 1,$$
$$d = -\left| X_{L,(k-1)} - X_{L,(k)} \right|^2 \tag{3.7}$$

If the discriminant is greater than zero, then there are three distinct real solutions; on the other hand, if the discriminant is smaller than zero, then the solution consists of one real solution and a complex conjugate pair. The points where the discriminant is zero are the exact points where the jump phenomenon occurs. The interval where the discriminant is positive corresponds to the region of multi-valued response, where the response changes depending on approaching from lower or upper frequencies.

A typical single-degree-of-freedom mass-spring-damper system is shown in the figure below. Spring is assumed to have a cubic stiffness behavior.

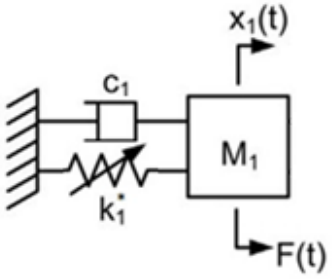

Figure 3.1 The System Model of a Single-Degree-of-Freedom System with Cubic Stiffness

Since the nonlinearity is between the ground and the mass for a SDOF system, α_{NLC} becomes simply the receptance of the linear system.

$$\alpha_{NLC} = \frac{1}{k_1 - \omega^2 m_1 + i\omega c_1} \tag{3.8}$$

Similarly, linear displacement term becomes:

$$\left|X_{L,1}\right| = F|\alpha_{NLC}| \tag{3.9}$$

Hence, Equation 3.3 becomes:

$$\frac{9}{16}k_c^2|\alpha_{NLC}|^2 t^3 + \frac{3}{2}k_c Re(\alpha_{NLC})t^2 + t - F|\alpha_{NLC}|^2 = 0 \tag{3.10}$$

where,

$$t = \left|X_{NL,1}\right|^2 \tag{3.11}$$

By using Equation 3.10, the response of the system with varying frequency graph looks like the figure below for a system parameter set.

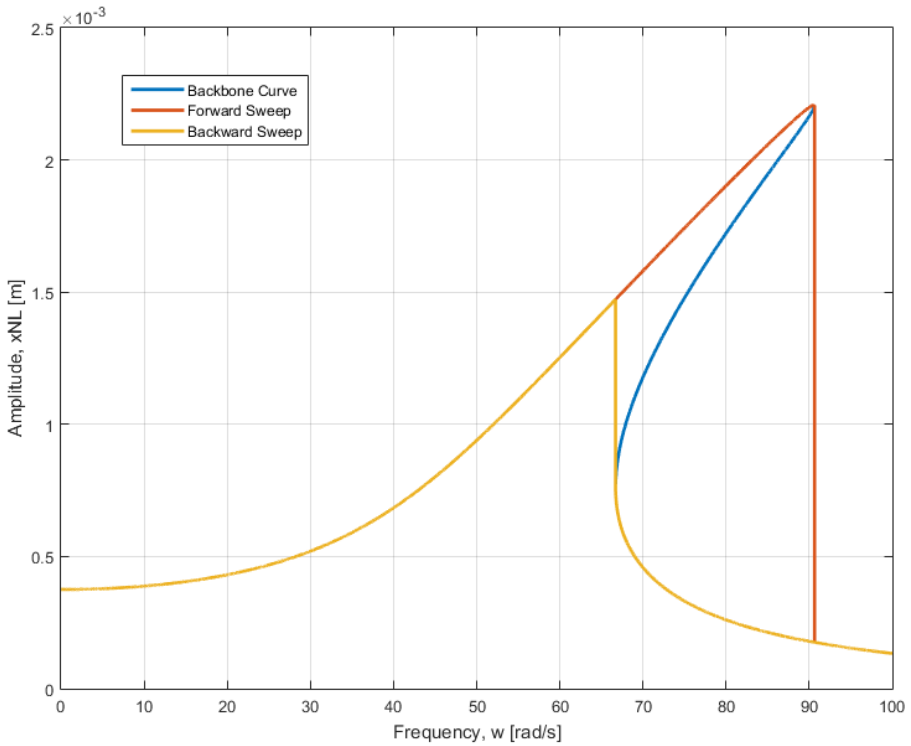

Figure 3.2 An Example of Frequency vs Amplitude Graph of a SDOF System Found with Describing Function Method

Parameters are chosen as $m_1 = 1\ kg, k_1 = 2500\frac{N}{m}, c_1 = 5\frac{Ns}{m}, k_c = 7.8 * 10^8\frac{N}{m^3}, F = 1\ N.$

The linear system graph would be a single peak around $\sqrt{\frac{k_1}{m_1}} = 50\ rad/s$ since it is a lightly damped system. Instead, there is a region of nonlinearity between 66.7 rad/s and 90.6 rad/s since the nonlinearity effect is highly dominant.

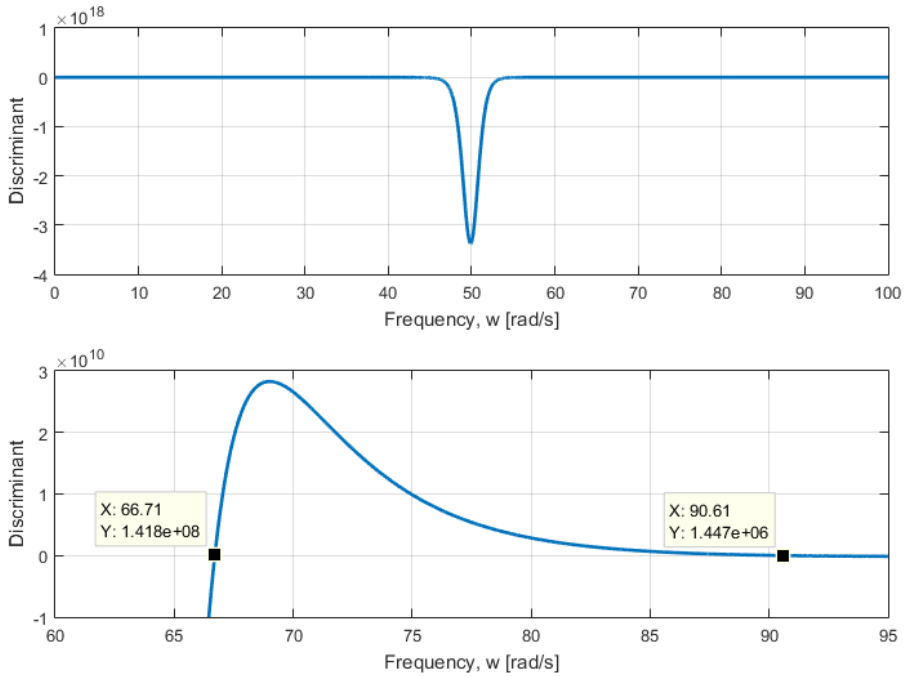

Figure 3.3 Frequency vs Discriminant Graph for the Example SDOF System

The discriminant is negative for frequencies under 66.7 rad/s and over 90.6 rad/s and the real root of the main equation gives the nonlinear displacement. Between these frequencies, the discriminant is positive, and Equation 3.9 returns three distinct roots for nonlinear displacement. The responses can be seen in three different colors in this frequency range in Figure 3.2.

The red plot is the forward sweep. This is the response when the frequency is increasing from lower frequencies to 90.6 rad/s. At 90.6 rad/s there is a jump-down behavior.

The yellow plot is backward sweep. This is the response when the frequency is decreasing from higher frequencies to 66.7 rad/s. At 66.7 rad/s there is a jump-up behavior.

The blue plot shows the third solution. The curve shows that there is a hardening spring present in the system. While nonlinear system responses traditionally shown

with this curve, this root does not correspond to a physical system response, i.e. the system does not vibrate at this amplitude.

When a vibration absorber is attached, the new system becomes a two-degree-of-freedom system.

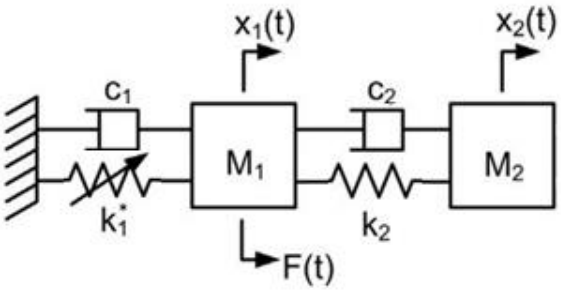

Figure 3.4 The 2-DOF System Model of a Tuned Vibration Absorber Attached to the Main System

When nonlinearity is between the ground and the first mass, α_{NLC} is equal to $\alpha_{1,1}$ of the linear receptance matrix of a 2-DOF system.

$$\alpha_{NLC} = \alpha_{1,1} = \frac{k_2 - \omega^2 m_2 + i\omega c_2}{\begin{matrix} m_1 m_2 \omega^4 - (k_1 k_2 + k_2 m_1 + k_2 m_2 + c_1 c_2)\omega^2 + k_1 k_2 \\ +i\omega[c_1 k_2 + c_2 k_1 - \omega^2 (c_1 m_2 + c_2 m_1 + c_2 m_2)] \end{matrix}} \qquad (3.12)$$

If the TVA parameters are selected as in Den Hartog's method, for a mass of $m_2 = 0.1\ kg, k_2 = 350\frac{N}{m}, c_2 = 0.1\frac{Ns}{m}$ the response of the system is given below.

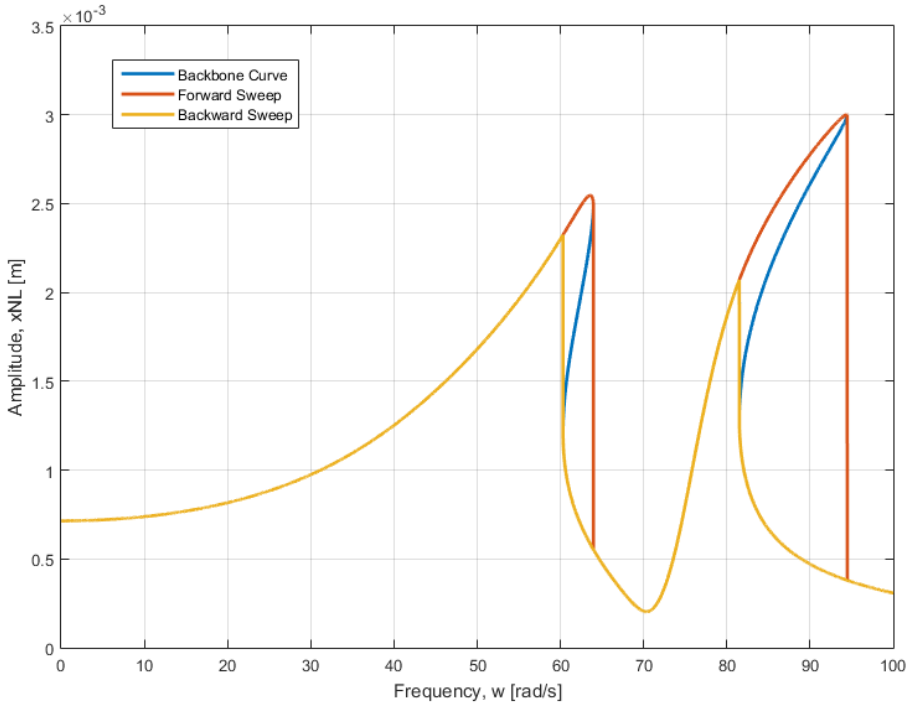

Figure 3.5 The Frequency vs Amplitude Graphs for the First TVA Parameter Set

Now that there are two masses in the system, there might be two different regions of nonlinearity. Moreover, there are two peaks that are not smaller than SDOF case. Only positive outcome is a local vibration reduction around 70 rad/s.

If the TVA parameters are selected as in Den Hartog's method, for a mass of $m_2 = 0.1\ kg$, the stiffness and damping become $k_2 = 207\frac{N}{m}, c_2 = 1.6\frac{Ns}{m}$ the response of the system is given below.

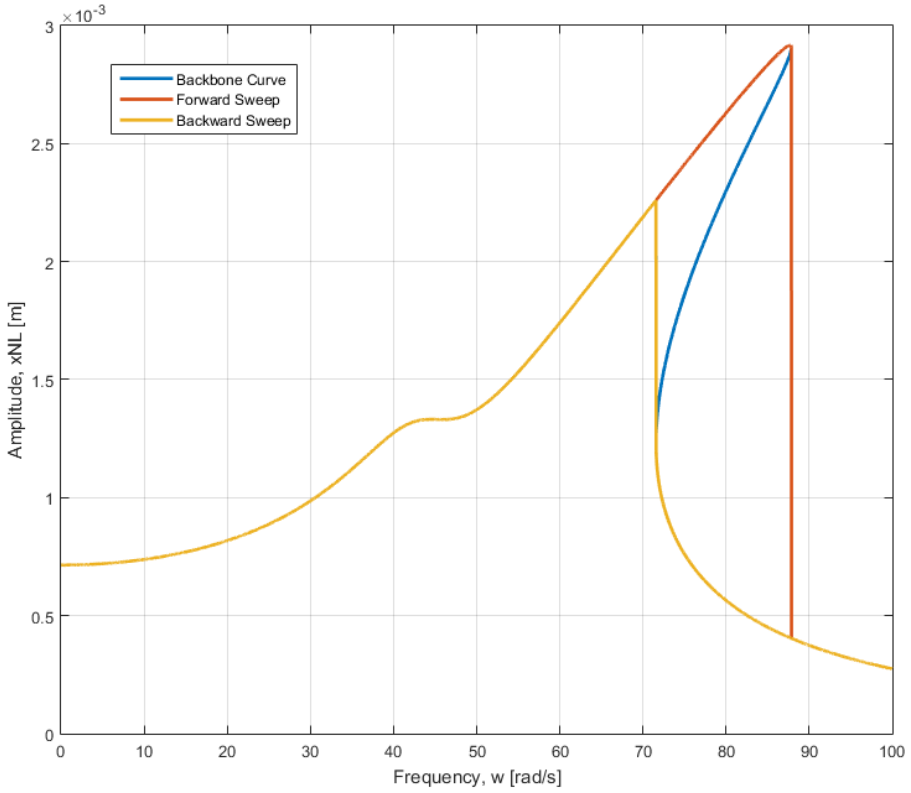

Figure 3.6 The Frequency vs Amplitude Graphs for the Second TVA Parameter Set

Selecting Den Hartog parameters helped remove the first multi-valued region, but the second one is even bigger than the SDOF case. In this particular case, using TVA that is tuned with respect to Den Hartog yields worse results than the system without a TVA. Hence, having a dominant cubic stiffness element in the system makes the Den Hartog tuning equations invalid.

If the TVA parameters are selected as $m_2 = 0.1\,kg, k_2 = 250\frac{N}{m}, c_2 = 2\frac{N}{ms}$ the response of the system is given below.

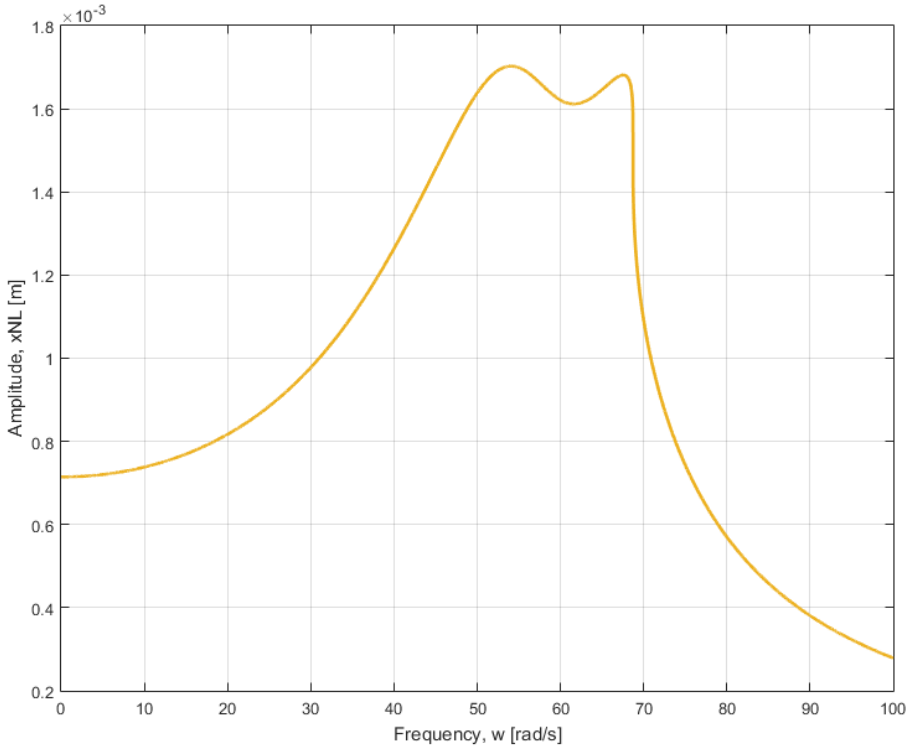

Figure 3.7 The Frequency vs Amplitude Graphs for the Third TVA Parameter Set

In this case, the overall vibration amplitudes are reduced, and the multi-valued regions are gone. By choosing the correct parameters, i.e. by optimally tuning the vibration absorber, a similar equally-peaked response graph can be achieved.

Another important point to consider is to implement the method to a variety of systems, from small MEMS systems to large buildings, or whether using SI or imperial units, bringing the equation into non-dimensional form is necessary.

Non-dimensional parameters on linear mass-spring-damper systems with TVA attached are traditionally taken as below.

$$\zeta_1 = \frac{c_1}{2m_1\sqrt{k_1/m_1}},\ \zeta_2 = \frac{c_2}{2m_2\sqrt{k_2/m_2}},\ \mu = \frac{m_2}{m_1},\ \omega_r = \sqrt{\frac{k_2/m_2}{k_1/m_1}}$$

ζ_1 and ζ_2 are the damping ratios, μ is the mass ratio and ω_r is the frequency ratio.

With these changes, and taking non-dimensional frequency as $\Omega = \frac{\omega}{\sqrt{k_1/m_1}}$, normalized α_{NLC} becomes:

$$\alpha_{NLC} = \frac{\omega_r^2 - \Omega^2 + i2\Omega\zeta_2\omega_r}{\Omega^4 - [1 + \omega_r^2(\mu+1) + 4\zeta_1\zeta_2\omega_r]\Omega^2 + \omega_r^2 + i2\Omega\left[\zeta_1\omega_r^2 + \zeta_2\omega_r - \Omega^2\left(\zeta_1 + \zeta_2\omega_r(\mu+1)\right)\right]} \tag{3.13}$$

where,

$$\alpha_{NLC,normalized} = k_1\alpha_{NLC,unnormalized}$$

To avoid confusion and to keep the equations organized, $\alpha_{NLC,normalized}$ and $\alpha_{NLC,unnormalized}$ denotations will not be used. After this point in the thesis, α_{NLC} always refers to non-dimensional formula.

Compared to linear systems, there is another parameter γ, which contains the cubic stiffness term in it. Note that, all the terms in γ belong to the main system constants and the amplitude of external forcing.

$$\gamma = \frac{k_c F^2}{k_1^3}$$

Hence, rewriting the Equation 3.10 with normalized terms

$$\frac{9}{16}\gamma^2|\alpha_{NLC}|^2T^3 + \frac{3}{2}\gamma Re(\alpha_{NLC})T^2 + T - |\alpha_{NLC}|^2 = 0 \tag{3.14}$$

where,

$$T = \frac{t}{\left(\frac{F}{k_1}\right)^2} = \frac{\left|X_{NL,1}\right|^2}{\left(\frac{F}{k_1}\right)^2} \tag{3.15}$$

Previous SDOF example with parameter set with $m_1 = 1\,kg, k_1 = 2500\frac{N}{m}, c_1 = 5\frac{Ns}{m}, k_c = 7.8 * 10^8\frac{N}{m^3}$, $F = 1\,N$, now becomes $m_1 = 1\,kg,\ \gamma = 0.2, \zeta_1 = 0.05$

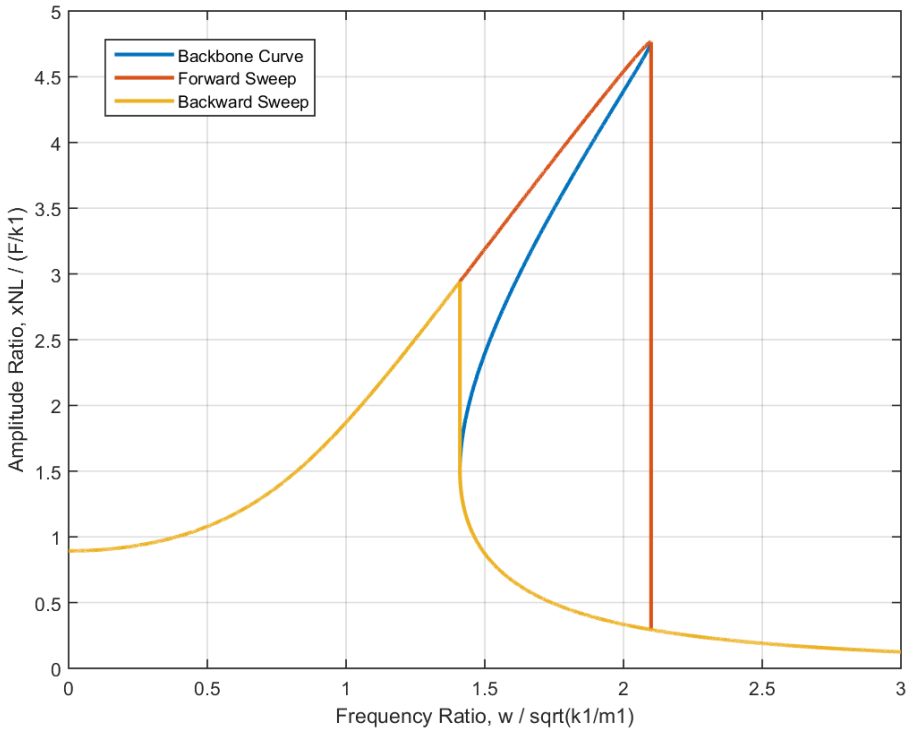

Figure 3.8 Non-Dimensional Version of the Graph in Figure 3.2

Similarly, TVA parameters become $\mu = 0.1, \omega_r = 1.414, \zeta_2 = 0.0283$ for the first example and $\mu = 0.1, \omega_r = 1.158, \zeta_2 = 0.2$ for the third example.

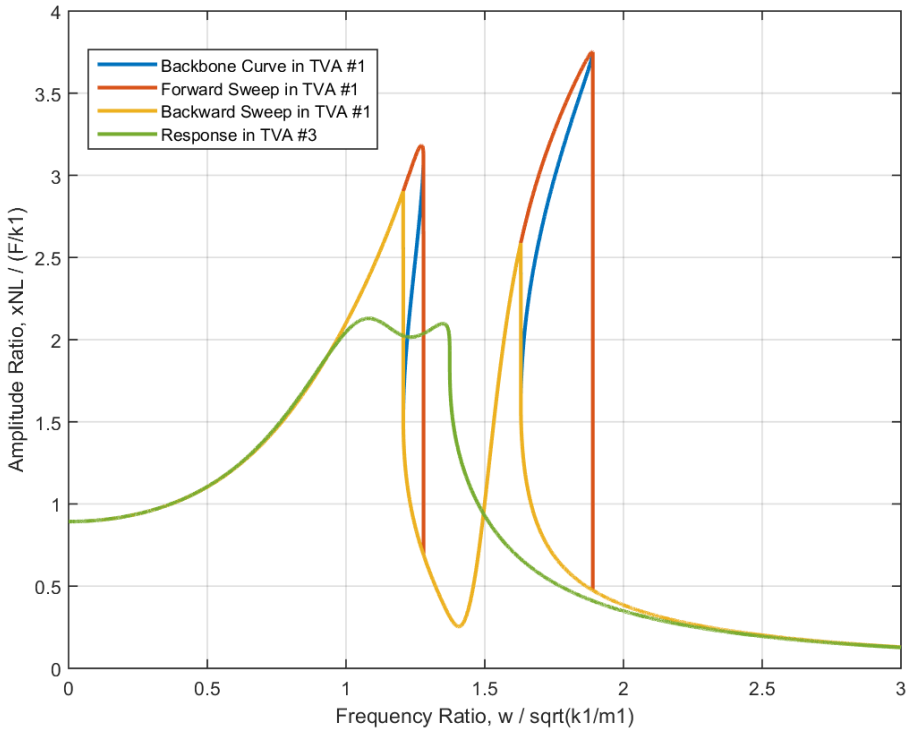

Figure 3.9 Non-Dimensional Version of the Graph in Figure 3.4 and Figure 3.5

When the parameters are selected properly, it is possible to reduce the vibrations at a local point or on a broadband range. The details on tuning the vibration absorber according to the need are given in the upcoming sections of the study.

3.1.1 Undamped System with Cubic Stiffness

At the start of the investigation, an undamped main system and an undamped absorber are assumed. This case significantly simplifies the main equations because no damping means no complex numbers in receptance and linear displacement terms.

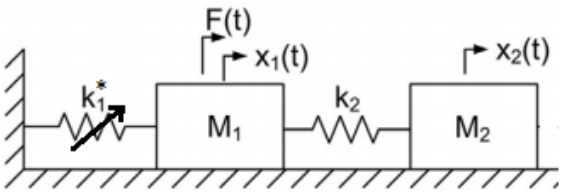

Figure 3.10 The 2-DOF Undamped System Model with Cubic Stiffness Between First Mass and the Ground

With zero damping ratios, α_{NLC} term is also simplified.

$$\alpha_{NLC} = \frac{\omega_r^2 - \Omega^2}{\Omega^4 - [1 + \omega_r^2(\mu + 1)]\Omega^2 + \omega_r^2} \tag{3.16}$$

Considering the simplification mentioned above, Equation 3.14 becomes,

$$\frac{9}{16}\gamma^2 {\alpha_{NLC}}^2 T^3 + \frac{3}{2}\gamma \alpha_{NLC} T^2 + T - {\alpha_{NLC}}^2 = 0 \tag{3.17}$$

Where,

$$T = \frac{\left|X_{NL,1}\right|^2}{\left(\frac{F}{k_1}\right)^2} \tag{3.18}$$

Discriminant of the above equation in (3.17) can be simplified as:

$$\Delta = {\alpha_{NLC}}^5 \left(\frac{27\gamma^3}{16} - \frac{2187\gamma^4}{256}{\alpha_{NLC}}^3\right) \tag{3.18}$$

Investigating $\Delta = 0$ to find jump locations,

$${\alpha_{NLC}}^3 = -\frac{16}{81\gamma} \; and \; {\alpha_{NLC}}^5 = 0 \tag{3.20a, b}$$

The above equations give the jump frequencies. For the sake of simplicity,

$$\gamma_u = \frac{81\gamma}{16} \tag{3.21}$$

Hence, the jump frequencies are found as:

$$\Omega_1 = \sqrt{\frac{1}{2}[\gamma_u + \omega_r^2(\mu+1) + 1 - \sqrt{(\gamma_u + \omega_r^2(\mu+1)+1)^2 - 4\omega_r^2(\gamma_u+1)}]}$$

$$\Omega_2 = \omega_r$$

$$\Omega_3 = \sqrt{\frac{1}{2}[\gamma_u + \omega_r^2(\mu+1) + 1 + \sqrt{(\gamma_u + \omega_r^2(\mu+1)+1)^2 - 4\omega_r^2(\gamma_u+1)}]}$$

$$(3.22a, b, c)$$

Ω_1 and Ω_3 are found from Eqn. 3.20a and Ω_2 comes from the numerator in α_{NLC} (i.e. Eqn. 3.20b).

While Ω_1 and Ω_3 depends on the excitation force, Ω_2 is independent of it. At this frequency, α_{NLC} and consequently the response becomes zero.

Between Ω_1 and Ω_2 is the first nonlinear region. Note that there is no fourth frequency for zero discriminant. This means there is no limit for second nonlinear region, i.e. it is between Ω_3 and infinity.

For Ω_1 and Ω_3, local peaks can be found from third-degree polynomial with zero discriminant solution.

The roots of a cubic equation with zero discriminant can be found with the equations below. Since $b^2 - 3ac \neq 0$, at zero discriminant frequency Eqn. 3.17 has a double root and a single root.

$$T_{double} = \frac{9ad - bc}{2(b^2 - 3ac)}$$

$$T_{single} = \frac{4abc - 9a^2d - b^3}{a(b^2 - 3ac)} \qquad (3.23a, b)$$

Where a, b, c, and d are the coefficients of the main equation used in the discriminant equation in Equation 3.6.

Single root equation gives the displacement at jump-up frequencies. Double root equation gives a result, but it does not correspond to physical value on the frequency response. The displacement at jump-down frequency is zero for a completely undamped system, but also it is the peak point of the system, so the displacement is also infinite for a backward sweep.

$$T = \frac{4abc - 9a^2d - b^3}{a(b^2 - 3ac)} = 9{\alpha_{NLC}}^2 \tag{3.24}$$

Note that α_{NLC} is constant for Ω_1 and Ω_3 frequencies (in Equation 3.20a), hence T is same for both frequencies.

If only the displacement of main system mass is in the scope of interest, finding T value is enough with Equation 3.18, but the displacement of the TVA, $X_{NL,2}$ can also be found from the equation derived from Sherman-Morrison.

$$\left|X_{NL,1}\right| = \sqrt{T\left(\frac{F}{k_1}\right)^2} = |3\alpha_{NLC}|\left(\frac{F}{k_1}\right) = 3\left|X_{L,1}\right| \; at \; \Omega_1 \text{ and } \Omega_3 \tag{3.25}$$

$$\frac{\left|X_{NL,1}\right|}{\frac{F}{k_1}} = \sqrt[3]{\frac{16}{3\gamma}} \; at \; \Omega_1 \text{ and } \Omega_3 \tag{3.26}$$

Let $\gamma = 0.5, \mu = 0.1, \omega_r = 2.0, \zeta_1 = \zeta_2 = 0$. Before the TVA is attached, the response graph is below.

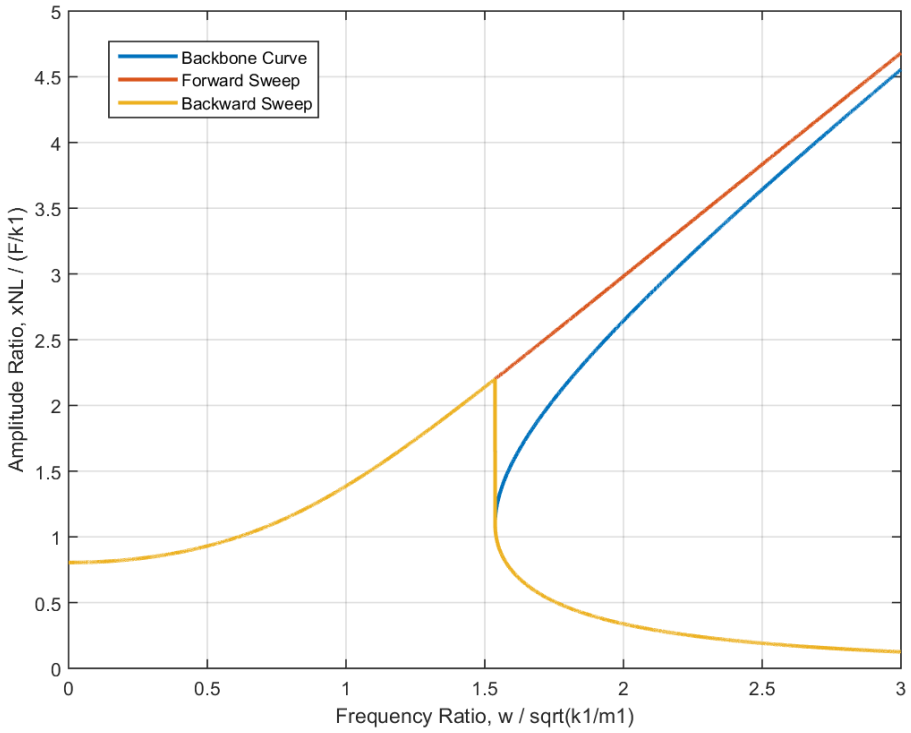

Figure 3.11 The Frequency vs Amplitude Graphs for the SDOF System with Parameters $\gamma = 0.5, \zeta_1 = 0$

The jump frequencies become $\Omega_1 = 1.405, \Omega_2 = 2.0, \Omega_3 = 2.188$ and the non-dimensional amplitude at Ω_1 and Ω_3 becomes $\frac{|X_{NL,1}|}{\frac{F}{k_1}} = 2.201$.

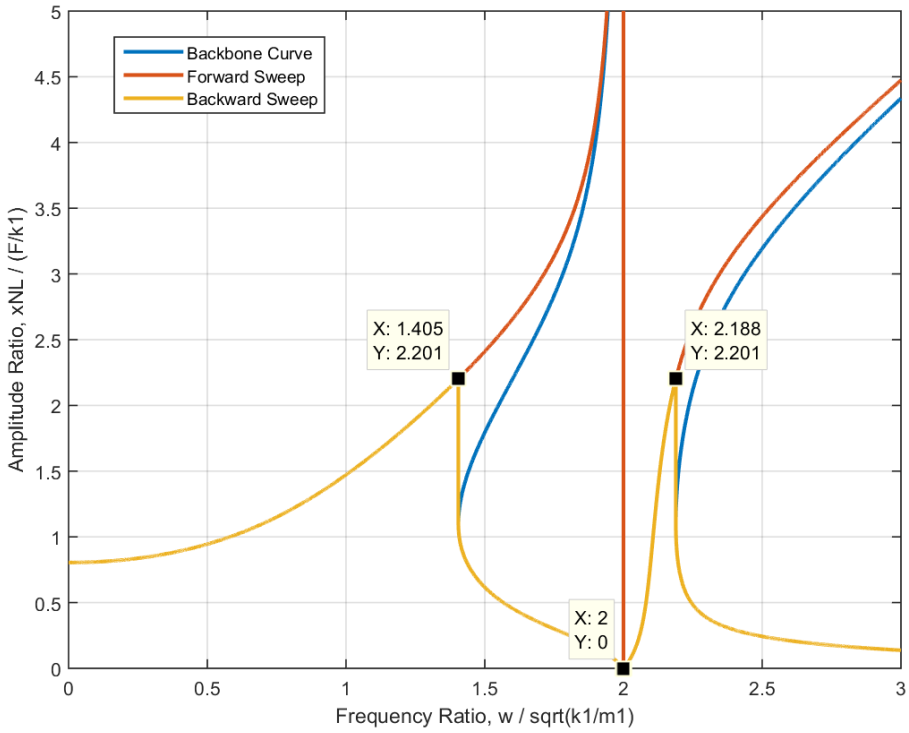

Figure 3.12 The Frequency vs Amplitude Graphs with Jump Frequencies for the 2-DOF System with Parameters $\gamma = 0.5, \mu = 0.1, \omega_r = 2.0, \zeta_1 = \zeta_2 = 0$

As Equation 3.25 demonstrates, nonlinear displacement is directly proportional to linear displacement at jump frequencies. More precisely, it is three times bigger. At Ω_2, α_{NLC} and the response become zero, meaning the linear and nonlinear displacements are both equal to zero.

Without damping added, there is not much that can be done in terms of reducing vibration and removing the regions of nonlinearity. As Equation 3.26 demonstrates, nonlinear displacement at jump frequencies is only dependent on main system's linear spring and cubic stiffness constants, and excitation force, which are assumed to be as main system properties and cannot be changed. However, there is a way to use these equations to obtain a vibration absorber that works for a range of frequencies. The displacement becomes zero around the frequency Ω_2 for the

undamped case. Since this point can be found analytically, it is possible to use the same equations on some damped systems for an approximate solution. This idea will be analyzed in the next section.

3.1.2 Damped Main System with an Undamped TVA

Assume that the main system has damping, but the vibration absorber is assumed to be undamped.

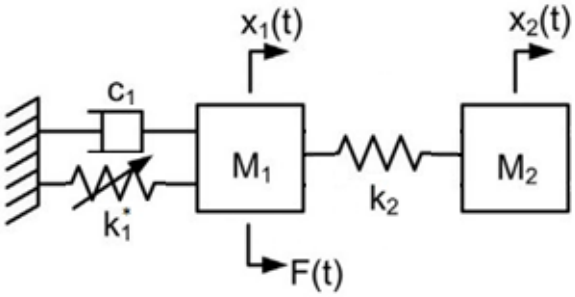

Figure 3.13 The 2-DOF System Model with Damped Main System with Cubic Stiffness and Undamped TVA

When selecting $\zeta_2 = 0$ in Equation 3.13, α_{NLC} term simplifies as:

$$\alpha_{NLC} = \frac{\omega_r^2 - \Omega^2}{\Omega^4 - [1 + \omega_r^2(\mu + 1)]\Omega^2 + \omega_r^2 + i2\Omega\zeta_1(\omega_r^2 - \Omega^2)} \tag{3.27}$$

The difference between α_{NLC} terms in undamped system case and damped main system + undamped TVA case is the complex term in the denominator. Note that, numerators of both terms are equal, and $\Omega = \omega_r$ makes $\alpha_{NLC} = 0$ in both cases.

Let $\gamma = 0.5, \mu = 0.1, \omega_r = 2.0, \zeta_2 = 0$ like before, but also $\zeta_1 = 0.1$

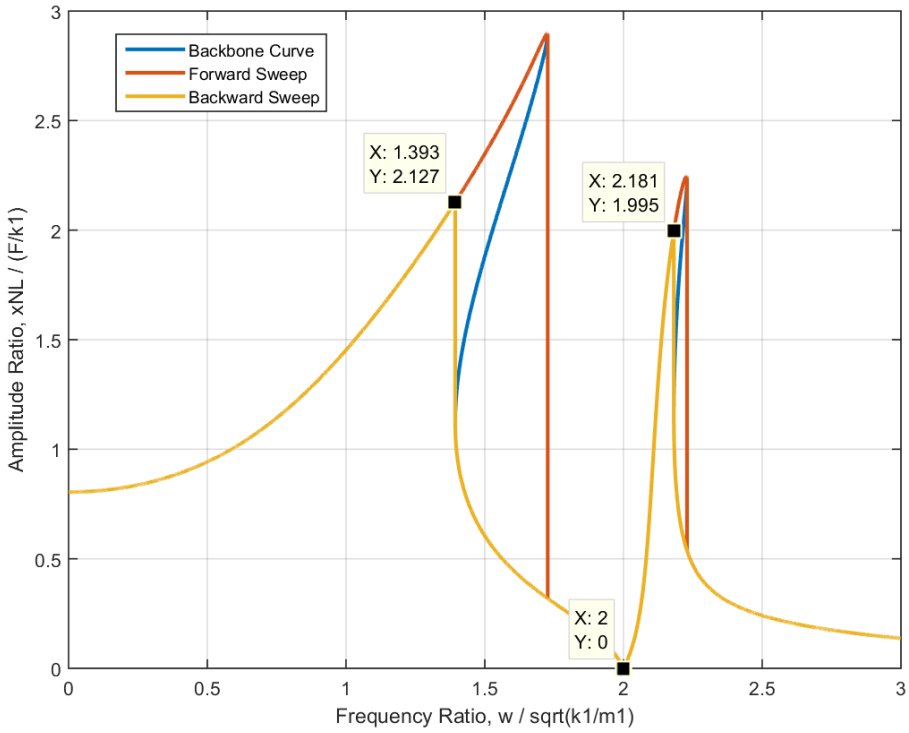

Figure 3.14 The Frequency vs Amplitude Graphs with Jump Frequencies for the 2-DOF System with Parameters $\gamma = 0.5, \mu = 0.1, \omega_r = 2.0, \zeta_1 = 0.1, \zeta_2 = 0$

$\Omega = \omega_r = 2$ still returns zero amplitude as expected. Jump-down frequencies and their corresponding response amplitudes are still close to the undamped case, especially the first one.

The response of the system is also found with the time domain solution at the frequency $\Omega = \omega_r = 2$. After the few steps at the initial transient state, the system response becomes zero at the steady state, as shown in Figure 3.15.

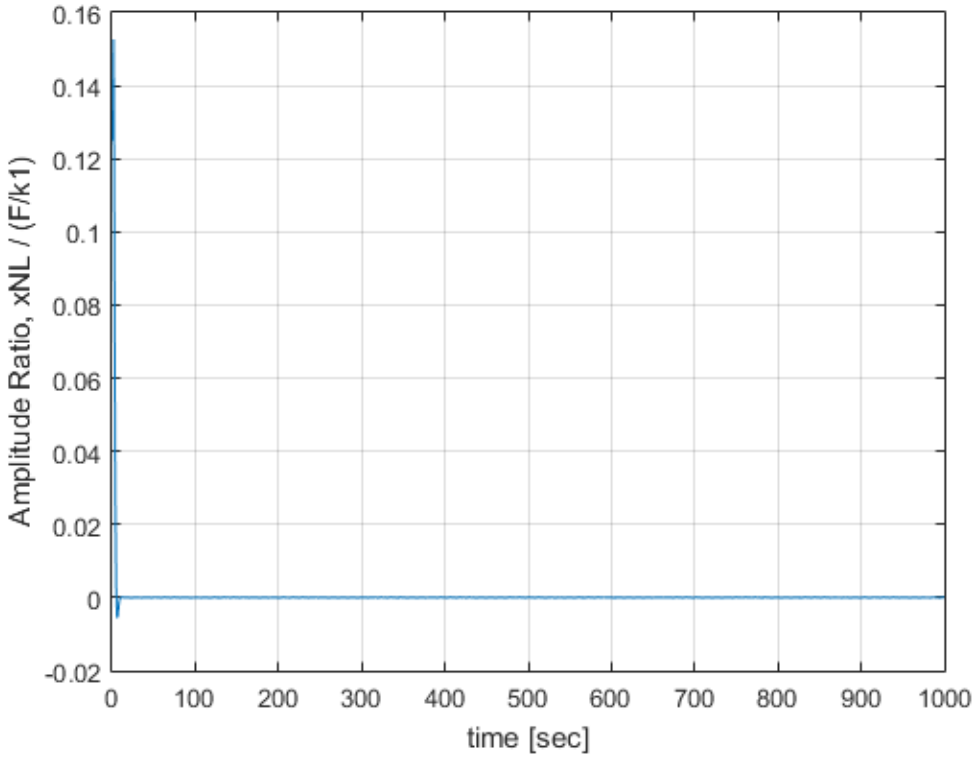

Figure 3.15 The Time Domain Solution for the 2-DOF System with Parameters $\gamma = 0.5, \mu = 0.1, \omega_r = 2.0, \zeta_1 = 0.1, \zeta_2 = 0$ at the Frequency Ratio $\Omega = \omega_r = 2$

Hence, it is guaranteed that there will be no jump behavior around the frequency Ω_2. This might be useful for a device working at a frequency around Ω_2, or a device working at a frequency bandwidth between Ω_2 and Ω_3, where the frequencies and the amplitudes are known approximately. There is also a safe area between the jump-down frequency and Ω_2 as well. Although there is no easy formulation to obtain jump-down frequency, it can be found numerically with the equations provided in this study.

The effect of other parameters on the jump-down frequency and the effective bandwidth of the absorbers will be analyzed in detail with case studies in Chapter 4.

3.1.3 Undamped Main System with a Damped TVA

Similar to Den Hartog's work, the main system is assumed to be undamped, while a damped TVA is attached. It is possible to observe the invariant points in the nonlinear case as well, which are the points that are not dependent on the damping of the TVA, ζ_2.

The frequency vs amplitude graphs are given for a set of parameters in the figure below. Notice that the curves still pass through the invariant points even though there is a multi-valued region present (e.g. the green curves).

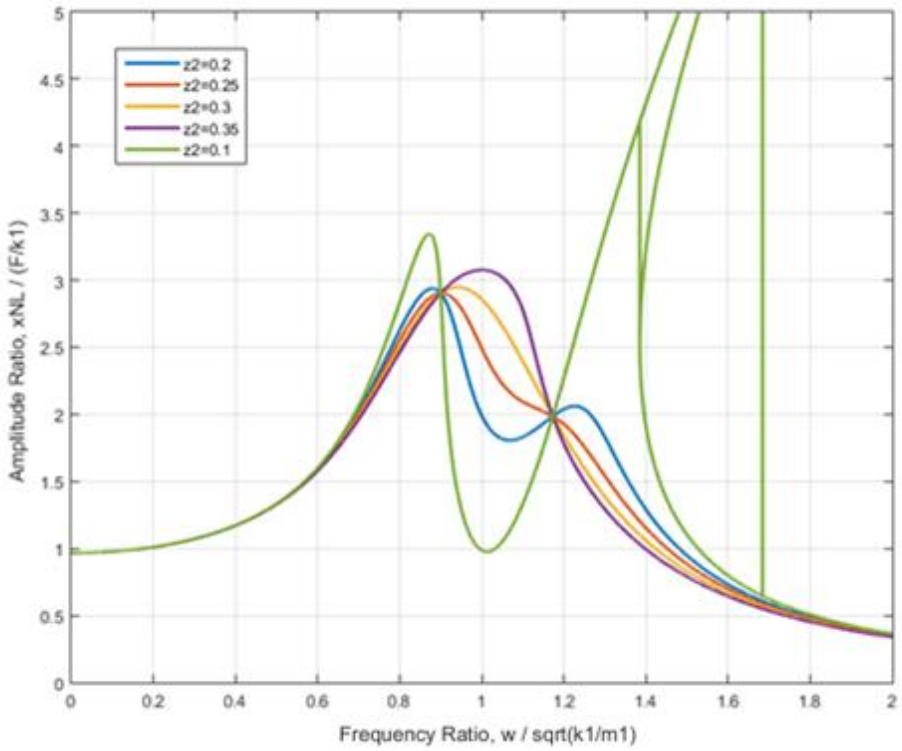

Figure 3.16 The Frequency vs Amplitude Graphs with varying ζ_2

In this case, α_{NLC} becomes the exact same expression in the Den Hartog's work since it is a linear response expression. Hence, invariant points of α_{NLC} is known. However, linear and nonlinear systems do not yield the same invariant points. The invariant points for both cases occur at different frequencies.

The invariant points of α_{NLC} and $X_{NL,1}$ for two sets of parameters can be seen in the figure below. All the parameters except ζ_2 are chosen the same for the two sets of parameters.

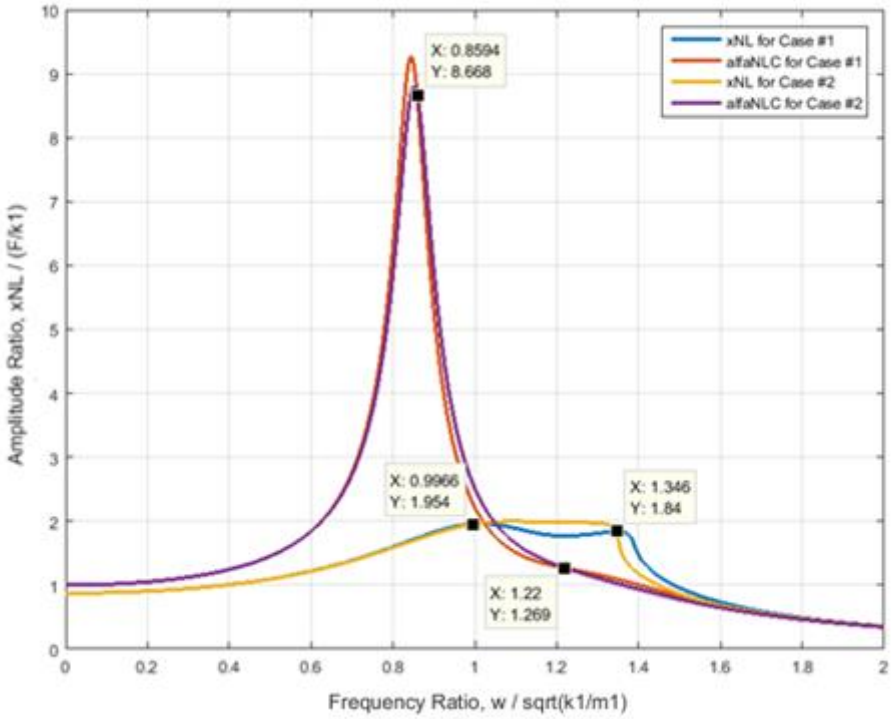

Figure 3.17 The Invariant Points of α_{NLC} and $X_{NL,1}$

No analytical solution is found to obtain the invariant points on the nonlinear response curves. Numerical methods are always useful if it is desired to find the frequency of these points. Then, they can be used for an optimization method similar to Den Hartog's.

3.1.4 Damped System with Cubic Stiffness

To obtain a more realistic case, damping is added to both the main system and the absorber. Since nonlinearity is between the mass and the ground, Equation 3.9 still

holds. As a drawback, the main equation becomes complicated to obtain simple analytical relations.

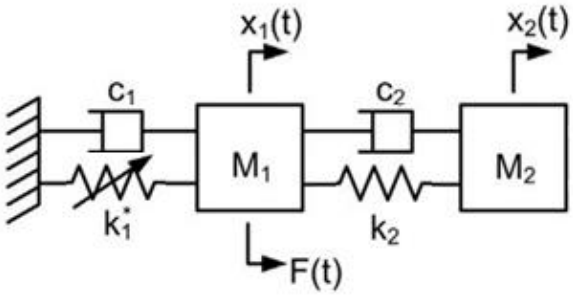

Figure 3.18 The 2-DOF Damped System Model with Cubic Stiffness Between First Mass and the Ground

The main equation and α_{NLC} terms were investigated under Section 3.1 and found in Equations 3.13 and 3.14

By using these equations, the discriminant equation can be found below.

$$\Delta = \frac{9\gamma^2(Re(\alpha_{NLC})^2 - |\alpha_{NLC}|^2)}{4} + \frac{27\gamma^3 Re(\alpha_{NLC})^3|\alpha_{NLC}|^2}{2} - \frac{2187\gamma^4|\alpha_{NLC}|^8}{256} - \frac{243\gamma^3 Re(\alpha_{NLC})|\alpha_{NLC}|^4}{16} \quad (3.28)$$

As can be seen, $\Delta = 0$ equation becomes extremely complicated. When expanded, the discriminant contains frequency (squared) terms up to the 12th power. No real way to simplify it were found because the absolute and real values of α_{NLC} are all different. Whether there is damping in the main system or not does not result in an easy way to obtain an analytical solution for the main equation or the discriminant.

Making a series of assumptions and ignoring small numbers and some terms may simplify the discriminant and jump frequencies may be obtained approximately.

There are some examples in the literature that find approximate jump frequency and corresponding amplitudes for a similar system [18].

Instead, tuning of absorber parameters is done with different approaches, with the aim of no jump phenomena in the frequency response. If there are no jump frequencies, the tuning process can be achieved with optimum damping and spring constant similar to the equal peak method of Den Hartog's.

3.1.4.1 Investigating the Damping Ratio on the Main System Response

Starting with the damping ratio, a series of parameter sets are examined to see the effect of ζ_2. Some examples are given in below amplitude vs frequency graphs with varying ζ_2.

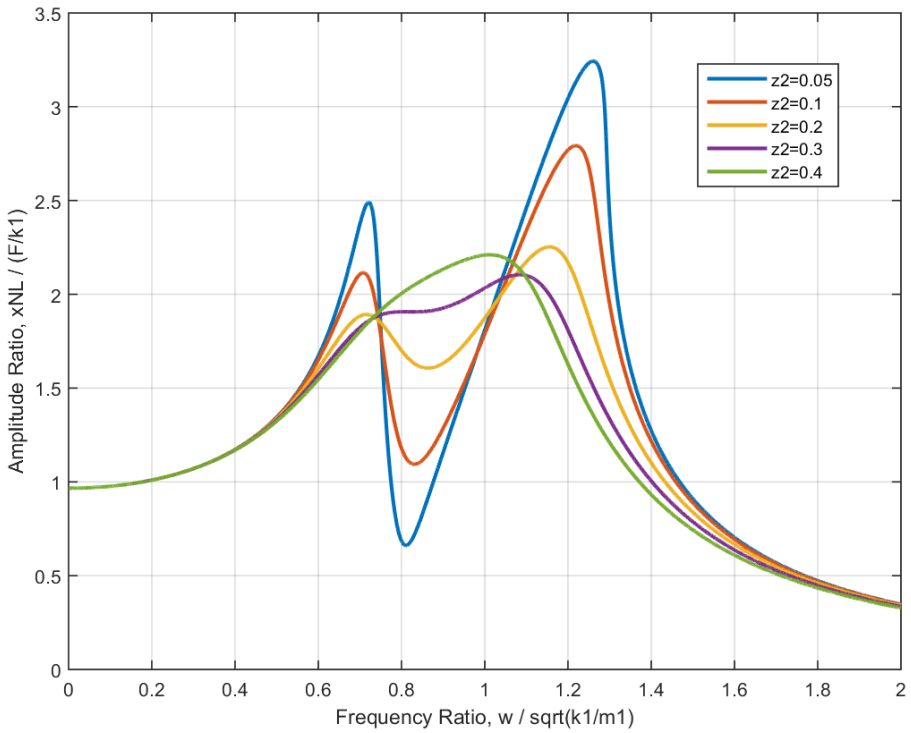

Figure 3.19 The Effect of ζ_2 on the Frequency vs Amplitude Graphs

Up to a certain point, increasing ζ_2 has a benefit in reducing the amplitude. However, after that point, total amplitude and maximum amplitude increases as ζ_2 increases. Therefore, similar to Den Hartog method for linear systems, there is a sweet spot for the optimum amplitude reduction. But unlike Den Hartog's method, there are no invariant points that are not affected by damping ratio.

This is also the same case in tuned vibration absorbers for damped linear systems. There is an optimum ζ_2 for the optimum amplitude. The optimum ζ_2 is given in Asami's work [5] as below.

$$\zeta_2 = \frac{\sqrt{8 + 9\mu - 4\sqrt{4 + 3\mu}}}{4(\mu + 1)} \tag{3.29}$$

While this is an equation for linear main system, it also works rather successfully for the main system with cubic stiffness. It is possible that damping is assumed to be linear in both systems, it gives a good approximation. For cases like cubic damping, or coulomb damping, this solution is not expected to work.

3.1.4.2 Investigation the Frequency Ratio on the Main System Response

Same parameter work is done for ω_r, which is the natural frequency ratio of the absorber to the main system. Below are the amplitude vs frequency graphs with varying ω_r for a set of parameters.

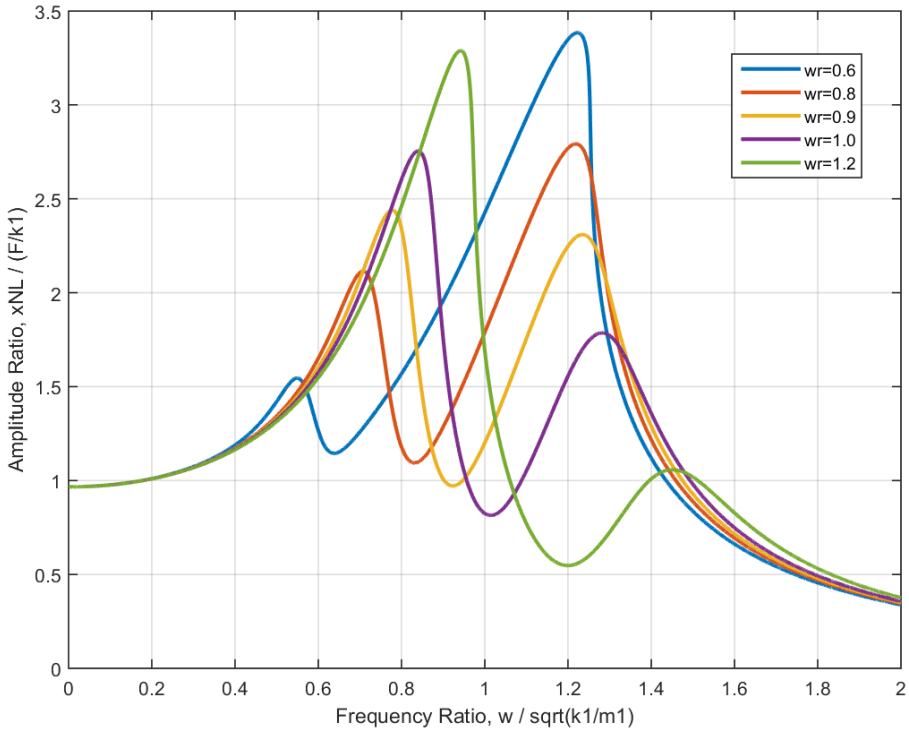

Figure 3.20 The Effect of ω_r on the Frequency vs Amplitude Graphs

The effect of ω_r is similar to the frequency ratio in the linear main system case. For low ω_r values, the right peak is bigger, and for high ω_r values, the left peak is bigger. For some optimum ω_r value, two peaks are equal to each other, just like Den Hartog's equal peak method.

In order to obtain the optimum ω_r value, multivariable regression is done. First, the effect of the parameters is observed with subset analysis on the Minitab software.

Best Subsets Regression: wr versus gama; z1; z2; mu

Response is wr

Vars	R-Sq	R-Sq (adj)	R-Sq (pred)	Mallows Cp	S	gama	z1	z2	mu
1	28,4	28,3	28,1	15117,0	0,12776				X
1	28,3	28,2	28,0	15144,9	0,12787	X			
2	66,9	66,8	66,7	6389,1	0,086914	X			X
2	66,8	66,7	66,6	6410,5	0,087038	X		X	
3	94,2	94,2	94,1	204,1	0,036485	X	X		X
3	94,0	94,0	94,0	233,1	0,036883	X	X	X	
4	95,1	95,0	95,0	5,0	0,033611	X	X	X	X

Figure 3.21 The Best Subsets for ω_r in Minitab

γ and ζ_1 are found to be the most important terms for the optimum ω_r value. Second important observation is that combine effect of μ and ζ_2 has a very little effect on ω_r and one of them can be omitted. Since ζ_2 is a function of μ alone, this was an expected result. Between the two of them, ζ_2 is chosen in the regression model.

Hence, the multivariable regression model is prepared in Minitab software with the parameters γ, ζ_1 and ζ_2 and their powers and cross products. For a realistic case, regression is done with the parameters ranges of $0 < \zeta_1 < 0.3$, $0 < \mu < 0.3$ and $0 < \gamma < 2$.

The minimized term in the regression was the difference between two peaks of the response curve. For every parameter set within the range mentioned above and the optimum damping ratio equation, different frequency ratios are used and the optimum frequency ratio that returns zero peak difference is selected. The peaks of the curves are found with the MATLAB function “peaks”.

Regression model is prepared with the aim of 0 p-value and VIF (Variance Inflation Factor) under 10. In statistical terms, p-value refers to the likelihood of obtaining a

result as extreme or more so than what was observed, assuming no effect or difference (null hypothesis). Meanwhile, the VIF quantifies the degree to which the variance of a given estimated regression coefficient is amplified by correlated predictors.

In very simple terms, p-value gives how much the term is related with ω_r, and VIF gives how good the coefficient estimation for parameter sets other than used in the regression. For both of these parameters, smaller values are better for the precision of the model.

The optimum ω_r equation are found as below.

$$\omega_r = c_0 + c_1\gamma + c_2\gamma^2 + c_3\gamma^3 \tag{3.30}$$

Where,

$$c_0 = 1.423 - 1.757\zeta_1 - 1.602\zeta_2 + 0.341\zeta_1^2 - 1.076\zeta_2^2 + 2.487\zeta_1\zeta_2$$

$$c_1 = 1.033 - 1.042\zeta_1 - 2.056\zeta_2 + 0.305\zeta_1^2 - 1.002\zeta_2^2 + 1.733\zeta_1\zeta_2$$

$$c_2 = -0.368 + 0.151\zeta_1 + 0.332\zeta_2$$

$$c_3 = 0.059 \tag{3.31a, b, c, d}$$

Regression Equation in Uncoded Units

w0 = 1,42332 + 1,0329 gama - 1,7567 z1 - 1,6019 z2 - 0,36836 gama*gama + 0,3411 z1*z1 - 1,0759 z2*z2 - 1,0420 gama*z1 - 2,0563 gama*z2 + 2,4869 z1*z2 + 0,05913 gama*gama*gama + 0,15088 gama*gama*z1 + 0,3315 gama*gama*z2 + 0,3053 gama*z1*z1 + 1,733 gama*z1*z2 + 1,002 gama*z2*z2

Coded Coefficients

Term	Coef	SE Coef	T-Value	P-Value	VIF
Constant	1,08333	0,00034	3155,18	0,000	
gama	0,191218	0,000748	255,60	0,000	7,57
z1	-1,40297	0,00444	-316,22	0,000	3,84
z2	-2,57540	0,00590	-436,76	0,000	4,81
gama*gama	-0,119052	0,000875	-136,00	0,000	3,34
z1*z1	0,5944	0,0394	15,10	0,000	2,00
z2*z2	-0,2447	0,0598	-4,09	0,000	4,64
gama*z1	-0,28598	0,00632	-45,27	0,000	2,60
gama*z2	-0,75922	0,00851	-89,22	0,000	3,24
z1*z2	3,9251	0,0805	48,77	0,000	3,64
gama*gama*gama	0,05913	0,00115	51,50	0,000	10,28
gama*gama*z1	0,15088	0,00926	16,29	0,000	3,64
gama*gama*z2	0,3315	0,0126	26,26	0,000	4,26
gama*z1*z1	0,3053	0,0675	4,52	0,000	3,39
gama*z1*z2	1,733	0,140	12,40	0,000	4,22
gama*z2*z2	1,002	0,106	9,49	0,000	6,36

Model Summary

S	R-sq	R-sq(adj)	R-sq(pred)
0,0053621	99,88%	99,87%	99,87%

Figure 3.22 The Summary of Regression Work for ω_r in Minitab

p-value of zero on all the terms and VIF under 10 all the terms except γ^3 is obtained. VIF of γ^3 is came as 10.28, which is acceptable. High squared terms tend to have bigger VIF values, and more datasets may help reduce this value. In addition, $R^2 = 0.9988$ is obtained. It is possible to obtain a higher R^2 value by adding more terms such as $\zeta_1\gamma^3$ and $\zeta_2\gamma^3$, but by observation and investigation of the accuracy of the equations, this regression model is found as sufficient.

3.1.4.3 Investigating the Mass Ratio on the Main System Response

The last parameter is to be tuned is the mass ratio, μ. Traditionally in linear systems, the mass ratio is selected by the designer based on system requirements, because there is no optimum value of this parameter, and bigger values always give better results. It is similar in nonlinear systems, but a different approach is required.

Let the main system parameters $\gamma = 0.256, \zeta_1 = 0.1$. The non-dimensional amplitude vs the non-dimensional frequency graph is given below for this single-degree-of-freedom system with cubic stiffness.

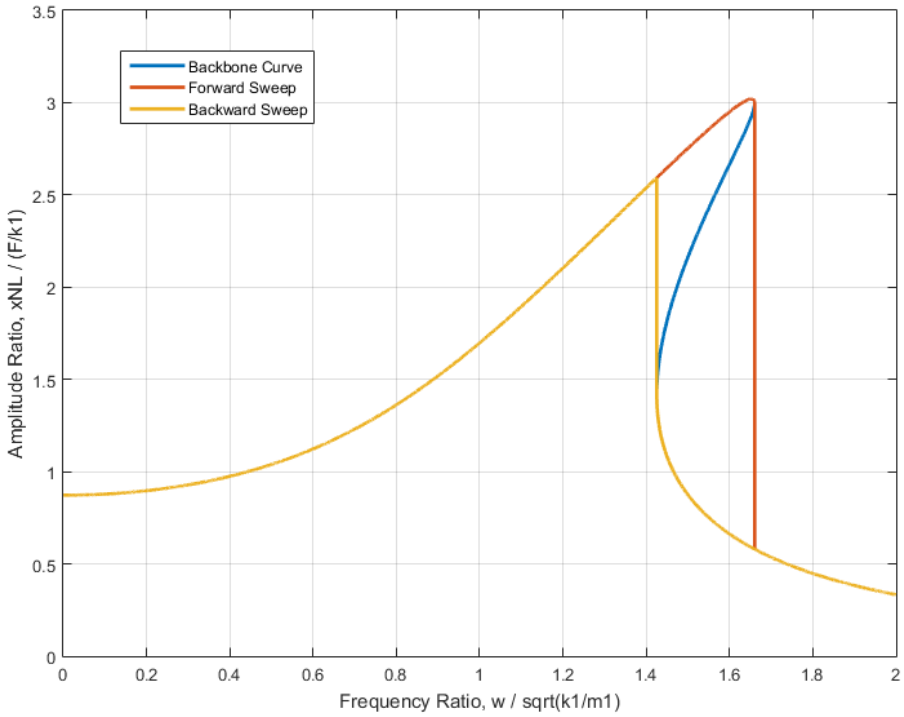

Figure 3.23 The Frequency vs Amplitude Graphs for the SDOF System with Parameters $\gamma = 0.256, \zeta_1 = 0.1$

The effect of mass ratio will be observed by selecting various mass ratios for the same case.

If $\mu = 0.02$ is selected, the system still demonstrates multi-valued behavior. Selecting too small of a mass ratio results in multi-valued region, even though optimum damping ratio is used.

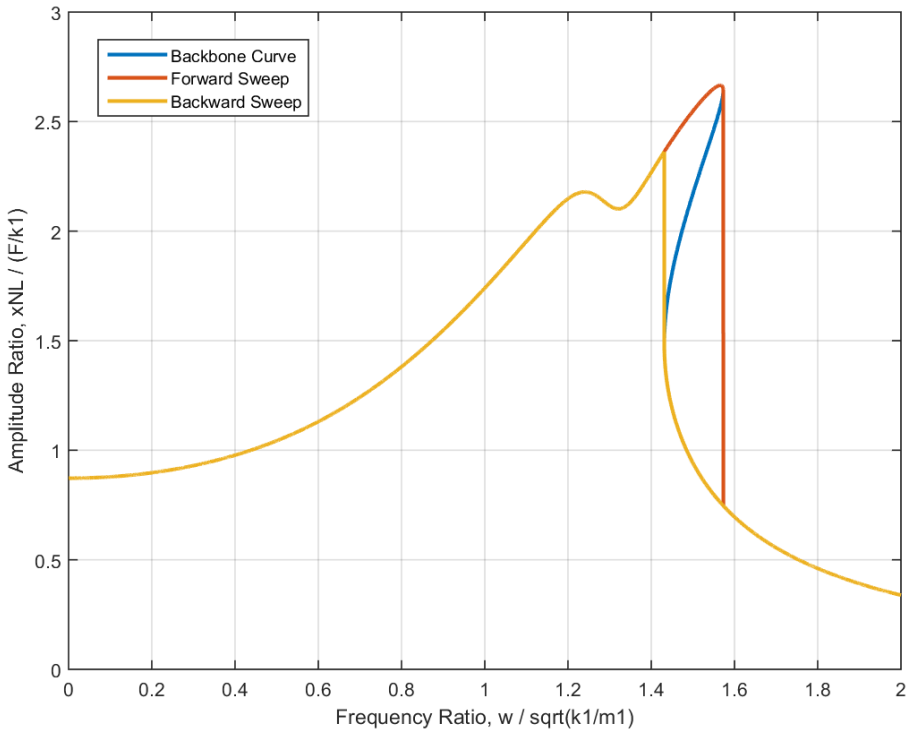

Figure 3.24 The Frequency vs Amplitude Graphs for the SDOF System for $\mu = 0.02$

If $\mu = 0.1$ is selected, the optimum parameters become $\zeta_2 = 0.18, \omega_r = 1.11$ and 40% peak amplitude reduction is reached.

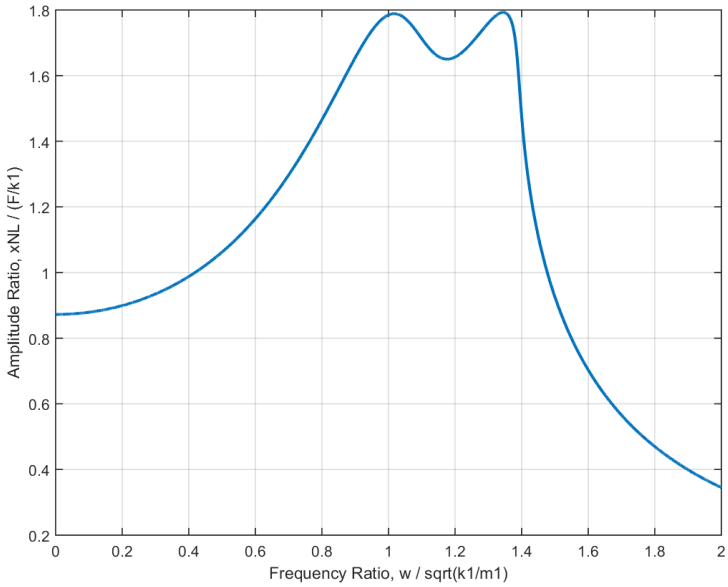

Figure 3.25 The Frequency vs Amplitude Graphs for the SDOF System for $\mu = 0.1$

If $\mu = 0.5$ is selected, the optimum parameters become $\zeta_2 = 0.36, \omega_r = 0.71$ and 55% peak amplitude reduction is reached.

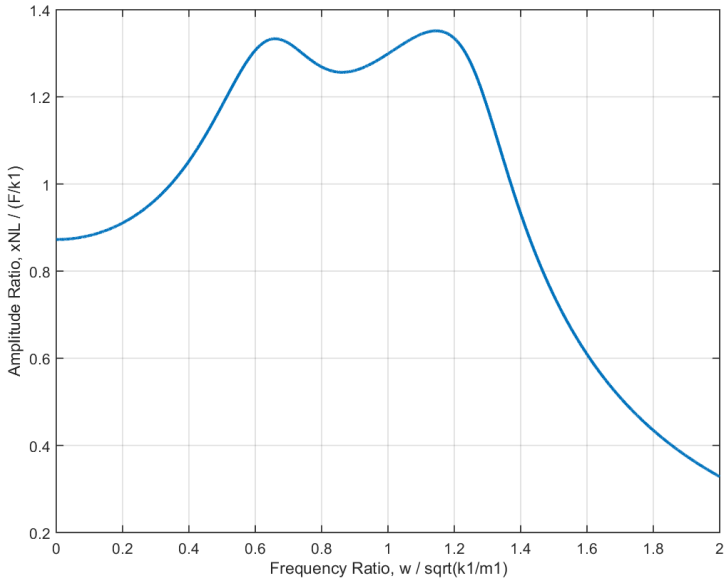

Figure 3.26 The Frequency vs Amplitude Graphs for the SDOF System for $\mu = 0.5$

Note that reaching from 40% to 55% peak reduction requires a five times heavier vibration absorber. The effective bandwidth is also wider, but in real life applications minimization of system total mass is desired and significant increase in mass for moderate to low performance improvement is not desired. Moreover, if the selected mass ratio is too small, it may yield multi-valued region in response curves. For these reasons, there is an optimum mass ratio that should be selected.

A minimum μ value can be obtained with respect to γ value that yields amplitude graphs without jump phenomena. The relation between γ and jump phenomena is given in Gatti's work [18]. Instead of solving $\Delta = 0$ equation for α_{NLC}, solving $\Delta = 0$ equation for the nonlinearity ratio, γ.

$$\gamma_{1,2} = \frac{8Re(\alpha_{NLC})^3 - 9Re(\alpha_{NLC})|\alpha_{NLC}|^2 \mp 8\sqrt{(4Re(\alpha_{NLC})^2 - 3|\alpha_{NLC}|^2)^3}}{81|\alpha_{NLC}|^6} \quad (3.32)$$

Equation 3.32 is plotted as frequency vs k_c for a set of parameters at below figure.

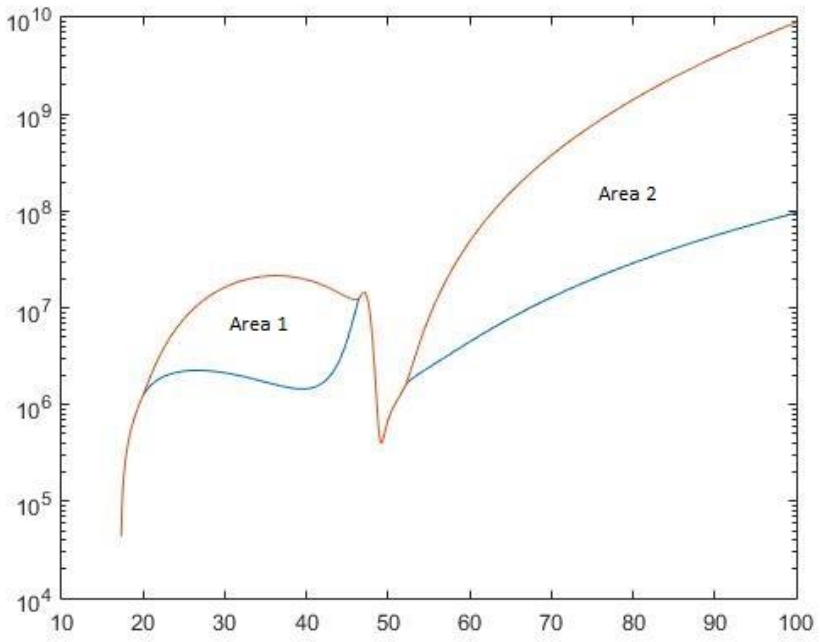

Figure 3.27 The Frequency vs k_c Graphs

If selected k_c value intersects upper and lower curve, i.e. passes through Area-1 or Area-2, there is a multi-valued behavior in the response, and jump frequencies are where k_c value intersects these areas.

For example, assume that $k_c = 5 \cdot 10^6$ N/m^3 with the same parameter set.

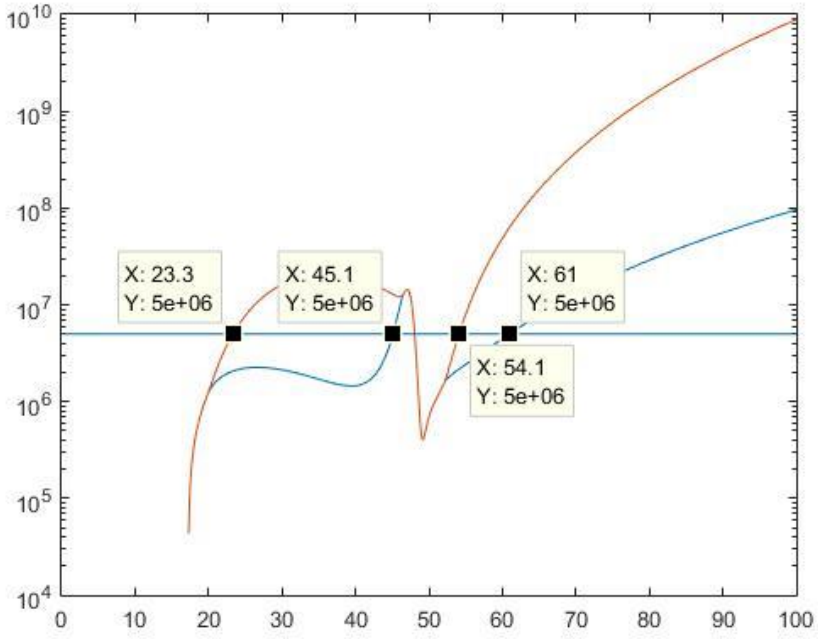

Figure 3.28 The Frequency vs k_c Graphs with $k_c = 5 * 10^6$ Plotted

In this case, the response curves become:

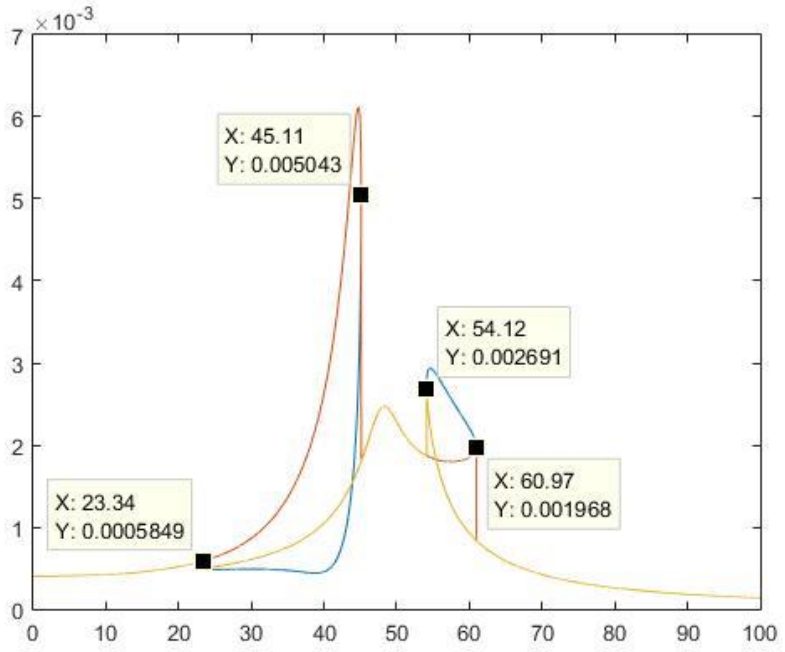

Figure 3.29 The Frequency vs Amplitude Graph for $k_c = 5 * 10^6$ Case

Notice that jump frequencies are the same as intersection points shown in Figure 3.28.

The multi-valuedness of response is related to the term in the square root in Equation 3.32. When the term in root is positive, there are two different real values for γ and two curves are plotted. When γ values are low enough, the root term is negative and real γ terms become complex with equal real parts. Hence, if the root term is always negative for various frequencies, there will be no jump phenomena.

In order to find the critical γ value which will result in a system with jump in the frequency response, the case where the root term is equal to zero should be investigated.

$$4Re(\alpha_{NLC})^2 = 3|\alpha_{NLC}|^2 \tag{3.33}$$

However, the above equation yields complex terms that could not be solved analytically. To obtain an analytical solution, a multivariable regression work is done for the mass ratio μ, similar to the work done for ω_r.

The best subsets for μ are given below. It can be seen that it is enough to use γ and ζ_1 for a good fit. While ω_r alone seems to have a high impact, using it with γ and ζ_1 in the regression does not yield any significant difference. ζ_2 is not used on purpose, because it is directly related to the mass ratio.

Best Subsets Regression: mu versus gama; z1; wr

Response is mu

Vars	R-Sq	R-Sq (adj)	R-Sq (pred)	Mallows Cp	S	gama	z1	wr
1	83,3	83,2	82,9	657,0	0,041112		X	
1	56,3	56,0	55,2	1993,1	0,066513			X
2	96,3	96,3	96,2	13,9	0,019294	X	X	
2	91,1	91,0	90,7	273,3	0,030103	X		X
3	96,6	96,5	96,3	4,0	0,018705	X	X	X

Figure 3.30 The Best Subsets for the Mass Ratio Regression in Minitab

The mass ratio is found as below. Although ζ_1 seems to have a very high impact alone, anything larger than square terms tend to have high p-values.

$$\mu = c_0 + c_1\gamma + c_2\gamma^2 + c_3\gamma^3 + c_4\gamma^4 \tag{3.34}$$

Where,

$$c_0 = 0.133 - 1.541\zeta_1 + 2.537\zeta_1^2$$

$$c_1 = 0.564 - 1.416\zeta_1$$

$$c_2 = -0.986 + 3.258\zeta_1$$

$$c_3 = 0.782 - 2.867\zeta_1$$

$$c_4 = 0.204 + 0.783\zeta_1 \qquad (3.35a, b, c, d, e)$$

This time, some of the terms are VIF terms bigger than 10, but still in the range of reasonable values. The effect of this, with the obtained R^2 and residual values will be analyzed in the discussion chapter.

Regression Equation in Uncoded Units

mu = 0,13252 + 0,5642 gama - 1,5412 z1 - 0,9857 gama*gama + 2,5374 z1*z1 - 1,416 gama*z1 + 0,7823 gama*gama*gama + 3,258 gama*gama*z1 - 0,20404 gama*gama*gama*gama - 2,867 gama*gama*gama*z1 + 0,7827 gama*gama*gama*gama*z1

Coded Coefficients

Term	Coef	SE Coef	T-Value	P-Value	VIF
Constant	0,123042	0,000443	278,03	0,000	
gama	0,094607	0,000944	100,22	0,000	6,42
z1	-1,23687	0,00457	-270,75	0,000	3,20
gama*gama	0,04152	0,00266	15,59	0,000	12,43
z1*z1	2,5374	0,0413	61,47	0,000	1,14
gama*z1	-0,5408	0,0124	-43,68	0,000	6,07
gama*gama*gama	-0,06924	0,00177	-39,11	0,000	7,42
gama*gama*z1	-0,4101	0,0352	-11,66	0,000	25,62
gama*gama*gama*gama	-0,10861	0,00353	-30,76	0,000	13,94
gama*gama*gama*z1	0,7508	0,0228	32,90	0,000	6,55
gama*gama*gama*gama*z1	0,7827	0,0466	16,78	0,000	19,23

Model Summary

S	R-sq	R-sq(adj)	R-sq(pred)
0,0025807	99,94%	99,93%	99,92%

Figure 3.31 The Summary of Regression Work for μ in Minitab

3.1.4.4 Investigating the Frequency Ratio with a Predetermined Mass Ratio

With using this μ term, the regression is redone for ω_r in order to obtain a better R^2 value with less residuals.

Best Subsets Regression: wr versus gama; z1; z2; mu

Response is wr

Vars	R-Sq	R-Sq (adj)	R-Sq (pred)	Mallows Cp	S	gama	z1	z2	mu
1	84,2	84,1	84,1	1242,0	0,039033		X		
1	46,2	46,1	46,0	6411,6	0,071915			X	
2	93,2	93,2	93,1	14,3	0,025622	X	X		
2	92,4	92,3	92,3	127,2	0,027134		X		X
3	93,3	93,2	93,2	4,9	0,025478	X	X		X
3	93,2	93,2	93,1	13,9	0,025603	X	X	X	
4	93,3	93,2	93,2	5,0	0,025466	X	X	X	X

Figure 3.32 The Best Subsets for ω_r Regression with Predetermined Mass Ratio in Minitab

In this case, the best subsets for ω_r suggests that using γ and ζ_1 are enough for a good fit. Since the μ term is a function of γ and ζ_1, and the μ that can be selected is limited, its effect on ω_r seems to diminish. Similarly, ζ_2 is not added to the regression model as well.

The new ω_r regression model is given below.

$$\omega_r = c_0 + c_1\gamma + c_2\gamma^2 \tag{3.36}$$

Where,

$$c_0 = 1.306 - 1.707\zeta_1 - 2.883\zeta_2 + 1.400\zeta_1^2 + 5.506\zeta_1\zeta_2$$

$$c_1 = 0.191 - 0.744\zeta_1 - 1.180\zeta_2 + 4.528\zeta_1^2 - 5.989\zeta_2^2 - 8.790\zeta_1\zeta_2$$

$$c_2 = -0.040 + 1.068\zeta_1 + 1.122\zeta_2 - 9.114\zeta_1^2 - 5.351\zeta_2^2 - 16.210\zeta_1\zeta_2$$

$$(3.37a, b, c)$$

Regression Equation in Coded Units

wr = 1,30596 + 0,19086 gama - 1,7068 z1 - 2,8830 z2 - 0,04044 gama*gama + 1,400 z1*z1 - 0,7436 gama*z1 - 1,1800 gama*z2 + 5,506 z1*z2 + 1,0680 gama*gama*z1 + 1,1221 gama*gama*z2 - 4,528 gama*z1*z1 - 8,79 gama*z1*z2 - 5,989 gama*z2*z2 - 9,114 gama*gama*z1*z1 - 16,21 gama*gama*z1*z2 - 5,351 gama*gama*z2*z2

Coded Coefficients

Term	Coef	SE Coef	T-Value	P-Value	VIF
Constant	1,30596	0,00031	4169,05	0,000	
gama	0,19086	0,00101	188,30	0,000	68,13
z1	-1,7068	0,0196	-87,30	0,000	445,38
z2	-2,8830	0,0204	-141,65	0,000	487,46
gama*gama	-0,04044	0,00169	-23,88	0,000	51,04
z1*z1	1,400	0,125	11,23	0,000	83,60
gama*z1	-0,7436	0,0402	-18,50	0,000	499,49
gama*z2	-1,1800	0,0419	-28,18	0,000	526,75
z1*z2	5,506	0,126	43,63	0,000	83,78
gama*gama*z1	1,0680	0,0479	22,29	0,000	408,78
gama*gama*z2	1,1221	0,0517	21,68	0,000	457,39
gama*z1*z1	-4,528	0,793	-5,71	0,000	1930,84
gama*z1*z2	-8,79	1,62	-5,44	0,000	5374,30
gama*z2*z2	-5,989	0,811	-7,38	0,000	2298,03
gama*gama*z1*z1	-9,114	0,522	-17,48	0,000	338,08
gama*gama*z1*z2	-16,21	1,09	-14,90	0,000	813,98
gama*gama*z2*z2	-5,351	0,637	-8,40	0,000	586,68

Model Summary

S	R-sq	R-sq(adj)	R-sq(pred)
0,0020216	99,96%	99,96%	99,95%

Figure 3.33 The Summary of Regression Work for ω_r with Predetermined Mass Ratio in Minitab

In this case, VIF values are all very high. However, this is an expected result because of the predetermined μ and ζ_2 values.

To sum up, using Equations 3.29, 3.34 and 3.36, it is possible to obtain an analytical solution that gives the system response with minimum amplitudes and an optimum mass ratio.

Note that this ω_r regression is done for the minimum μ that gives amplitude graphs without jump phenomena. If the mass ratio is selected bigger than this value, equations 3.29 and 3.30 should be used for tuning instead for a better fit. High VIF on the ω_r model in Equation 3.36 supports that.

An interesting outcome of this method is observed when the main system is undamped. The invariant points discussed in Section 3.1.3. are approximately equal and near the maximum points of nonlinear response curves. In the figure below, blue and red curves are found from the method developed, green and purple curves are drawn for the sole purpose of identifying the invariant points. This is also a proof of how well the regression model works.

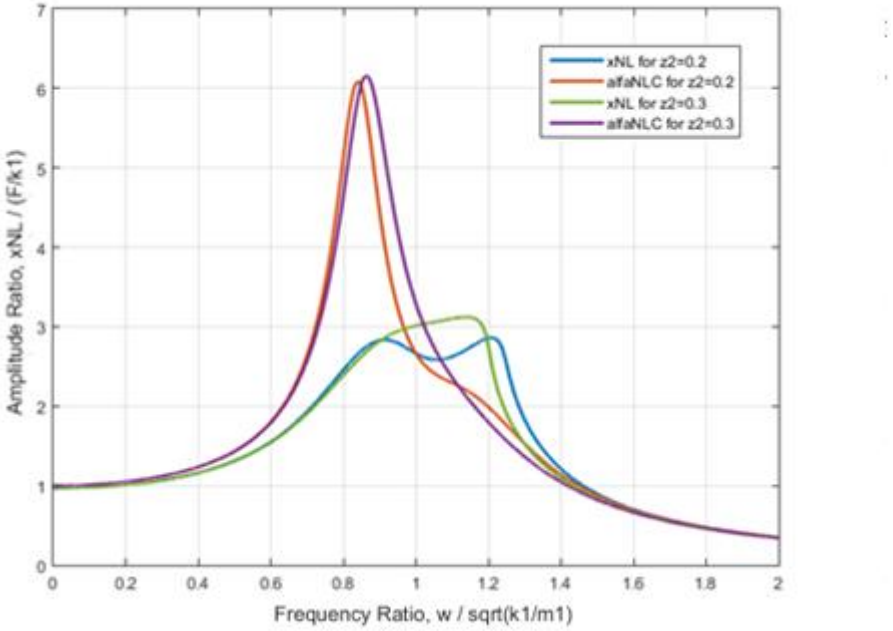

Figure 3.34 The Invariant Points of α_{NLC} and $X_{NL,1}$ with the Method Developed

Instead of this methodology, using numerical methods with the same equations is always a possibility. Computational time would not be unbearable since the equations are still very easy to solve by a computer. This should be the case for nonlinearities other than cubic stiffness which return too complex to solve equations. This method is also used in case studies with the purpose of investigating whether the regression model is accurate or not.

For the cubic stiffness case, the pseudo-code in Appendix A provides a basic framework for iterating through the parameter space to find the combination of parameters ζ_2 and ω_r that yield the smallest area under the graph and the smallest difference between the two peak points.

3.2 Tuned Vibration Absorber Attached on A Multi Degree of Freedom Nonlinear System

It is possible to obtain a tuning method by using the same equations for MDOF systems by applying Sherman-Morrison method to scale and find amplitudes on other points. Unlike the single-degree-of-freedom system solution, this is only possible with numerical methods because the equations are getting too complex as the number of degree-of-freedom increases.

An n-DOF system with the nonlinear element between the first mass and the ground is given in the below figure.

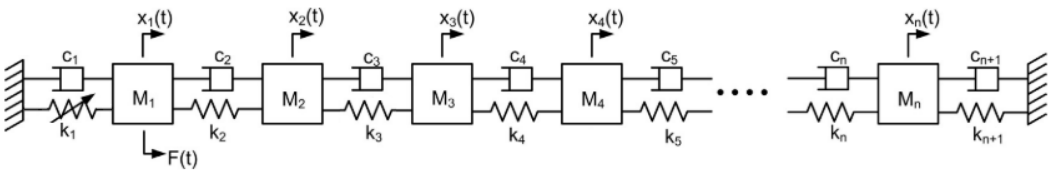

Figure 3.35 A MDOF System with Nonlinear Element Between the First Mass and The Ground

The advantage of this method is that the numerical optimization is done by using receptance of the system. Finding receptance curves of the system is an easy task with simple tests. The other significant advantage of this method is the computation time. The computation time for large scale systems with traditional methods is drastically long, but using these analytical equations can reduce the computation time significantly. Another advantage would be to obtain a system-specific and requirement-based optimization method. This is also a system identification method, and the optimization capabilities depend on the algorithm used in optimization. Usually, it is preferred to reduce the vibration amplitudes by minimizing the peak points or the area under the graphs. For some systems, it may be desired to reduce the response amplitude only for a specific range of frequencies. For some other systems, the requirement may be to reduce the vibration amplitudes for a specific degree of freedom only and/or mode only. This method provides freedom to tune the system based on any requirements quickly.

The comparison is made to demonstrate the computational time gained by using this method. Two algorithms are developed in order to try thousands of parameter sets and find the optimum one for the TVA. One of the algorithms uses a traditional iterative method to find the response curves and the other one uses Describing Function Method to obtain the response. Note that the TVA is included in the number of DOF in the left column.

Table 3.1 The Comparison of Computational Time for Iterative and DF Methods

# of Degree-of-Freedom	**Iterative Method**	**Analytical DF Method**
2 DOF	1.21 min	1.14 min
5 DOF	1.97 min	1.25 min
50 DOF	175 min	3.08 min
500 DOF	~15450 min	205 min

As the degree of freedom increases, the inverse of a big matrix is taken repetitively (for each iteration step) for the iterative method. Since there are no iterations in DF Method, matrix inversion is taken only once for each set. Hence, the computational burden is significantly bigger for the high-DOF system.

It is possible to use the equations developed for the damped SDOF system in Section 3.1.4. for certain MDOF systems. If the MDOF graph has similarities and can be represented with a SDOF equivalent system, then SDOF solutions can be used on this equivalent system. A detailed case study will be presented in Chapter 4 on this topic.

It is also possible to use this method for nonlinearities other than cubic stiffness, or for a nonlinearity between two masses instead of ground connection, but these cases are not in the scope of this thesis work.

CHAPTER 4

CASE STUDIES AND VALIDATION

In this chapter, case studies to demonstrate the validity and efficiency of the presented methods are given. The analytical formulation for 2-DOF systems is validated with different sets of parameters, and the numerical method for MDOF systems is validated with different cases with various sets of parameters and degrees of freedom.

The results are also compared with the time domain solution. The 'ode45' command in MATLAB is used to solve the nonlinear differential equation set and obtain the time domain solution of the system. This command executes the Runge-Kutta (4,5) formula. When solving for a specific frequency, the number of equations solved is twice the total degree of freedom of the system. This is because the second-order differential equations are converted to first-order differential equations to apply the Runge-Kutta method.

4.1 2-Degree-of-Freedom Case Studies

This section presents the implementation of the method shown in Section 3.1.2. The parameters change with different cases since the system is always the same.

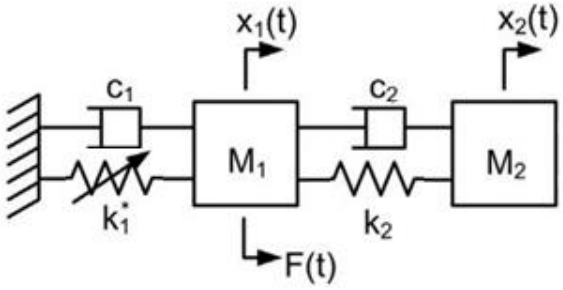

Figure 4.1 A 2-DOF System Model

4.1.1 Case Study #1 (Undamped & lightly damped 2-DOF system)

The first case study will analyze the equations obtained in the undamped system in 3.1.1.

The system parameters chosen for Case Study #1 are given below.

$$\gamma = 0.256, \mu = 0.2, \omega_r = 1.42, \zeta_1 = \zeta_2 = 0$$

The frequency vs response graph of the main system for the SDOF case is given below.

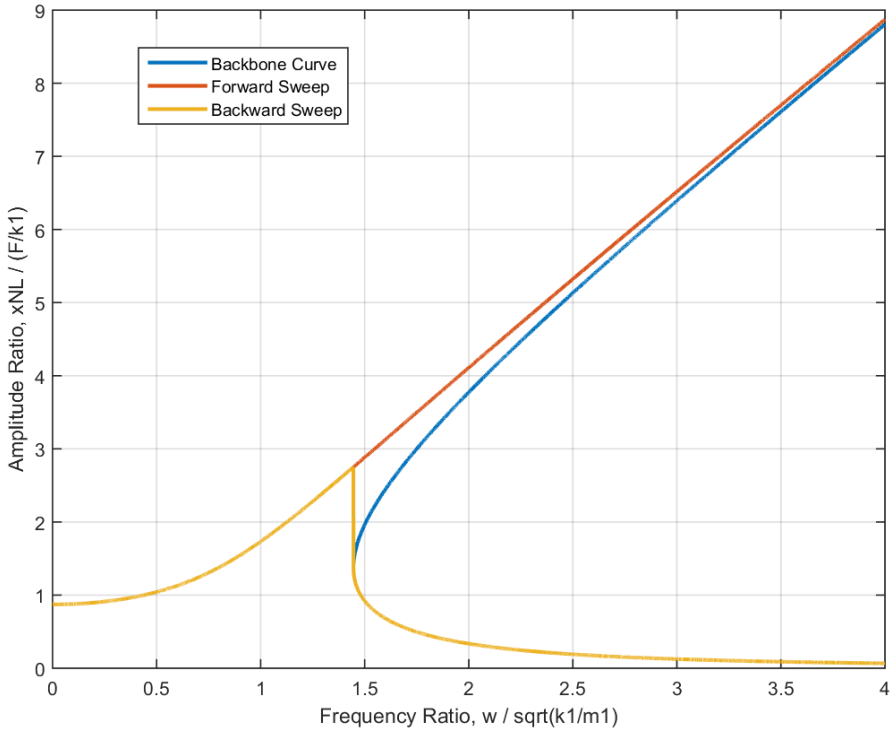

Figure 4.2 The Response Curves for SDOF System with $\gamma = 0.256, \zeta_1 = 0$

The frequency vs response graph with TVA attached is given below.

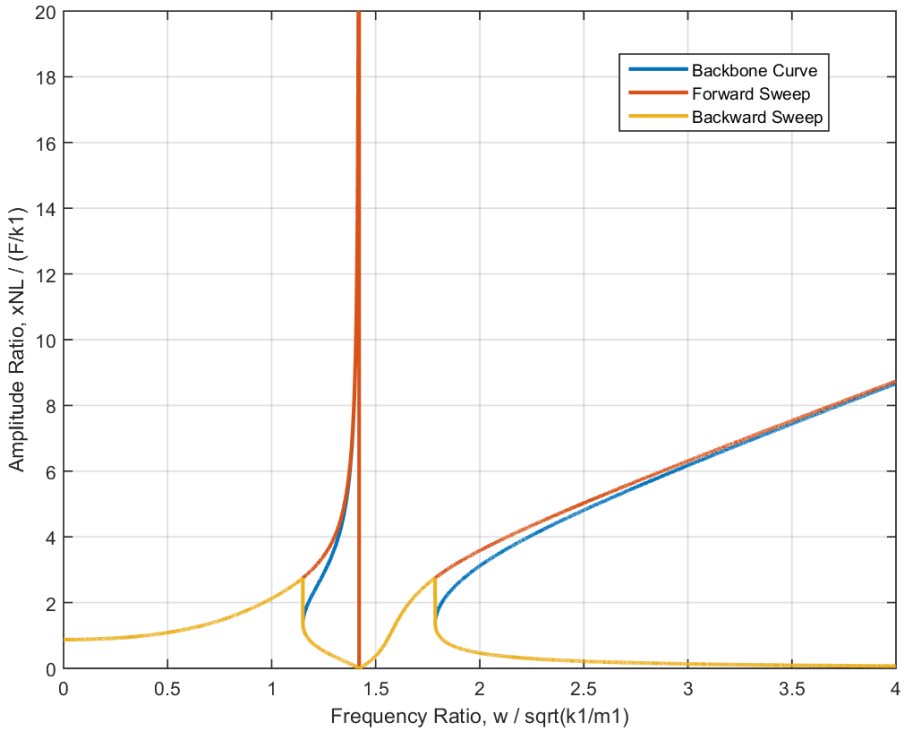

Figure 4.3 The Response Curves for the Parameter Set of $\gamma = 0.256, \mu = 0.2, \omega_r = 1.42, \zeta_1 = \zeta_2 = 0$

By using Equations 3.22 and 3.26, jump frequencies and the corresponding response are found as below.

$$\Omega_1 = 1.150, \Omega_2 = 1.42, \Omega_3 = 1.785$$

$$X_{NL} = 2.751$$

The jump-up frequencies Ω_1 and Ω_3, the response at these points, and the jump-down frequency Ω_2 are investigated on the graph.

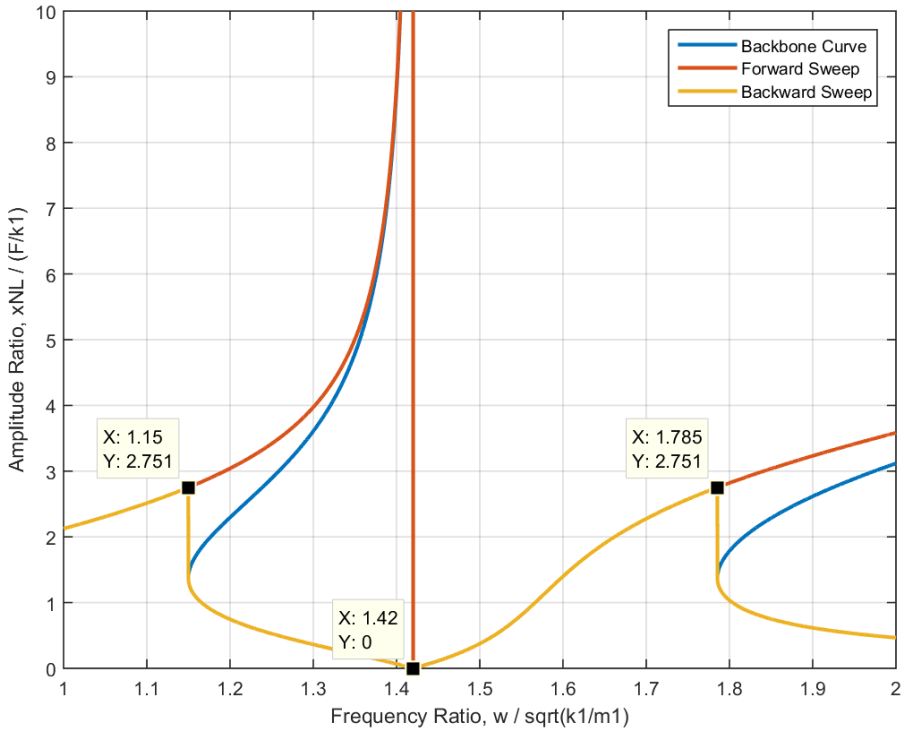

Figure 4.4 The Response Curves with Jump Frequencies for the Parameter Set of $\gamma = 0.256, \mu = 0.2, \omega_r = 1.42, \zeta_1 = \zeta_2 = 0$

In the case of a very lightly damped system, the equations are working as well.

For example, in the case of $\zeta_1 = \zeta_2 = 0.001$ the jump frequencies and the response are found as below.

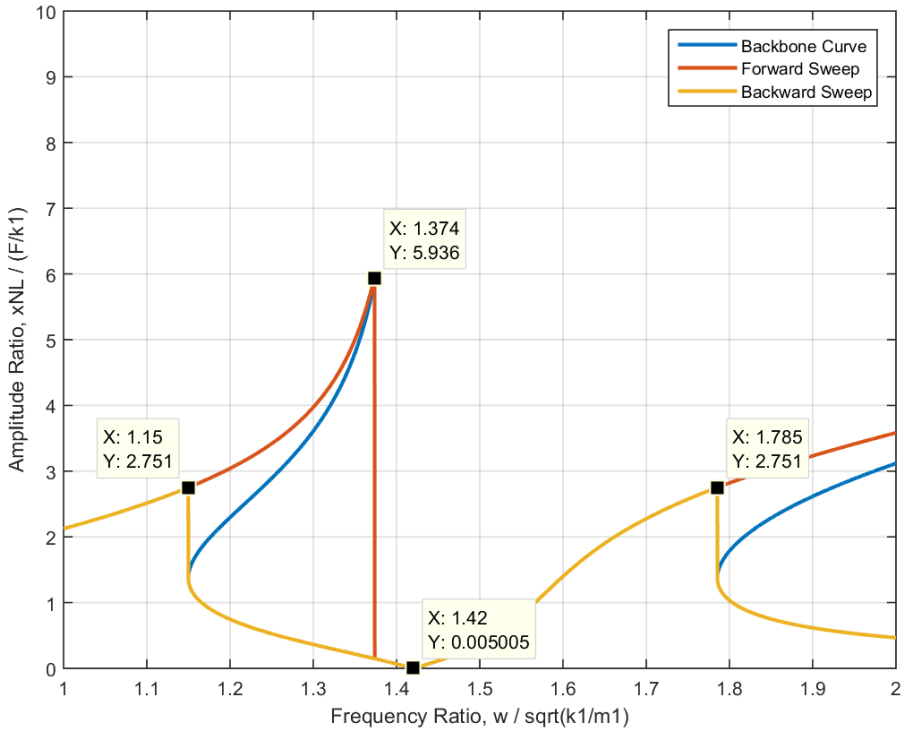

Figure 4.5 The Response Curves with Jump Frequencies for $\zeta_1 = \zeta_2 = 0.001$

In the case of $\zeta_1 = \zeta_2 = 0.001$, jump-down frequencies and corresponding responses are still the same.$\Omega_2 = \omega_r$ is still a local minimum point. However, the jump-down frequency moved significantly. Hence, ω_2 is not a good estimate for jump-down frequency for lightly damped case.

Further investigation of the effect of increasing damping on jump frequencies is presented below.

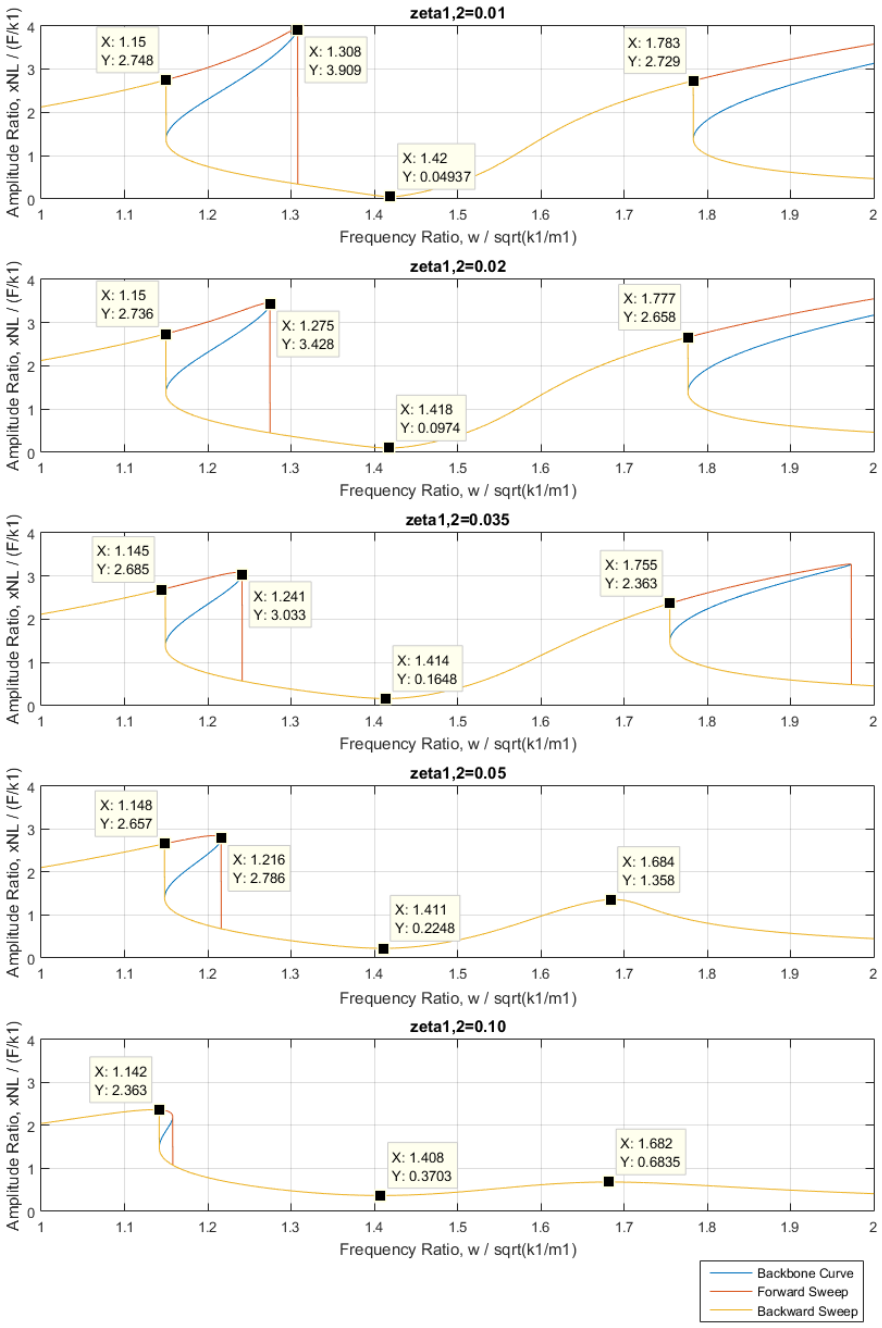

Figure 4.6 The Response Curves with Jump Frequencies for Various Damping Ratios

In the case of a lightly damped system, the equations are working as well. As the damping increases, the accuracy of the equations falls as expected. However, even with a moderate damping of 0.1, jump frequencies and the corresponding response are still close to the undamped case if jumping occurs. Moreover, the local minima point is still close to ω_r, for this specific case with only a 0.8% error.

The response amplitude at the second jump-down frequency has the highest error and should be considered as a bad approximation for moderate or high damping ratios. Similarly, the second jump-up frequency has a bigger error than the first one, but still a good approximation to a degree.

Overall, the reason behind the size of the error lies in whether there is a jump phenomenon. The error on the first jumping area when $\zeta_1 = \zeta_2 = 0.1$ also got bigger because the area is small and almost disappeared.

4.1.2 Case Study #2 (Damped Main System & Undamped Absorber)

In this case study the main system damping exists but damping of the vibration absorber is selected as $\zeta_2 = 0$ as investigated in Section 3.1.2.

The system parameters are chosen similarly to the previous case, except for the damping ratios.

$$\gamma = 0.256, \mu = 0.2, \omega_r = 1.42, \zeta_1 = 0.1, \zeta_2 = 0$$

The frequency vs response of the main system graph is given below.

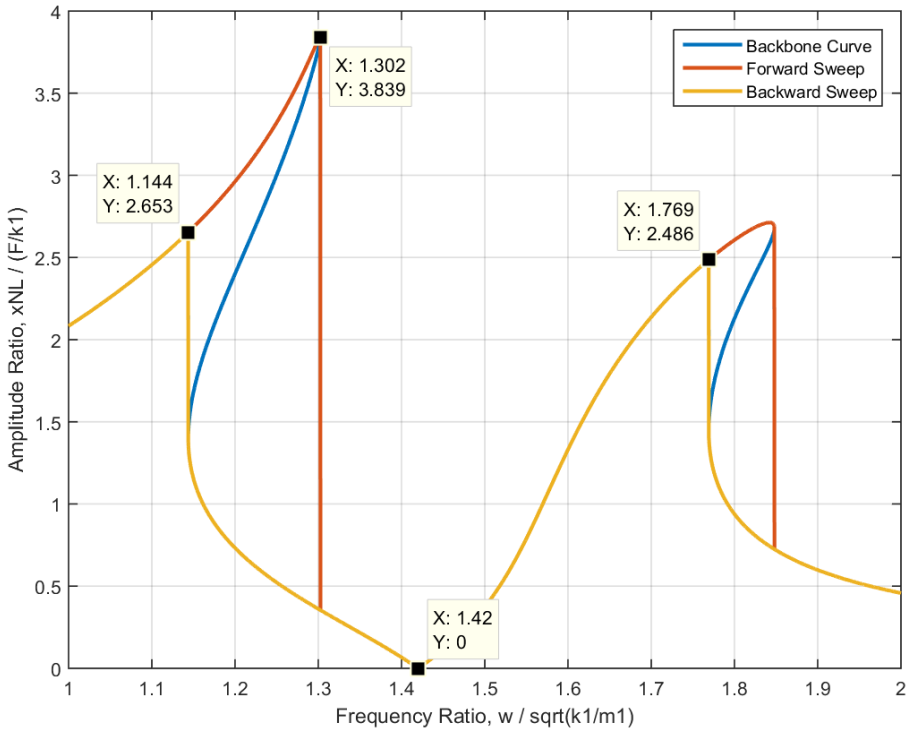

Figure 4.7 The Response Curves with Jump Frequencies for the Parameter Set of $\gamma = 0.256, \mu = 0.2, \omega_r = 1.42, \zeta_1 = 0.1, \zeta_2 = 0$

The undamped equations still yield good approximate results for jump-up frequencies and the responses even though there is damping in the main system. Moreover, the local minimum point gives the exact result. Local minimum equation is found from numerator of the α_{NLC} and the numerator does not contain any ζ_1 terms in it. Hence, it is expected to find the minimum point exactly as zero at the frequency ω_r when $\zeta_2 = 0$ selected.

Finally, the effect of the mass ratio μ is investigated. The jump frequencies are calculated again for different mass ratios. The response does not depend on the mass ratio, so it is always $X_{NL} = 2.752$ for this case.

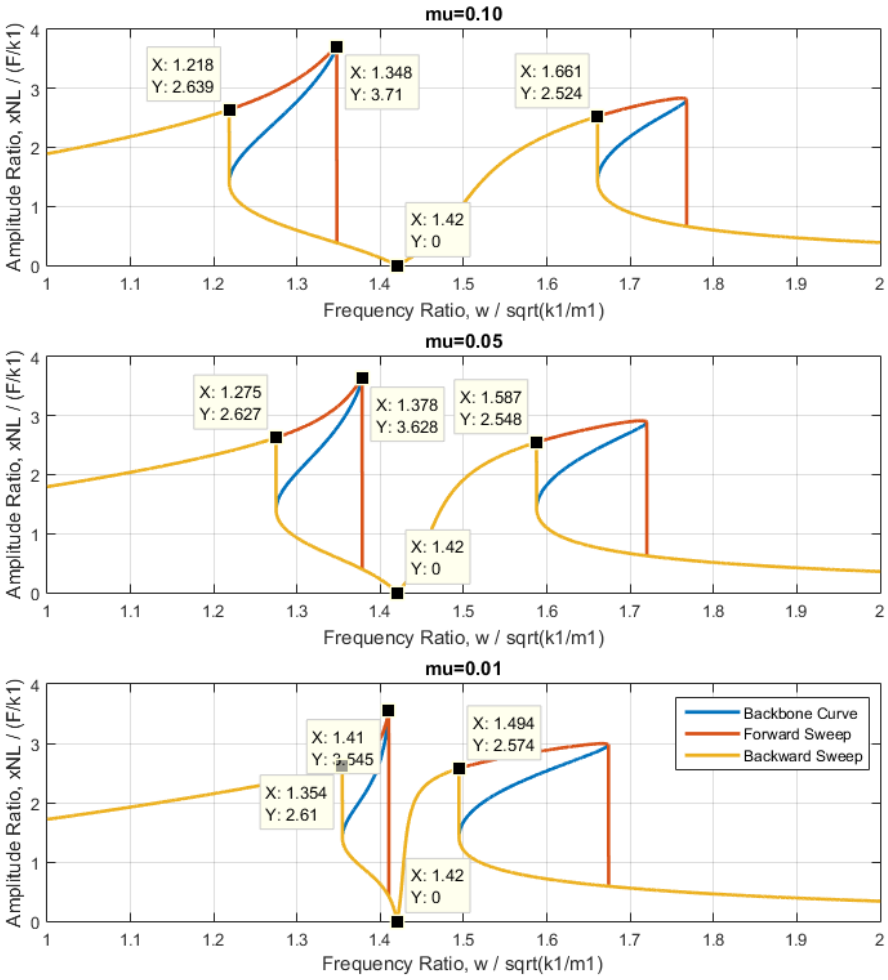

Figure 4.8 The Response Curves with Jump Frequencies for Various Mass Ratios

For $\mu = 0.1$, the Equations 3.22a and 3.22c yield $\Omega_1 = 1.226,\ \Omega_3 = 1.675$

For $\mu = 0.05$, the Equations 3.22a and 3.22c yield $\Omega_1 = 1.282,\ \Omega_3 = 1.601$

For $\mu = 0.01$, the Equations 3.22a and 3.22c yield $\Omega_1 = 1.363,\ \Omega_3 = 1.507$

When the mass ratio decreases, the first jump-down frequency and the second jump-up frequency get closer to local minimum points. Hence, selecting high mass ratio provides a broad bandwidth of small amplitudes around ω_r.

4.1.3 Case Study #3 (Damped Main System & Vibration Absorber with low nonlinearity and high main system damping)

The case studies between #3 and #6 will analyze the equations obtained in the damped system in 3.1.3.

The system parameters chosen for Case Study #3 are given below.

$$\gamma = 0.25, \zeta_1 = 0.15$$

Frequency vs response of the main system is found with Describing Function Method

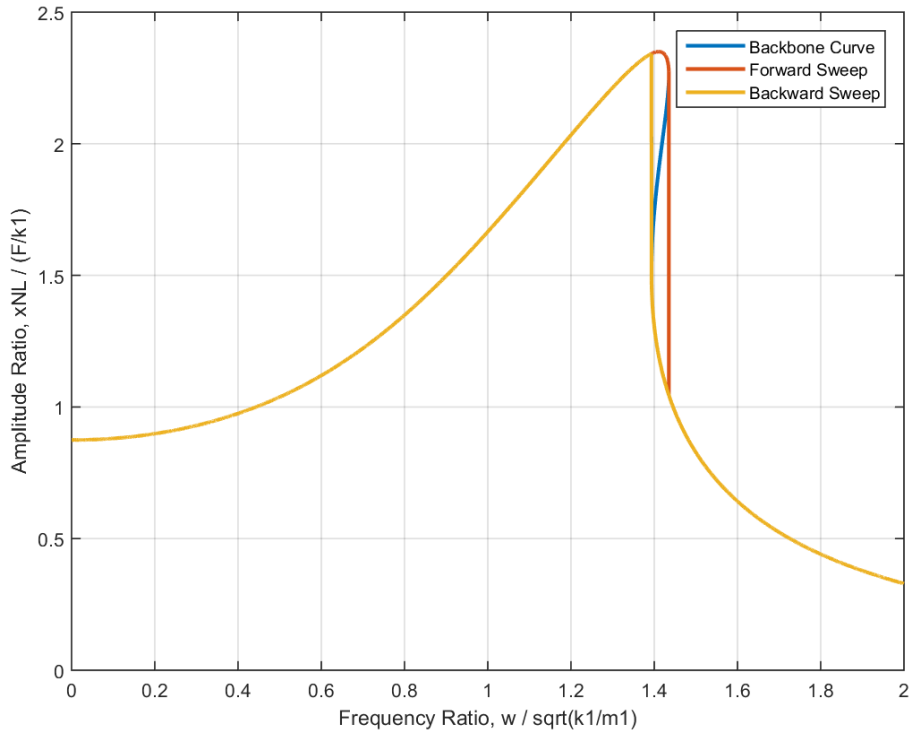

Figure 4.9 The Response Curves for SDOF System with $\gamma = 0.25, \zeta_1 = 0.15$

Same graph with ODE45 solution is given below.

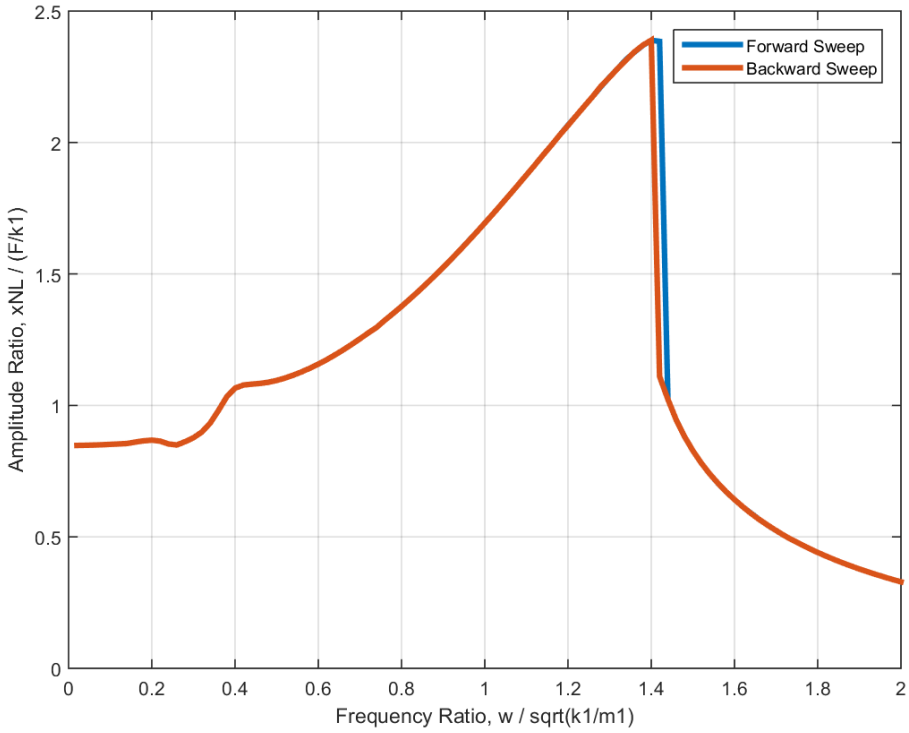

Figure 4.10 ODE Solution for the Response Curves for SDOF System with $\gamma = 0.25, \zeta_1 = 0.15$

From Equations 3.29, 3.34 and 3.36, the vibration absorber parameters can be found quickly.

$$\mu = 0.0205, \omega_r = 1.232, \zeta_2 = 0.0868$$

The two-degree-of-freedom system with TVA response graphs is found using Describing Function Method

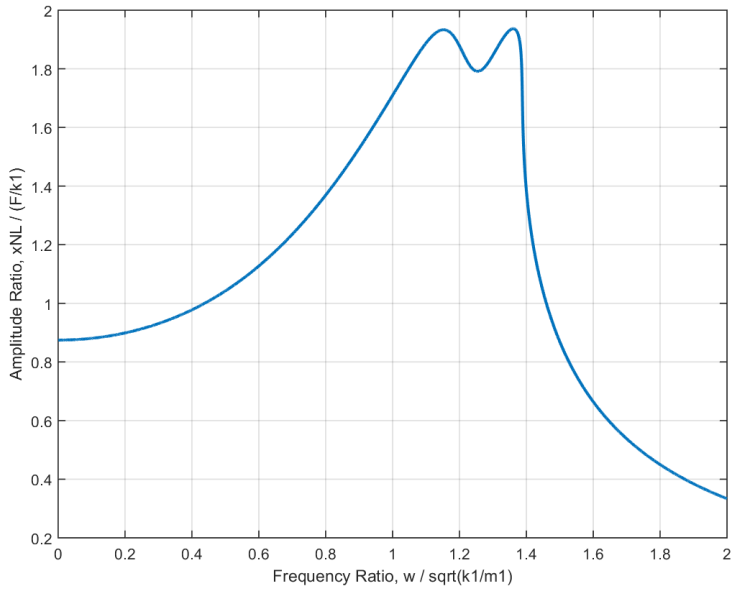

Figure 4.11 The Response Curves for 2DOF System with $\gamma = 0.25, \zeta_1 = 0.15, \mu = 0.0205, \omega_r = 1.232, \zeta_2 = 0.0868$

Comparing with ODE45 solutions:

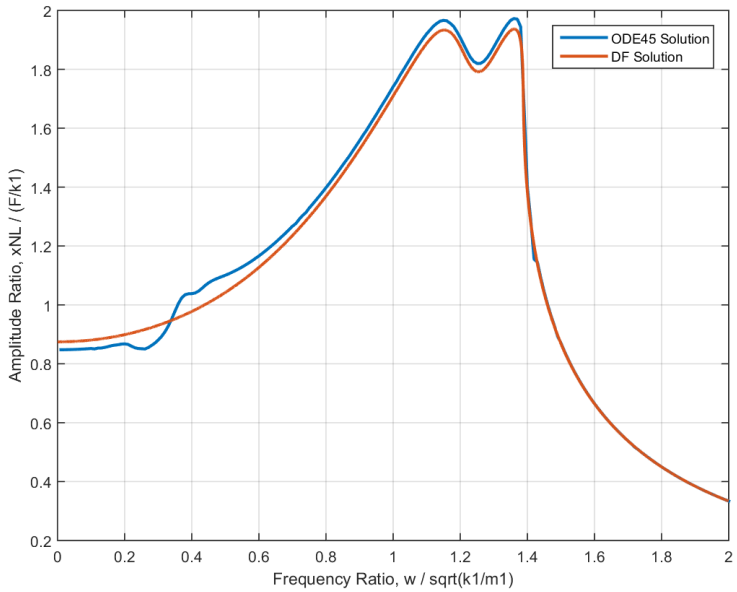

Figure 4.12 The Comparison of ODE Solution and Describing Function Method Solution for Case Study #3

Instead of using the equations, parameter sweep is done. Parameter sweep gives the lowest peak with the smallest area under the graph. The mass ratio is chosen as the same because it is the most dominant parameter to reduce the amplitude.

$$\mu = 0.0205, \omega_r = 1.230, \zeta_2 = 0.102$$

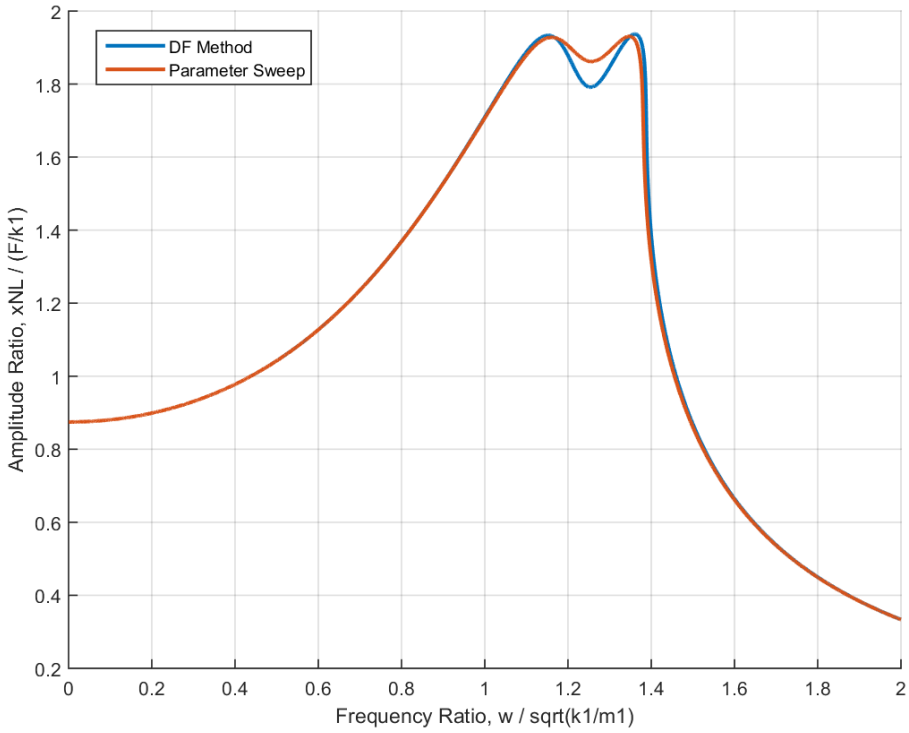

Figure 4.13 The Comparison of Describing Function Method and Parameter Sweep for Case Study #3

4.1.4 Case Study #4 (Damped Main System & Damped Vibration Absorber with high nonlinearity and high main system damping)

The system parameters chosen for Case Study #4 are given below.

$$\gamma = 1.50, \zeta_1 = 0.15$$

Frequency vs response of the main system is found with Describing Function Method

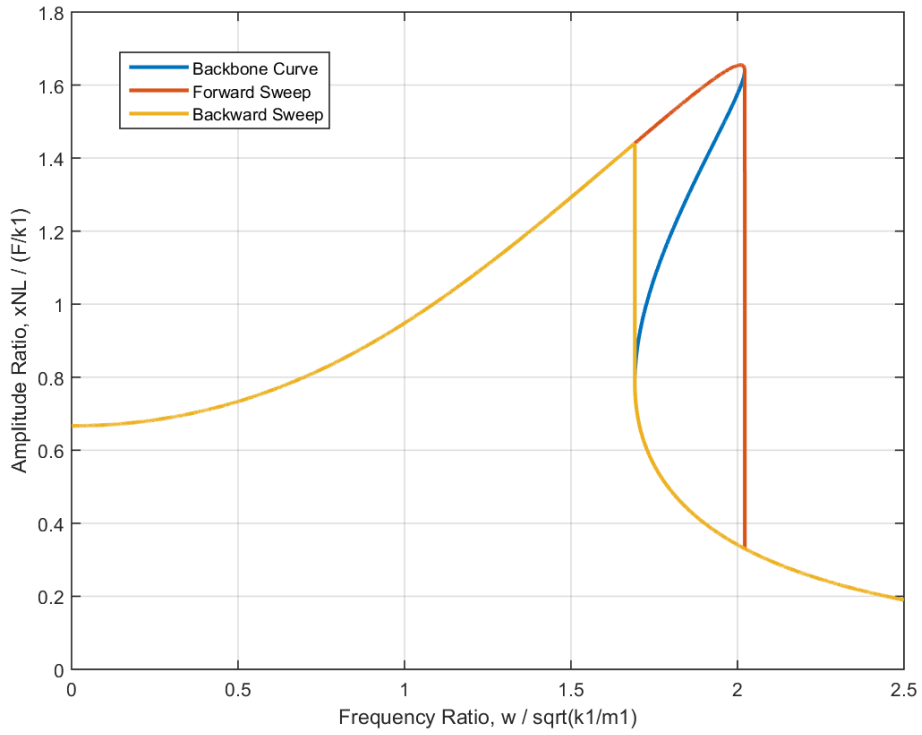

Figure 4.14 The Response Curves for SDOF System with $\gamma = 1.50, \zeta_1 = 0.15$

From Equations 3.29, 3.34 and 3.36, the vibration absorber parameters can be found quickly.

$$\mu = 0.118, \omega_r = 1.295, \zeta_2 = 0.200$$

The two-degree-of-freedom system with TVA response graphs is found usingh Describing Function Method

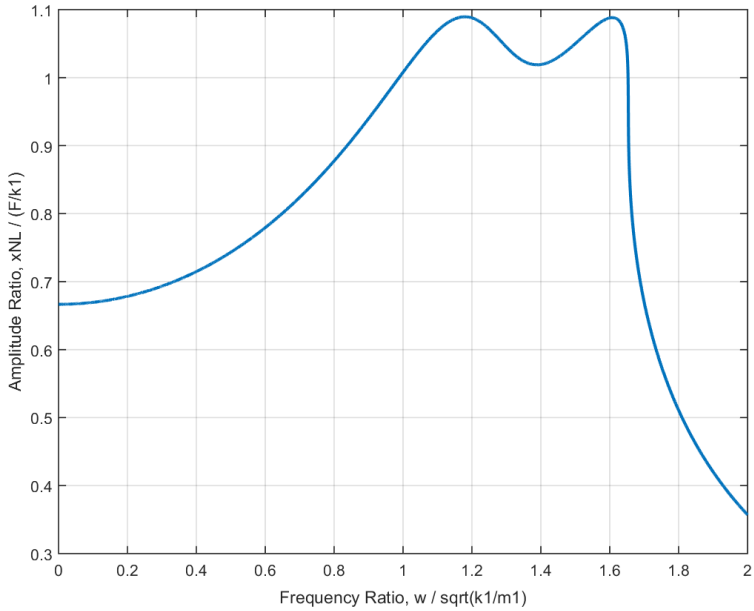

Figure 4.15 The Response Curves for 2DOF System with $\gamma = 1.50, \zeta_1 = 0.15, \mu = 0.118, \omega_r = 1.295, \zeta_2 = 0.200$

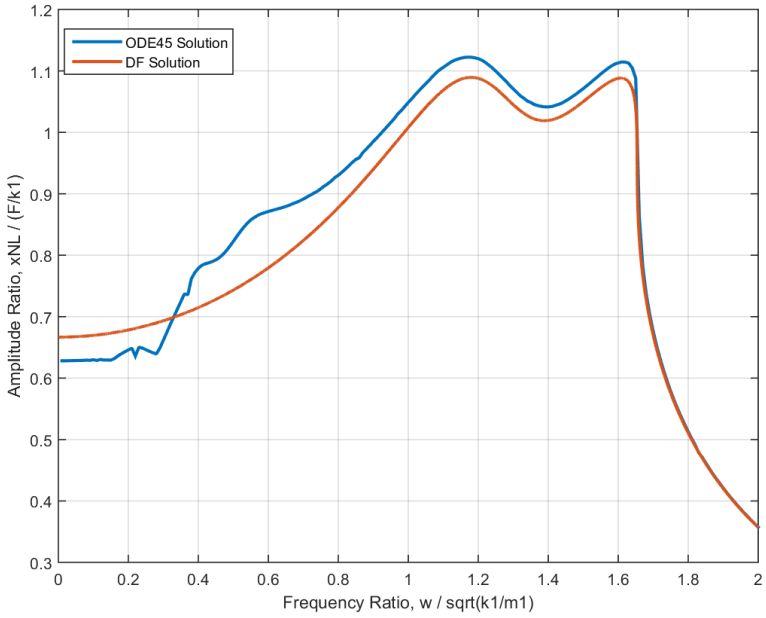

Figure 4.16 The Comparison of ODE Solution and Describing Function Method Solution for Case Study #4

Parameter sweep solution gives $\mu = 0.118, \omega_r = 1.290, \zeta_2 = 0.2196$

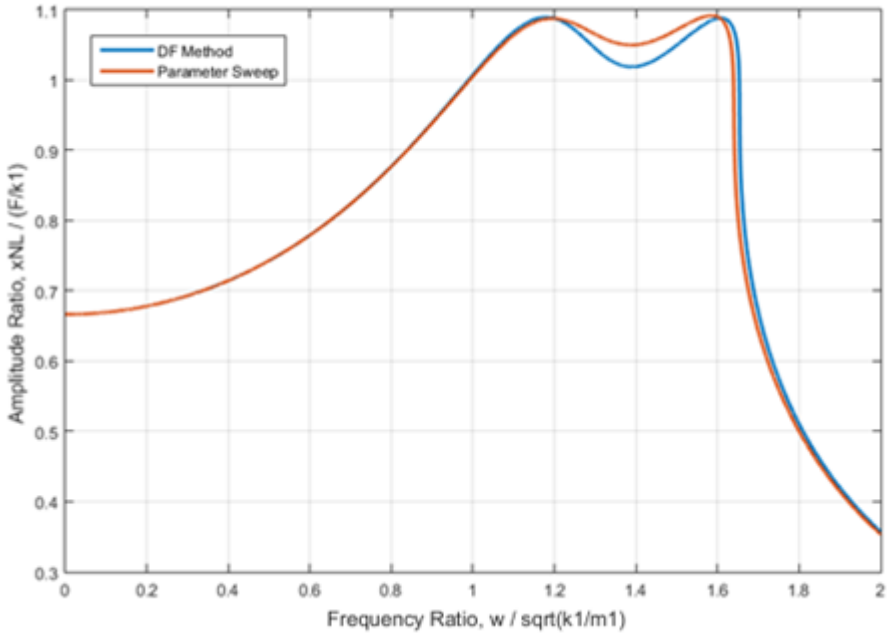

Figure 4.17 The Comparison of Describing Function Method and Parameter Sweep for Case Study #4

4.1.5 Case Study #5 (Damped Main System & Damped Vibration Absorber with low nonlinearity and low main system damping)

The system parameters chosen for Case Study #5 are given below.

$$\gamma = 0.25, \zeta_1 = 0.05$$

Frequency vs response of the main system is found with Describing Function Method

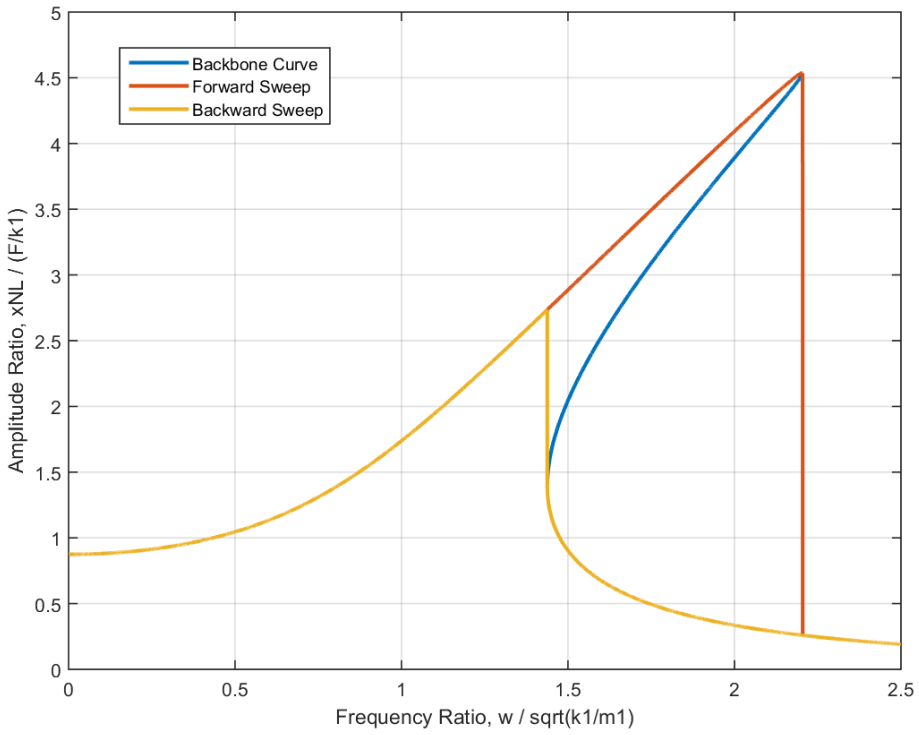

Figure 4.18 The Response Curves for SDOF System with $\gamma = 0.25, \zeta_1 = 0.05$

From Equations 3.29, 3.34 and 3.36, the vibration absorber parameters can be found quickly.

$$\mu = 0.143, \omega_r = 1.106, \zeta_2 = 0.218$$

The two-degree-of-freedom system with TVA response graphs is found using Describing Function Method

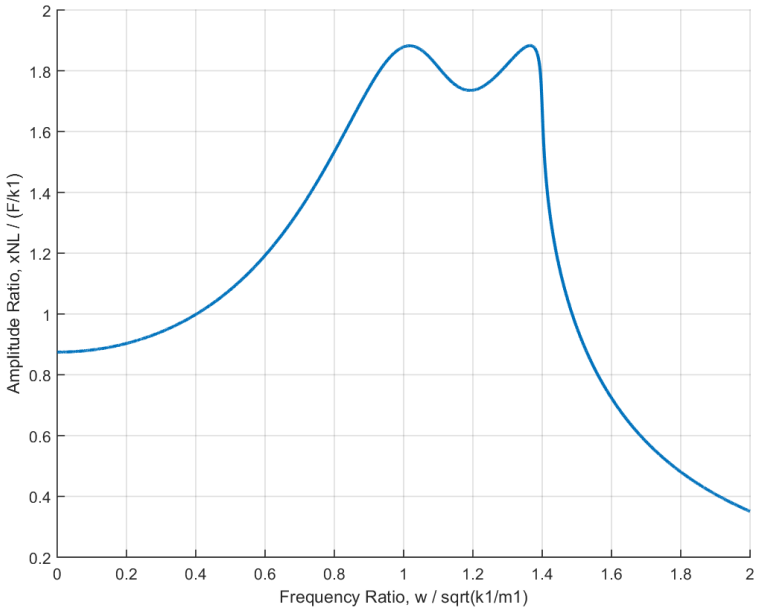

Figure 4.19 The Response Curves for 2DOF System with $\gamma = 0.25, \zeta_1 = 0.05, \mu = 0.143, \omega_r = 1.106, \zeta_2 = 0.218$

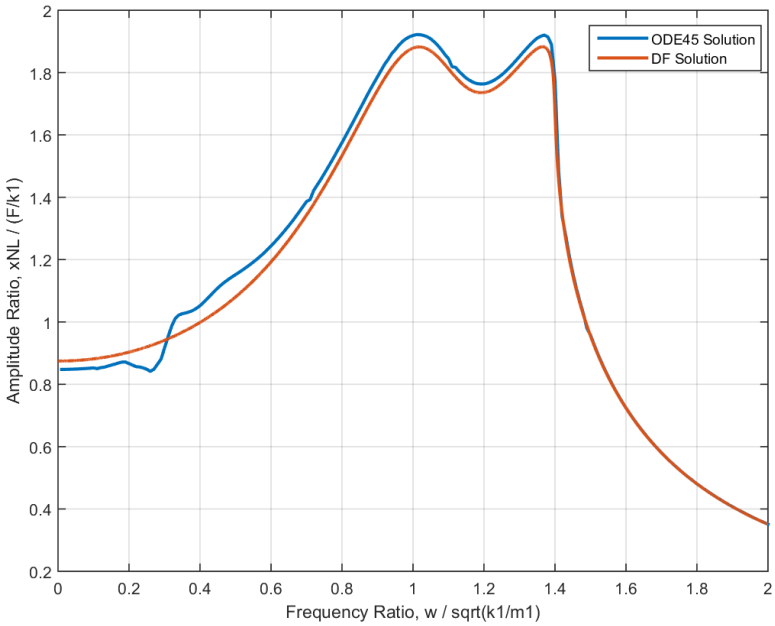

Figure 4.20 The Comparison of ODE Solution and Describing Function Method Solution for Case Study #5

Parameter sweep solution gives $\mu = 0.143, \omega_r = 1.110, \zeta_2 = 0.206$

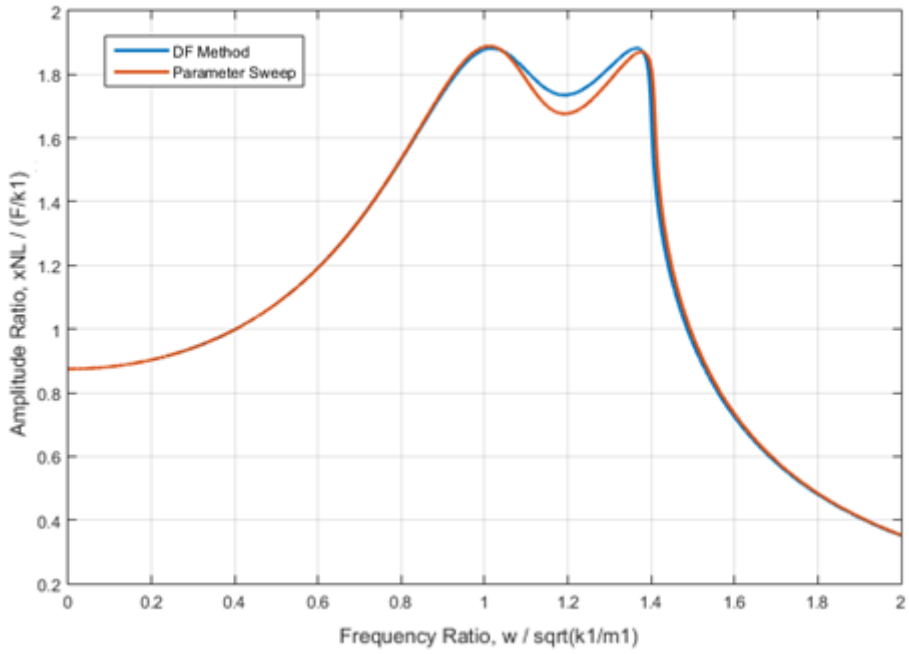

Figure 4.21 The Comparison of Describing Function Method and Parameter Sweep for Case Study #5

4.1.6 Case Study #6 (Damped Main System & Damped Vibration Absorber with high non-linearity and low main system damping)

The system parameters chosen for Case Study #6 are given below.

$$\gamma = 1.5, \zeta_1 = 0.05$$

Frequency vs response of the main system is found with Describing Function Method

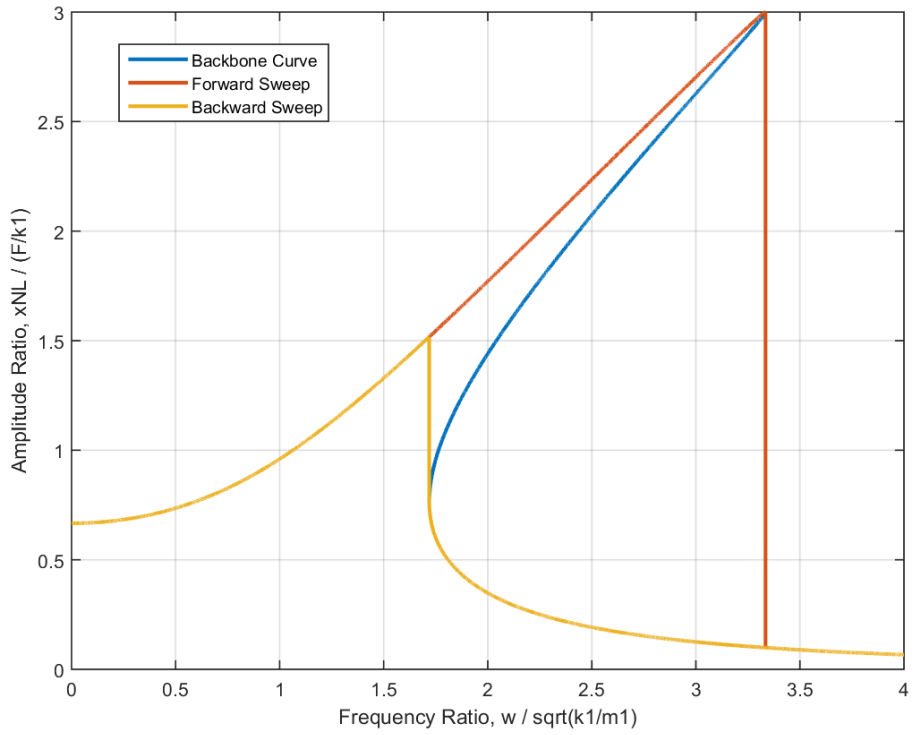

Figure 4.22 The Response Curves for SDOF System with $\gamma = 1.50, \zeta_1 = 0.05$

From Equations 3.29, 3.34 and 3.36, the vibration absorber parameters can be found quickly.

$$\mu = 0.272, \omega_r = 1.174, \zeta_2 = 0.286$$

The two-degree-of-freedom system with TVA response graphs is found using Describing Function Method

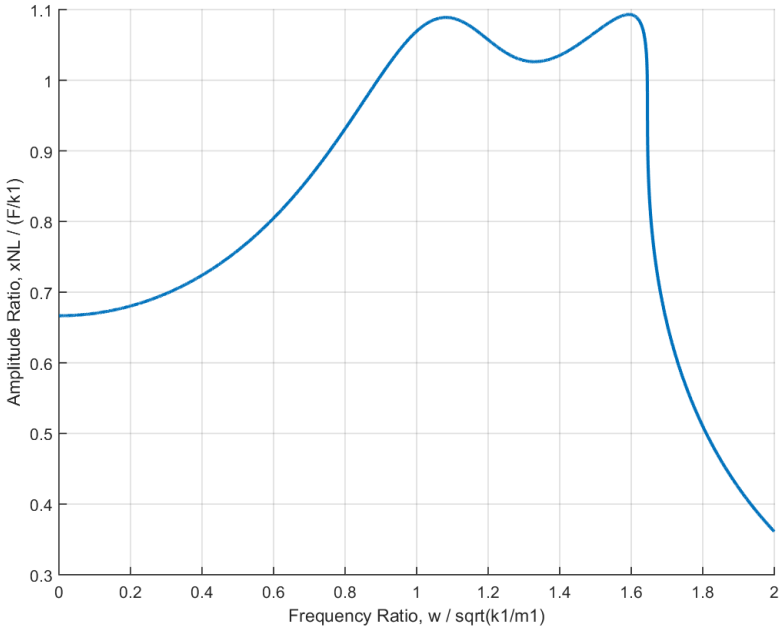

Figure 4.23 The Response Curves for 2DOF System with $\gamma = 1.50, \zeta_1 = 0.05, \mu = 0.272, \omega_r = 1.174, \zeta_2 = 0.286$

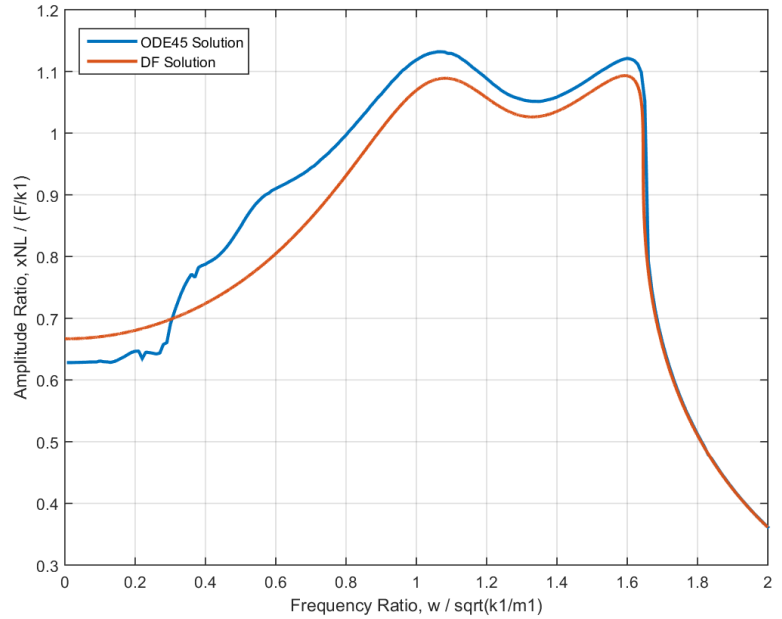

Figure 4.24 The Comparison of ODE Solution and Describing Function Method Solution for Case Study #6

Parameter sweep solution gives $\mu = 0.272, \omega_r = 1.180, \zeta_2 = 0.272$

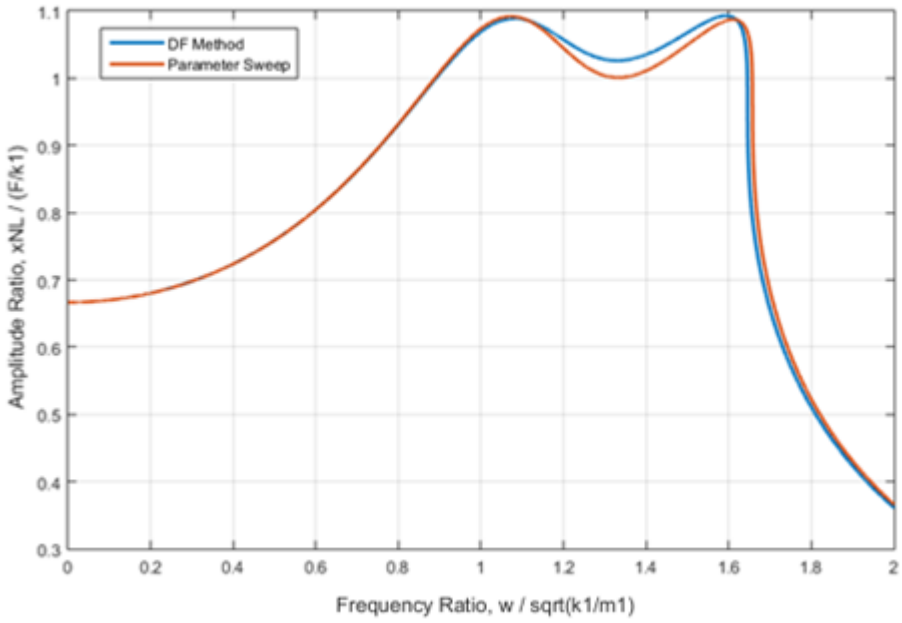

Figure 4.25 The Comparison of Describing Function Method and Parameter Sweep for Case Study #6

4.2 Multi-Degree-of-Freedom Case Studies

This section presents the implementation of the methods mentioned in Section 3.2.

4.2.1 Case Study #7

For a 4-degree-of-freedom system with cubic stiffness between the first mass and the ground, a linear TVA is attached to the first mass.

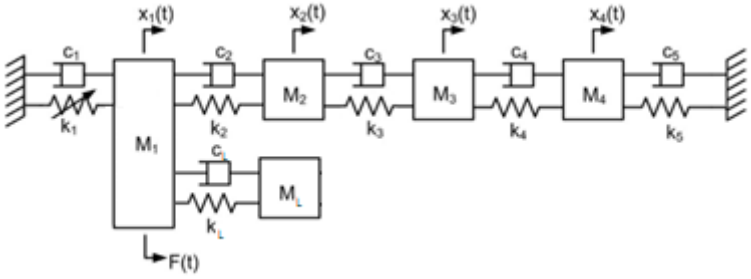

Figure 4.26 The System Model of a TVA Attached to 4-DOF System with Cubic Stiffness Connected Between the First Mass and the Ground

The main system parameters are assumed to be equal for each DOF.

$$m = 1\ kg, k = 2500\frac{N}{m}, c = 5\frac{N}{ms}, F = 5\ N, k_c = 10^9\frac{N}{m^3}$$

The mass of the absorber is selected as $m_L = 0.5\ kg$

Before the TVA is attached, there is a jump phenomenon between the frequencies 101 and 110 rad/s.

The parameter sweep returns the optimum damping with no jump behavior and minimum peaks.

$$c_L = 2.5\frac{N}{ms}, k_L = 559\frac{N}{m}$$

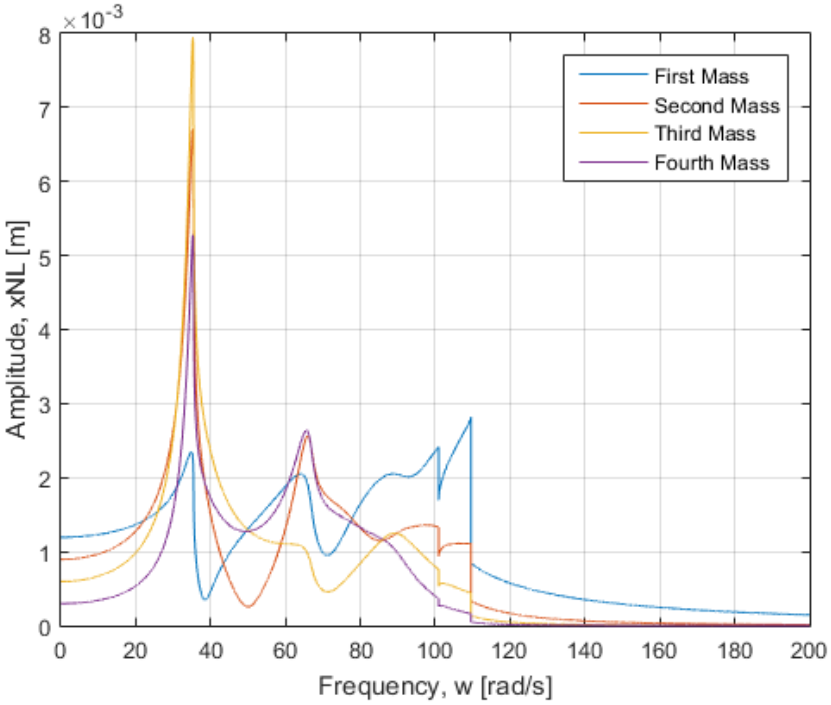

Figure 4.27 The Response Curves for Case Study #8 Before the TVA is Attached

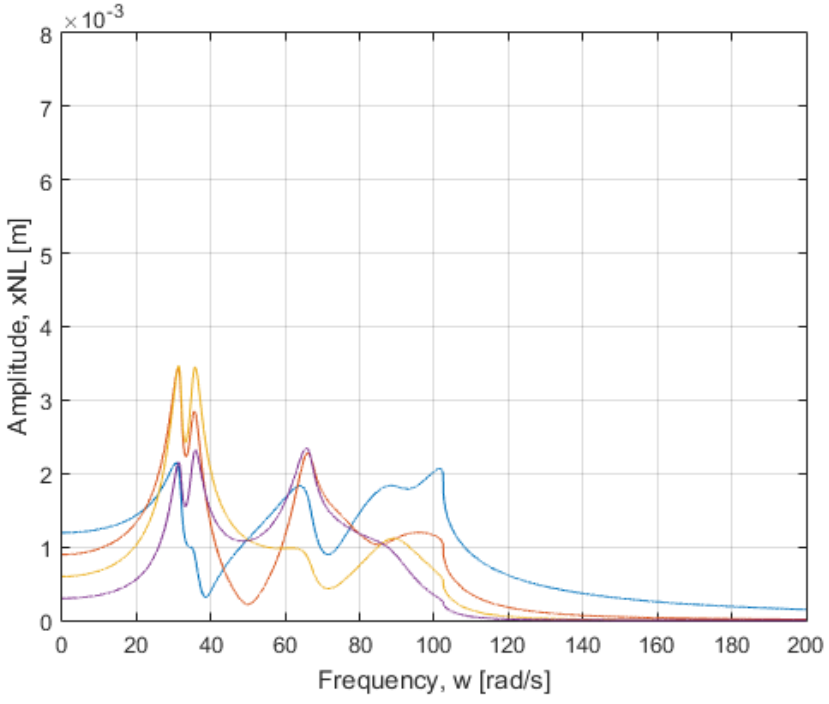

Figure 4.28 The Response Curves for Case Study #8 After the TVA is Attached

4.2.2 Case Study #8

For an MDOF system similar to the Case Study #7, the connection between the first mass and the ground demonstrates a cubic stiffness behavior, and an external forcing is applied on the first mass.

$$k_1 = 2500\frac{N}{m}, c_1 = 1\frac{N}{ms}, k_c = 10^9\frac{N}{m^3}, F = 1\ N$$

The other system parameters are assumed to be equal.

$$m_1 = m_2 = m_3 = \cdots = 1\ kg$$

$$k_2 = \ k_3 = \cdots = 500\frac{N}{m}$$

$$c_2 = c_3 = \cdots = 1\frac{N}{ms}$$

In this case, the system can be imagined as a homogenous cantilever beam with a cubic stiffness connection to the ground.

For 4-DOF system like Case Study #7, the response curves for the first mass are given in the figure below. If the first modes are neglected, the multi-valued region is very similar to an SDOF system. Hence, an SDOF equivalent system may be used to find an optimum TVA design. The response of the first mass in the 4-DOF system is shown in Figure 4.29.

If the system is assumed as 20-DOF with the same parameters, the multi-valued region does not change. Only small modes are added before the multi-valued region, so the assumption does not change as well. The response of the first mass in the 20-DOF system is shown in Figure 4.30.

The progression is continued with 4-DOF case for simplicity.

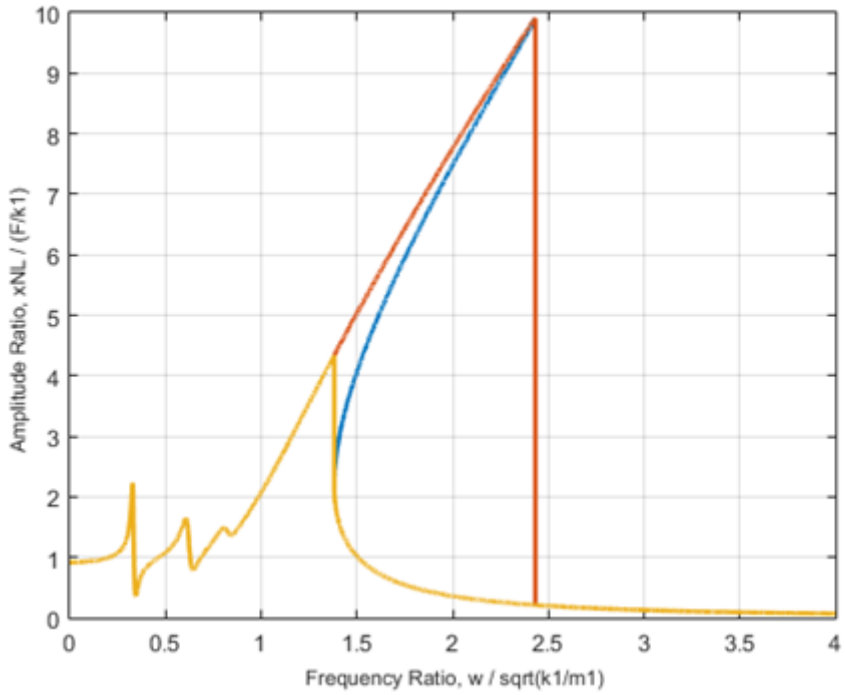

Figure 4.29 The Response of the First Mass in a 4-DOF System

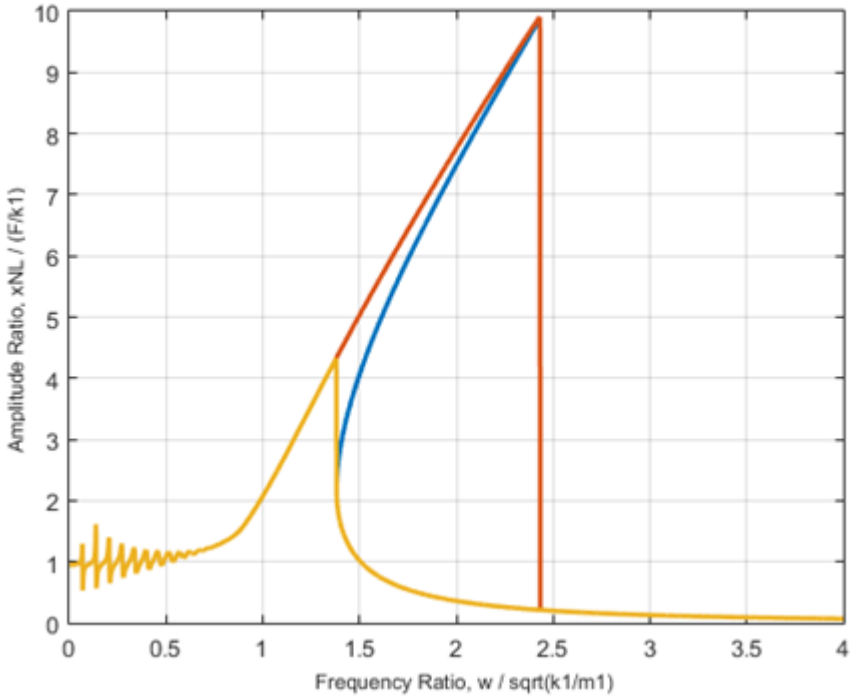

Figure 4.30 The Response of the First Mass in a 20-DOF System

Although the response resembles a SDOF system, it may not equal to an exact SDOF response. Unless k_2 and c_2 are selected perfectly, there will be some differences between the curves.

For an SDOF system with:

$$\gamma = 0.148, \zeta_1 = 0.01$$

The response curves are given below.

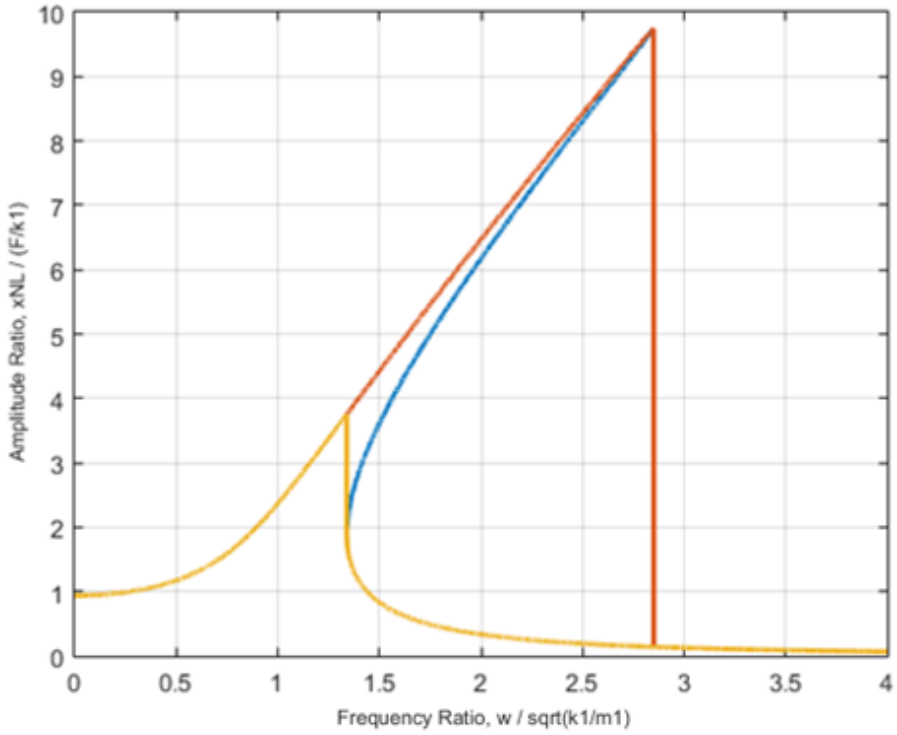

Figure 4.31 The Response Curves for SDOF System with $\gamma = 0.148, \zeta_1 = 0.01$

Comparing this curve with the first mass of 4-DOF system

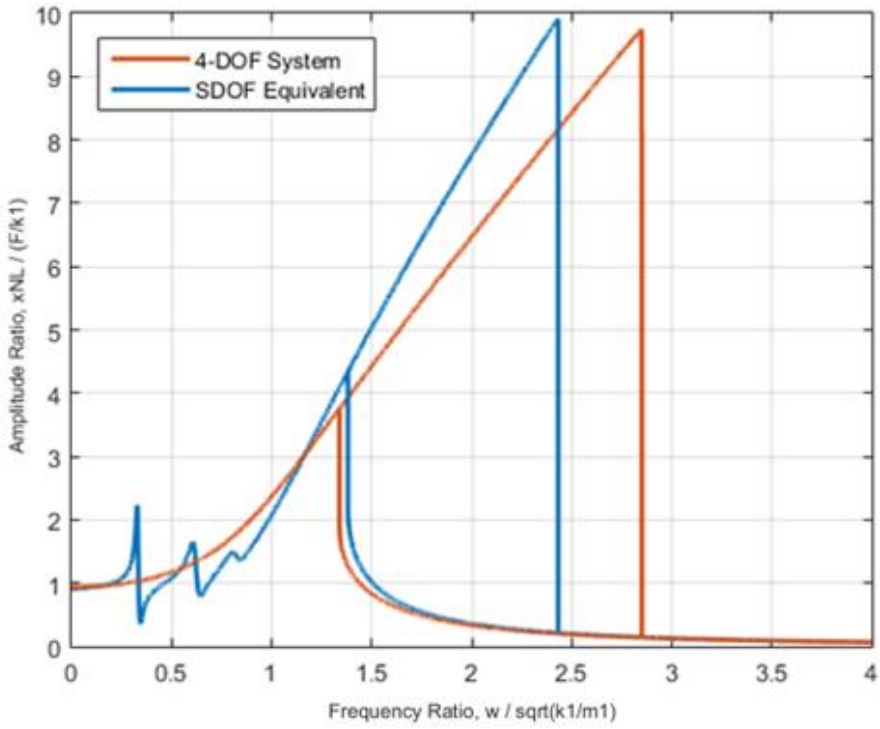

Figure 4.32 The Comparison of the First Mass of the 4-DOF System and its SDOF Equivalent

While the first jump location and the peak amplitude are close, the other jump location does not overlap. Another equivalent system may give the two overlapping jump locations, but this time peak amplitude would not be the same. Selecting such an equivalent system is not a wrong approach, it is just one out of these three parameters will not be the same with the equivalent system.

After attaching the TVA, the response of the first mass becomes as below. The idea is to find an approximation for the optimum values so that this SDOF equivalent system is found to be sufficient. Equating the other two parameters may or may not give a better result, but it will be very close to this one.

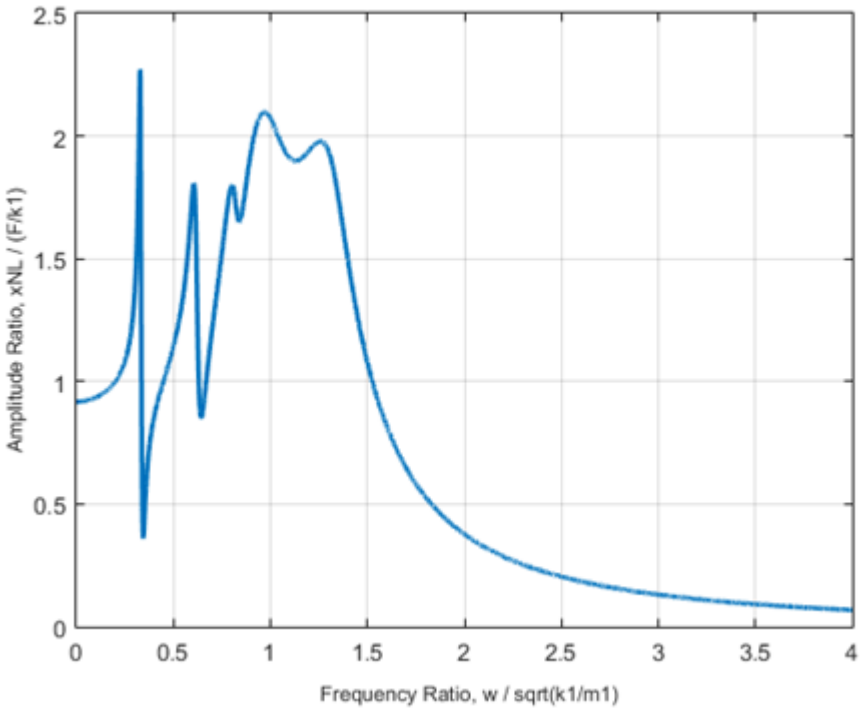

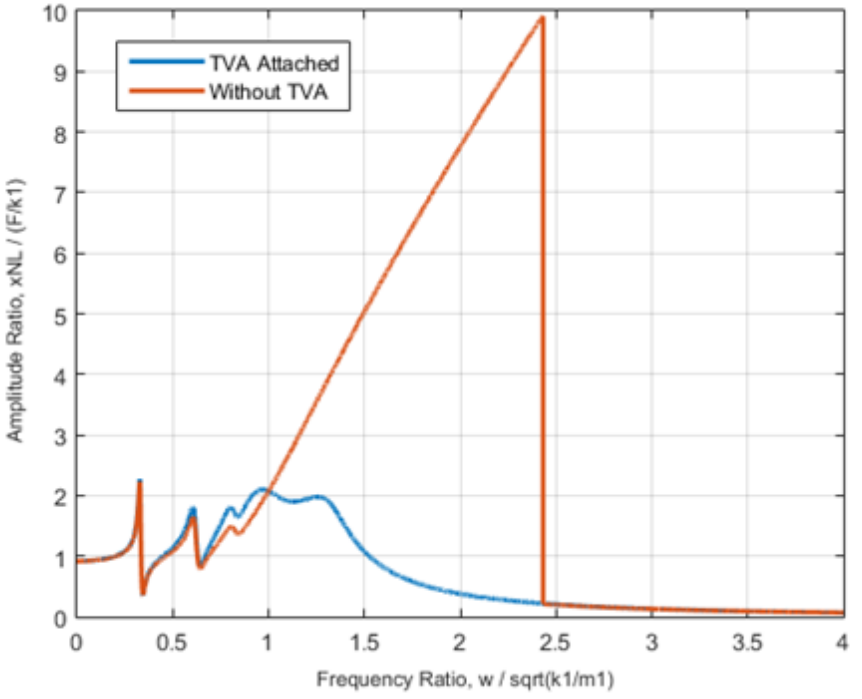

Figure 4.33: The Response Curves of The First Mass of the 4-DOF System with and without TVA Attached

ODE45 solution is almost the same as the DF Solution.

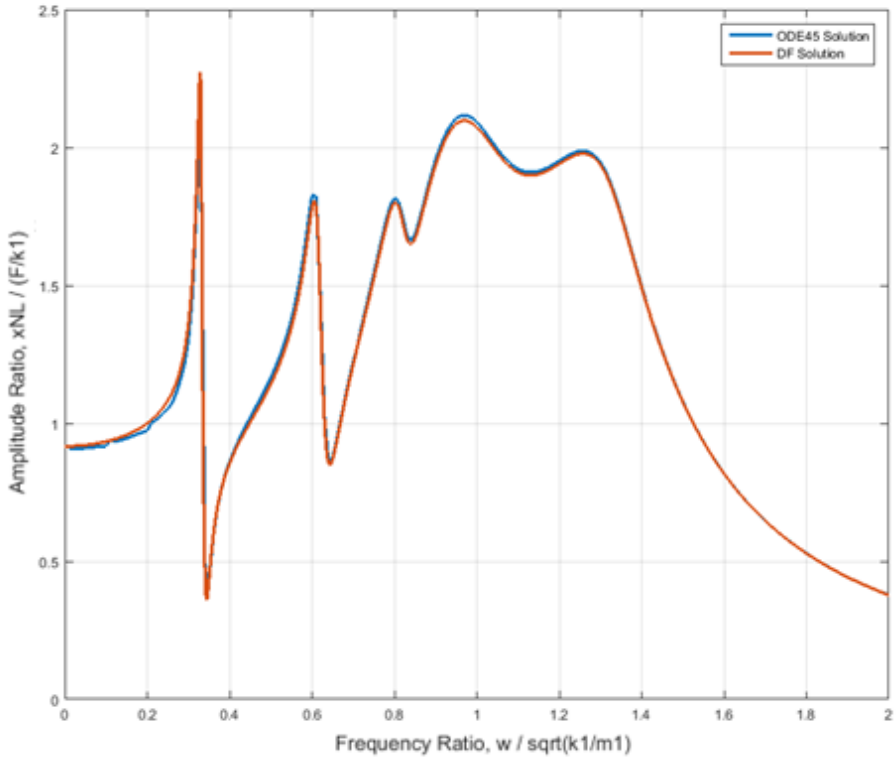

Figure 4.34 The Comparison of ODE Solution and Describing Function Method Solution for Case Study #8

4.3 Discussion of the Findings

Both local and broadband tuning methods result in good approximations, giving very close results for the perfectly optimum parameters. ODE solutions suggest that there is a slight difference between the method solution and the differential equations solution. This is due to the quasi-linearization and single harmonic approximations of describing functions. Parameter sweep work done in broadband tuning case studies shows that the suggested frequency ratio and damping ratio values are close to the actual values if brute force optimization was performed. In some cases, the

suggested damping ratio gives better results than parameter sweep in terms of lower local minimum point. This is because the parameter sweep selection algorithm does not consider the local minimum when selecting. If the algorithm is corrected, the solutions will be closer to each other.

Case Studies between #3 and #6 were the cases where the broadband tuning method was analyzed. The main system and TVA parameters and the results are summarized in the table below.

Table 4.1 Summary of the Case Studies #3-6

Main System		TVA Parameters			Results	
γ	ζ_1	μ	ω_r	ζ_2	Peak Amp	Area
0.25	0.15	0.021	1.232	0.087	1.93	2.23
1.5	0.15	0.118	1.295	0.200	1.09	1.64
0.25	0.05	0.143	1.107	0.218	1.89	2.32
1.5	0.05	0.272	1.174	0.287	1.09	1.67

The main system parameters are specifically chosen to observe the limit values. $\gamma = 0.25$ represents a very low nonlinear behavior and $\gamma = 1.5$ is a very high nonlinear behavior. Similarly, $\zeta_1 = 0.05$ is considered a low damping ratio, and $\zeta_1 = 0.15$ is a relatively high damping ratio.

By observing the mass ratio, it can be said that systems with low nonlinearity and high damping ratios are easier to isolate the vibrations from. A high nonlinearity with a low damping ratio resulted in a mass ratio of 0.272 in order to remove the region of nonlinearity. Practically speaking, this mass ratio may not be possible to obtain because the system gets 27% heavier, and it can cause other problems for the designer. If that is the case, then other possibilities should be considered. The local tuning method can be used if the system works on a narrow frequency range, or the

system has to perform around the region of nonlinearity. Using as high as possible mass ratio will protect the system from high jump-down amplitudes.

The frequency ratio required to obtain equal peaks seems to increase for high nonlinearity and high damping ratio. It is independent of the mass ratio or damping ratio of TVA, as expected.

The damping ratio of TVA is directly proportional to the mass ratio hence it is not an independent adjustment parameter.

About the results section, the nonlinearity constant γ seems to have a higher impact on peak amplitudes and the area under the graph. For high nonlinearities, the main system damping ratio almost has no impact on both. It is possible to obtain an approximate result for the peak amplitude in terms of γ and μ.

The effect of the main system damping ratio cannot be seen from the table. When the graphs are investigated, it can be seen that the damping ratio only has a bandwidth effect. A high damping ratio gives a narrower bandwidth between peaks and vice versa. The comparison of case studies #4 and #6 is given below to show the effect of damping ratio.

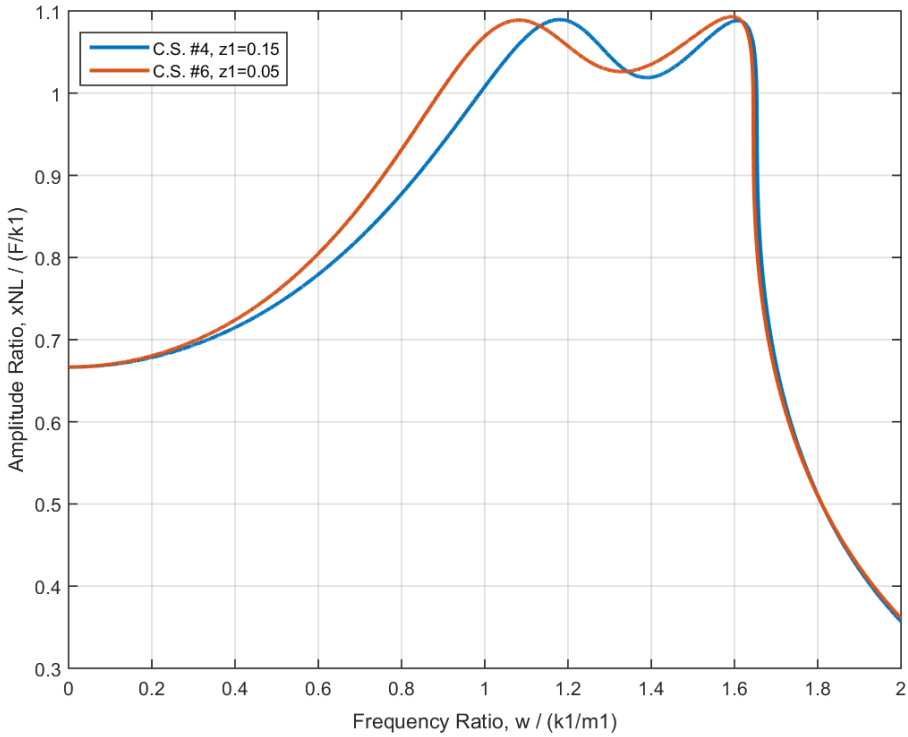

Figure 4.35 The Comparison of Case Studies #4 and #6

CHAPTER 5

CONCLUSION

This thesis aimed to develop a method similar to Den Hartog's equal-peak method for finding the optimal tuning parameters for vibration absorbers connected to systems exhibiting cubic stiffness behavior. To accomplish this, the new approach used Describing Functions for quasi-linearization of the nonlinearity and frequency response functions to analyze and optimize the system. The thesis suggested analytical methods for broadband tuning and local tuning for 2-DOF systems, wherein a linear tuned vibration absorber is coupled to the system with cubic stiffness nonlinearity. A numerical method extension for tuned vibration absorbers for weakly nonlinear MDOF systems is also suggested.

5.1 Advantages of the Method

The real power of this method lies in its foundations by using Describing Functions. There are several factors of using Describing Functions that give significant advantages. First, the Describing Functions method can serve as a system identification method. It enables us to understand and model the system when there is nonlinearity in the system since it provides a method to represent the nonlinearity in a closed form algebraic expression in frequency domain. Therefore, it enables us to understand the effects of nonlinearity on the tuning parameters of the tuned vibration absorber.

Secondly, the proposed method significantly simplifies the equation of motion. All these complicated terms are grouped as a single constant term α_{NLC}, making things easier to observe. The local tuning idea was found because of this easy term. The numerator of the term α_{NLC} was a key to come up with the idea.

The third advantage of the method is its analytical and fast solution opportunity. Instead of using ODEs or numerical methods to solve the equation of motion with different parameters for a varying frequency range, the linearized equations give a solution in less than a second. This was useful for obtaining the broadband tuning method. Although the solutions did not come up as smoothly as the examples in the literature survey, the Describing Function method allowed for a multivariate regression in a space with thousands of different parameter sets in a relatively short time, which resulted in a really good approximation of the optimum parameters.

Although the study focuses on cubic stiffness nonlinearity, the fundamentals of the method enable the user to handle other nonlinearities as well. With more complicated behaviors, obtaining analytical solutions may not be feasible; however, numerical approaches can still be employed. The method guarantees swift execution and results in significant time savings compared to traditional numerical methods.

The biggest advantage of the work done in this thesis is the simplicity of the proposed methods. A person without a mechanical vibration background can easily use the equations and find the optimum parameters for their SDOF system with cubic stiffness.

Another big advantage is the variety of solutions offered for different needs and problems. There is a local tuning possibility for a single frequency and a broadband tuning possibility through all frequencies. For broadband tuning, there is also a chance to find the smallest mass ratio possible from the formula or to use a different desired mass ratio and select the frequency ratio accordingly.

5.2 Disadvantages and Flaws of the Method

It is discussed in Chapter 1 that the amplitude of the excitation force affects the stiffness and the natural frequency of the system. The excitation force is in the nonlinearity term γ, and changing the force means changing the γ. Since the broadband tuning is done according to this parameter, changing it will have a high

impact. The region of nonlinearity may reappear, causing high jump-down amplitudes on certain frequencies and damaging the main system. Hence, if the force amplitude is not constant, this tuning method should not be used. There is no method in literature currently which can overcome this problem.

Similarly, as the name suggests, the local tuning is done for a certain frequency. If the frequency of the excitation changes over time, the system that is locally tuned may encounter similar dangerous effects. It can be generalized that, the broadband tuning should be used in the case of constant excitation amplitude, and the local tuning should be used in the case of constant excitation frequency otherwise the proposed broadband tuning method should be performed.

The case studies give good results since the parameters are selected to show and prove certain arguments in the thesis, but there are some flaws in the method developed that have to be mentioned.

When the nonlinearity is low, and the damping ratio is high, the regression equation for the mass ratio may give negative results. For example, a system with $\gamma = 0.1$ and $\zeta_1 = 0.15$ results in $\mu = -0.001$. This is due to the residual from regression being higher than this value of 0.001.

When the mass ratio returns a negative value, it is actually an indication that nonlinearities are significantly small, and a very small value of mass ratio is sufficient to remove the nonlinear region. In this case, the nonlinearities can be neglected, and the problem can be treated as a linear TVA attached to a linear primary system.

Another problem is the regression is not working perfectly at the parameter boundaries. The lower boundaries are discussed above, as the mass ratio may return negative results. Similarly, a very high nonlinearity with a low damping ratio case results in not-so-equal peaks. For example, selecting $\gamma = 2$ as the upper boundary and a low damping ratio of $\zeta_1 = 0.05$ gives the frequency-response graph below.

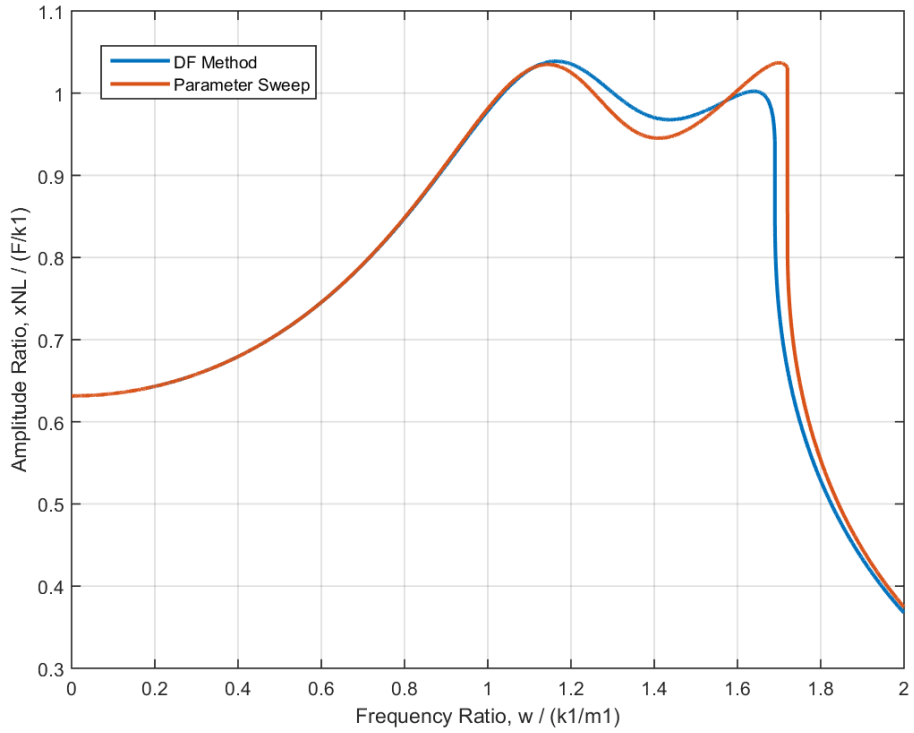

Figure 5.1 The Error at the Peaks for $\gamma = 2, \zeta_1 = 0.05$

In this case, although the peaks are not equal, the TVA parameters still results in a good performance with significant attenuation. A nonlinear constant bigger than $\gamma = 1$ means significantly high nonlinearity and $\gamma = 2$ may not be very likely to encounter in physical systems.

5.3 Future Work Improvements

There are some possible improvements for the work done in the future. Since there are no easy ways to find an analytical solution for the frequency ratio, a multivariate regression is done to the closed-form equation in order to obtain a solution. The application of Asami's H∞ optimization method [5] emerges as a valuable tool, offering a systematic approach to optimize system performance. Similar work can

be done for the frequency and mass ratios, and a complete analytical form may be obtained similar to examples in the literature.

There are also some possibilities of using these findings on diverse ideas and fields. One of the possibilities is to use these equations for connecting a linear system to the ground with a nonlinear isolator. Wire rope isolators are a good example, since their structural behavior is nonlinear and often modeled as cubic stiffness. This case has the same system model, except the main system is the second mass, and vibrations on the second mass is reduced by tuning μ, γ and ζ_1. The relationship between these parameters and the amplitudes can be observed in the findings discussed in Section 4.3.

Another possibility is to use these equations on signal filtering applications. Local tuning method is very similar to a notch filter, which is used to filter out noise on a certain frequency. Broadband tuning method can be used for control of gain by selecting proper γ and ζ_1 values. Such signal processing applications extend the relevance of these findings beyond structural engineering, presenting opportunities for advancements in communication systems, electronics, and related domains.

REFERENCES

[1] Frahm, H. (1910). Means for Damping the Rolling Motion of Ships, US970368A

[2] J P Den Hartog. (1934). Mechanical Vibrations. Dover Publications.

[3] Randall, S. E., Halsted, D. M., & Taylor, D. L. (1981). Optimum vibration absorbers for linear damped systems. Journal of Mechanical Design, 103(4), 908.

[4] Thompson, A. G. (1981). Optimum tuning and damping of a dynamic vibration absorber applied to a force excited and damped primary system. Journal of Sound and Vibration, 77(3), 403–415.

[5] Asami, T., & Nishihara, O. (2003). Closed-form exact solution to h∞ optimization of dynamic vibration absorbers (Application to different transfer functions and damping systems). Journal of Vibration and Acoustics, 125(3), 398.

[6] Casalotti, A., Arena, A., Lacarbonara, W. (2014). Mitigation of Post-flutter Oscillations in Suspension Bridges by Hysteretic Tuned Mass Dampers. Eng. Struct. 69, 62–71

[7] Lin, C., Hu, C., Wang, J., & Hu, R. (1994). Vibration control effectiveness of passive tuned mass dampers. Journal of the Chinese Institute of Engineers, 17(3), 367–376.

[8] Soto, M.G., Adeli, H., Tuned Mass Dampers, Architectural Computational Methods, 20(4), 419–431 (2013)

[9] Taylor, E. S. (1936). Eliminating crankshaft torsional vibration in radial aircraft engines, SAE International. 31, 81–89

[10] Zapfe, J. A., & Lesieutre, G. A. (1997). Broadband vibration damping using highly distributed tuned mass absorbers. AIAA Journal, 35(4), 753–755.

[11] Sims, N. D. (2007). Vibration absorbers for chatter suppression: A new analytical tuning methodology. Journal of Sound and Vibration, 301(3-5), 592–607.

[12] Rivin, E.I. (1999). Stiffness and Damping in Mechanical Design. CRC Press.

[13] Ibrahim, R. A. (2008). Recent advances in nonlinear passive vibration isolators. Journal of Sound and Vibration, 314(3-5), 371–452.

[14] Nagarajaiah, S., & Sonmez, E. (2007). Structures with semiactive variable stiffness single/multiple tuned mass dampers. Journal of Structural Engineering, 133(1), 67–77.

[15] Brennan, M. J., Kovacic, I., Carrella, A., & Waters, T. P. (2008). On the jump-up and jump-down frequencies of the Duffing oscillator. Journal of Sound and Vibration, 318(4-5), 1250–1261.

[16] Gatti, G., Kovacic, I., & Brennan, M. J. (2010). On the response of a harmonically excited two degree-of-freedom system consisting of a linear and a nonlinear quasi-zero stiffness oscillator. Journal of Sound and Vibration, 329(10), 1823–1835.

[17] Gatti, G., Brennan, M. J., & Kovacic, I. (2010). On the interaction of the responses at the resonance frequencies of a nonlinear two degrees-of-freedom system. Physica D: Nonlinear Phenomena, 239(10), 591–599.

[18] Gatti, G., & Brennan, M. J. (2011). On the effects of system parameters on the response of a harmonically excited system consisting of weakly coupled nonlinear and linear oscillators. Journal of Sound and Vibration, 330(18-19), 4538–4550.

[19] Rüdinger, F. (2007). Tuned mass damper with nonlinear viscous damping. Journal of Sound and Vibration, 300(3-5), 932–948.

[20] Habib, G., Detroux, T., Viguié, R., & Kerschen, G. (2015). Nonlinear generalization of Den Hartog′s equal-peak method. Mechanical Systems and Signal Processing, 52-53, 17–28.

[21] Chang, W., Jin, X., Huang, Z., & Cai, G. (2021). Random response of nonlinear system with inerter-based dynamic vibration absorber. Journal of Vibration Engineering & Technologies, 9(8), 1903–1909.

[22] Sgobba, S., & Marano, G. C. (2010). Optimum design of linear tuned mass dampers for structures with nonlinear behaviour. Mechanical Systems and Signal Processing, 24(6), 1739–1755.

[23] Mohebbi, M., & Joghataie, A. (2011). Designing optimal tuned mass dampers for nonlinear frames by distributed genetic algorithms. The Structural Design of Tall and Special Buildings, 21(1), 57–76.

[24] Tanrikulu, O., Kuran, B., Ozguven, H. N., & Imregun, M. (1993). Forced harmonic response analysis of nonlinear structures using describing functions. AIAA Journal, 31(7), 1313–1320.

[25] Özer, M. B. (2015). Closed form solutions of weakly nonlinear multi-degree of freedom systems with single nonlinear element. Journal of Sound and Vibration, 344, 345–362.

[26] Gelb, A., & Vander, W. E. (1968). Multiple-Input Describing Functions and Nonlinear System Design. McGraw-Hill.

[27] Brennan, M. (n.d.). Vibration Absorbers/Neutralisers. https://www.feis.unesp.br/Home/departamentos/engenhariamecanica/gmsint/14-vibration-absorbers.pdf

[28] Shock and Vibration Damping Components. https://www.vibrationmounts.com/media/wysiwyg/Catalog/VMC-V100-catalog.pdf

[29] Arslan, Ö. (2008). Modal identification of nonlinear substructures and implementation in structural coupling analysis [Master's Thesis, Middle East Technical University] https://open.metu.edu.tr/handle/11511/17955

APPENDICES

A. Pseudo-Code for Parameter Sweep to Obtain Optimum Damping and Frequency Ratio

```
% 1. Define the function to calculate the area under the graph
given the equation and parameters wr and zeta2:
function area = calculateArea(equation, wr, zeta2, mu)
    % Initialize area
    area = 0;
    % Define your algorithm to calculate the area under the graph
    % using the equation and parameters wr and zeta2
    % This could involve numerical integration techniques
    % Update the 'area' variable with the calculated area
end

% 2. Define the function to find the peak points of the graph given
the equation and parameters wr and zeta2:
function [peakPoint1, peakPoint2] = findPeakPoints(equation, wr,
zeta2, mu)
    % Define your algorithm to find the peak points of the graph
    % using the equation and parameters wr and zeta2
    % This could involve finding the critical points of the
equation
    % and then evaluating those points to find the peak points
end

% 3. Initialize the parameters wr and zeta2 with initial values or
ranges.
wr_range = [initial_wr_value:step:final_wr_value];
zeta2_range = [initial_zeta2_value:step:final_zeta2_value];

% 4. Initialize the smallestArea variable with a large value.
smallestArea = inf;

% 5. Initialize the smallestDifference variable with a large value.
smallestDifference = inf;

% 6. Iterate through the parameter space:
for wr = wr_range
    for zeta2 = zeta2_range
        % Calculate the area under the graph for the current
parameters
        currentArea = calculateArea(equation, wr, zeta2);

        % Find the peak points for the current parameters
        [peakPoint1, peakPoint2] = findPeakPoints(equation, wr,
zeta2, mu);

        % Calculate the difference between the two peak points
```

```
        currentDifference = abs(peakPoint1 - peakPoint2);

        % Check if the current area is smaller than the
smallestArea
        % and the current difference is smaller than the
smallestDifference
        if currentArea < smallestArea && currentDifference <
smallestDifference
            smallestArea = currentArea;
            smallestDifference = currentDifference;
            bestParameters = [wr, zeta2];
        end
    end
end

% 7. Output the bestParameters that result in the smallest area and
the smallest difference between peak points.
fprintf('Best Parameters: wr = %.2f, zeta2 = %.2f\n',
bestParameters(1), bestParameters(2));
fprintf('Smallest Area: %.2f\n', smallestArea);
fprintf('Smallest Difference: %.2f\n', smallestDifference);
```

B. Main Code for 2-DOF Analytical DF Method

```
gama=0.148;  z1=0.01;

mu = 0.13252 + 0.5642*gama - 1.5412*z1 - 0.9857*gama*gama +
2.5374*z1*z1 - 1.416*gama*z1 + 0.7823*gama*gama*gama +
3.258*gama*gama*z1 - 0.20404*gama*gama*gama*gama -
2.867*gama*gama*gama*z1 + 0.7827*gama*gama*gama*gama*z1

z2 = sqrt((8+9*mu-4*sqrt(4+3*mu))/(1+mu))/4;

wr = 0.9029 + 2.3455*gama + 2.294*z1 + 0.198*z2 - 1.0724*gama*gama
- 4.667*z1*z1 + 0.100*z2*z2 - 11.708*gama*z1 - 8.822*gama*z2 -
4.417*z1*z2 + 6.317*gama*gama*z1 + 5.078*gama*gama*z2 +
15.260*gama*z1*z1 + 26.32*gama*z1*z2 + 5.536*gama*z2*z2 -
9.083*gama*gama*z1*z1 - 16.16*gama*gama*z1*z2 -
5.341*gama*gama*z2*z2

omega=0.0002:0.0002:2;
for i=1:10000
    A=wr^2-omega(i).^2;
    B=2*z2*wr*omega(i);
    C=omega(i).^4-(1+wr^2*(mu+1)+4*z1*z2*wr)*omega(i).^2+wr^2;
    D=2*omega(i).*((z1*wr^2+z2*wr)-omega(i).^2*(z1+z2*wr*(mu+1)));
    alfa_NLC(:,i)=(A+1i*B)/(C+1i*D);

    xL(1,i)=alfa_NLC(:,i);

    a=(3/4*gama*abs(alfa_NLC(:,i))).^2;
    b=(3/2*gama*real(alfa_NLC(:,i)));
    c=1;
    d=-abs(xL(1,i))^2;
    co = [a b c d];
    s(:,i)=roots(co);

    disc(i)=18*a*b*c*d-4*b^3*d+b^2*c^2-4*a*c^3-27*a^2*d^2;
    if disc(i) < 0
        for j=1:3
            if isreal(s(j,i)) == 1
                t(1,i)=s(j,i);
                t(2,i)=s(j,i);
                t(3,i)=s(j,i);
            end
        end
    else
        t(1,i)=s(1,i);
        t(2,i)=s(2,i);
        t(3,i)=s(3,i);
    end
    for j=1:3
        xNL1(j,i)=sqrt(t(j,i));
    end
end
```

C. Main Code for 2-DOF Iterative Method

```
m1=1;
k1=2500;
m2=0.2;
k2=330;
kc=10^9;
c1=10;
c2=0.5;
F=1;

w=0.1:0.1:100;

for i=1:1:size(w,2)
    f = @(x1)(abs(x1)-abs(F*(m2*w(i).^2*1i + c2*w(i) -
k2*1i)/(c1*k2*w(i) - c1*m2*w(i).^3 - c2*m1*w(i).^3 - c2*m2*w(i).^3
- k2*kc*x1^2*1i + k1*m2*w(i).^2*1i + k2*m1*w(i).^2*1i +
k2*m2*w(i).^2*1i - m1*m2*w(i).^4*1i - k1*k2*1i + c2*k1*w(i) +
c1*c2*w(i).^2*1i + c2*kc*w(i)*x1^2 + kc*m2*w(i).^2*x1^2*1i)));
    a=0;
    b=0.1;
    while abs(f(b))>.00000001
        if f((a+b)/2)<0
            a=(a+b)/2;
        else
            b=(a+b)/2;
        end
    end
    xNL(i)=a;
end
```

D. Main Code for MDOF Analytical DF Method

```
clear
clc

dof = 100;

kc = 10^9;
F = 1;

m1 = 1;
k1 = 2500;
c1 = 1;

M=zeros(dof);
K=zeros(dof);
C=zeros(dof);

F0=zeros(dof,1);
F0(1,1)=F;

%Mass Matrix
M(1,1) = m1;
for i = 2:dof
    var_name = ['m', num2str(i)];
    eval([var_name, '= 1;']);
    M(i,i)=eval(var_name);
end

%Stiffness Matrix
for i = 2:dof
    var_name = ['k', num2str(i)];
    eval([var_name, '= 500;']);
end

K(1,1)=k1;
for i = 2:dof
    var_name = ['k', num2str(i)];
    K(i,i)=eval(var_name);
    K(i-1,i-1)=K(i-1,i-1)+eval(var_name);
    K(i,i-1)=-eval(var_name);
    K(i-1,i)=-eval(var_name);
end
K(dof,dof)=K(dof,dof)+eval(var_name); %% Sonda spring varsa

%Damping Matrix
for i = 2:dof
    var_name = ['c', num2str(i)];
    eval([var_name, '= 1;']);
end

C(1,1)=c1;
```

```
for i = 2:dof
    var_name = ['c', num2str(i)];
    C(i,i)=eval(var_name);
    C(i-1,i-1)=C(i-1,i-1)+eval(var_name);
    C(i,i-1)=-eval(var_name);
    C(i-1,i)=-eval(var_name);
end
C(dof,dof)=C(dof,dof)+eval(var_name); %% Sonda spring varsa

w=1:1:100;

for i=1:100
    alfa=inv(K-w(i).^2*M+1i*w(i)*C);
    alfa_NLC(:,i)=alfa(1,1);

    xL(:,i)=alfa*F0;

    a=(3/4*kc*abs(alfa_NLC(:,i))).^2;
    b=(3/2*kc*real(alfa_NLC(:,i)));
    c=1;
    d=-abs(xL(1,i))^2;
    co = [a b c d];
    s(:,i)=roots(co);

    disc(i)=18*a*b*c*d-4*b^3*d+b^2*c^2-4*a*c^3-27*a^2*d^2;
    if disc(i) < 0
        for j=1:3
            if isreal(s(j,i)) == 1
                t(1,i)=s(j,i);
                t(2,i)=s(j,i);
                t(3,i)=s(j,i);
            end
        end
    else
        t(1,i)=s(1,i);
        t(2,i)=s(2,i);
        t(3,i)=s(3,i);
    end
    for j=1:3
        xNL1(j,i)=xL(1,i)-
(3/4*kc*t(j,i))*(alfa(1,1))*(xL(1,i))/(1+(3/4*kc*t(j,i))*alfa_NLC(:
,i));
    end
end
```

E. Main Code for MDOF Iterative Method

```
dof = 5;

w = 1:1:100;
kc = 10^9;
F = 1;
m1 = 1;
k1 = 2500;
c1 = 1;

M=zeros(dof);
K=zeros(dof);
C=zeros(dof);
%D=zeros(dof);

%Mass Matrix
M(1,1) = m1;
for i = 2:dof
    var_name = ['m', num2str(i)];
    eval([var_name, '= 1;']);
    M(i,i)=eval(var_name);
end

%Stiffness Matrix
for i = 2:dof
    var_name = ['k', num2str(i)];
    eval([var_name, '= 500;']);
end

K(1,1)=k1;
for i = 2:dof
    var_name = ['k', num2str(i)];
    K(i,i)=eval(var_name);
    K(i-1,i-1)=K(i-1,i-1)+eval(var_name);
    K(i,i-1)=-eval(var_name);
    K(i-1,i)=-eval(var_name);
end
K(dof,dof)=K(dof,dof)+eval(var_name); %% Sonda spring varsa

%Damping Matrix
for i = 2:dof
    var_name = ['c', num2str(i)];
    eval([var_name, '= 1;']);
end

C(1,1)=c1;
for i = 2:dof
    var_name = ['c', num2str(i)];
    C(i,i)=eval(var_name);
    C(i-1,i-1)=C(i-1,i-1)+eval(var_name);
    C(i,i-1)=-eval(var_name);
```

```
    C(i-1,i)=-eval(var_name);
end
C(dof,dof)=C(dof,dof)+eval(var_name); %% Sonda spring varsa

%Delta Matrix
D = cell(dof,dof);
D{1,1} = @(x1)3/4*kc*x1^2;
for i = 1:dof
    for j = 1:dof
        if i == 1 && j == 1
        else
            D{i,j} = 0;
        end
    end
end

for ii = 1:size(w,2)
    a = 0;
    b = 10;
    for i = 1:dof
        for j = 1:dof
            if i == 1 && j == 1
                EOM(i,j) = (K(i,j) - w(ii).^2*M(i,j)
+1i*w(ii)*C(i,j) + D{i,j}((a+b)/2));
            else
                EOM(i,j) = (K(i,j) - w(ii).^2*M(i,j)
+1i*w(ii)*C(i,j) + D{i,j});
            end
        end
    end
    inv_result = inv(EOM);
    func = abs(a+b)/2 - abs(F*inv_result(1,1));
    while abs(func) > .0000001
        if func < 0
            a=(a+b)/2;
        else
            b=(a+b)/2;
        end
        for i = 1:dof
            for j = 1:dof
                if i == 1 && j == 1
                    EOM(i,j) = (K(i,j) - w(ii).^2*M(i,j)
+1i*w(ii)*C(i,j) + D{i,j}((a+b)/2));
                else
                    EOM(i,j) = (K(i,j) - w(ii).^2*M(i,j)
+1i*w(ii)*C(i,j) + D{i,j});
                end
            end
        end
        inv_result = inv(EOM);
        func = abs(a+b)/2 - abs(F*inv_result(1,1));
    end
    xNL(ii)=b;
    ii=ii+1;
end
```